ISSN 3102-0410 (Print)
ISSN 3102-0429(Online)

EVEREST ADVANCES
in Science and Technology (EAST)

November 1
2025

VOLUME-1
Issue-1

Editorial Board

Message from the CEO

It is with great pride and enthusiasm that I extend my heartfelt congratulations on the successful launch of the inaugural issue of Everest Advances in Science and Technology (EAST), a remarkable initiative by Everest Engineering College. I am confident that this journal is not just a publication and strongly believe that it is a reflection of our commitment to academic excellence, research-driven education, and our enduring mission to nurture innovation and critical inquiry.

We are in the era where science and technology are rapidly reshaping every aspect of our lives, the role of academic institutions as knowledge generator becomes more vital than ever. EAST is a timely and much-needed platform that brings together the ideas, experiments, and breakthroughs of both emerging and established researchers. It represents the intellectual heartbeat of our institution and signals our readiness to contribute meaningfully the global academic and scientific community.

I would like to express my sincere gratitude to all the editors for their tireless efforts, insightful contributions, and unwavering dedication throughout this process. My special thanks go to Er. Narayan Sapkota, whose patience and technical expertise brought this journal to life in LaTeX format, and to Er. Anil Thapa for his invaluable assistance in managing key administrative tasks behind the scenes.

We have begun our journey of working together with researchers and academicians inside, and outside the college including industrial communities through this first issue of EAST. I encourage scholars, students, faculty members, and industry professionals to actively participate in the growth of this journal, as contributors, reviewers, and readers.

Together, let us continue to build a strong academic research culture that inspires innovation, promotes critical thinking, and drives progress.

Arun Kumar Bhandari
Chief Executive Officer
Everest Engineering College

Message from the Principal and Editor-in-Chief

It gives me immense pleasure and a profound sense of pride to present the first-ever issue of Everest Advances in Science and Technology (EAST), the official research journal of Ever-est Engineering College. This publication marks a significant milestone in our institutional journey, a bold step toward foster-ing a strong culture of research, innovation, and academic excel-lence.

The vision behind EAST is to create a vibrant platform where curious minds, young researchers, seasoned academics, and industry experts can converge to share knowledge, challenge conventions, and push the boundaries of science and technology. In today's rapidly advancing world, it is imperative that educational institutions not only dissem-inate knowledge but also actively contribute to its creation. EAST is our humble yet ambitious response to this call.

This inaugural issue brings together a diverse range of scholarly articles, reflecting the interdisciplinary spirit we aim to nurture. We are committed to upholding the highest standards of academic integrity, peer review, and editorial excellence in every issue.

I extend my heartfelt thanks to our editorial board, reviewers, faculty, student researchers, and contributors who have made this publication possible. Your dedication has laid the foundation for what we hope will become a journal of national and international repute.

A special note of appreciation goes to Er. Narayan Sapkota, for meticulously converting the document into LaTeX format; a time-consuming yet essential task, and to Er. Anil Thapa, for his invaluable support in administrative coordination.

As we embark on this new academic endeavor, I warmly invite scholars, students, and professionals across the scientific and engineering spectrum to engage with EAST; as readers, contributors, and collaborators.

Let this be the beginning of a legacy in scientific thought, innovation, and discovery.

Prof. Dr. Hari Krishna Shrestha
Principal & Editor-in-Chief
Everest Advances in Science and Technology (EAST)
Everest Engineering College

Journal Name: Everest Advances in Science and Technology (EAST)
Volume: 1
Issue: 1
Date: November, 2025
ISSN: 3102-0410 (print), 3102-0429 (online)
Publisher: Everest Engineering College, Sanepa-2, Lalitpur

Table of Contents

Everest Advances in Science and Technology (EAST), Vol. 1, No. 1, 2025
ISSN: 3102-0410(print), 3102-0429(online)

Carbon Footprint Estimation in Road Construction: A Case Study of Pokhara-Mugling Road, Nepal

SABHYATA KHANAL[1*], ROBERT DONGOL[2]

Abstract. Road construction is a significant contributor to greenhouse gas emissions within the transport sector. This study attempted to quantify the Green House Gases (GHGs) emission of Pokhara - Mugling Road using Life Cycle Assessment (LCA). A Gate-to-Gate LCA was conducted to quantify emissions. Sensitivity analyses were conducted to assess the differential impacts of bitumen and aggregate on emissions during construction. The Relative Importance Index (RII) was calculated by distributing a questionnaire to experts and environmental safeguard specialists to gather insights on the most suitable mitigation measures for reducing emissions in Nepals' road sector. The findings revealed that the total carbon equivalent emissions from the construction of the Pokhara - Mugling Road amounted to 33.73 kilotons of CO_2e. Notably, 60.78% of these emissions were attributed to the materials used in the construction process. Fuel consumption by the Hot Mix Asphalt (HMA) plant contributed 70% of the emissions from the total fuel consumption, surpassing the emissions from all other plants and equipment involved in the pavement construction. Sensitivity analysis results indicated that changes in bitumen content have a more significant effect on GHG emissions compared to variations in aggregate. This suggests that the construction of a national highway substantially contributes to carbon emissions, and therefore, requires careful consideration to minimize its environmental footprint. Based on the RII analysis, optimizing construction and quality management plans is essential for reducing greenhouse gas emissions in road construction. Equally important is using electricity as a fuel source for heating in asphalt production can lower emissions compared to traditional fossil fuels. Implementing warm mix or cold asphalt technologies and incorporating recycled materials such as Reclaimed Asphalt Pavement (RAP) and crumb rubber in asphalt mixtures can significantly reduce emissions. Transitioning to low-emission equipment, including electric or biodiesel-powered machinery, and adopting alternative energy sources such as natural gas or biomass-based fuels in asphalt plants also can minimize the environmental impact. By integrating these sustainable practices, road construction in Nepal can significantly decrease its contribution to greenhouse gas emissions.

Keywords: Gate to Gate, Green House Gas, Hot Mix Asphalt, Life Cycle Assessment.

[1]Nepal Engineering College, Pokhara University, Bhaktapur, Nepal
E-mail: sabhyatakhanal77777@gmail.com
[2]Center for Postgraduate Studies, Nepal Engineering College, Nepal
E-mail: robert@nec.edu.np
* Corresponding author
Manuscript received: 12 July, 2025; revised: 15 August 2025; accepted: 5 September, 2025.
Everest Advances in Science and Technology (EAST), Vol. 1, No. 1, 2025

1. Introduction

Global warming is causing more frequent extreme weather events and the ongoing melting of the polar ice caps, which is being caused by an increase in greenhouse gas emissions. As a result of these negative effects of global warming, it is now urgently necessary to control and reduce greenhouse gas emissions in order to protect human life [1, 2, 3]. One of the primary global sources of carbon emissions is the road transportation sector [4]. Therefore, reducing the carbon emissions produced during construction is a crucial area for research to combat global warming. Infrastructure construction projects, especially road construction, are responsible for significant emissions [5]. Over the course of their entire life cycle, including the manufacturing of raw materials, building, operation, maintenance, and road repair, road infrastructure produces significant amounts of greenhouse gases (GHGs) [6, 7]. By 2050, it is anticipated that more than 25 million kilometers (a 60% increase from 2010) of new roads will have been constructed worldwide, 90% of which is anticipated to be constructed in the developing nations[8]. The World Bank study estimates that in 2018, around 17% of global greenhouse gas emissions came from the transport sector. Over the past 50 years, transport emissions have grown faster than nearly any other sector. If no measures are taken, these emissions are expected to rise by 60% by 2050 [9].

Nepal is among the most vulnerable nations to climate change and is at significant risk, due to its delicate topography, peoples' climate sensitive and subsistence lifestyles, and their limited potential for adaptation [10]. Despite its insignificant emissions, Nepal is committed to accelerating climate action while upholding the common but distinct obligations and unique capacities set forth in the Paris Agreement. Nepal's Nationally Determined Contribution (NDC) 3.0, submitted to the UNFCCC Secretariat in 2025, aims to reduce net GHG emissions by 8,866.53 Gg CO_2e (17.12%) by 2030 and 16,627.80 Gg CO_2 (26.79%) by 2035 through the implementation of quantified mitigation targets. Of the total expected reductions, the energy sector is projected to contribute around 53%, with the transport subsector accounting for 16% of the reduction by 2030 [11]. Nepal is committed to its long-term climate goals, based on recent reports from the Intergovernmental Panel on Climate Change (IPCC) and other scientific evidences. Nepal is strategically addressing climate change, aiming to achieve minimal or zero emissions and attain sustainable net-zero emissions by 2045 [10]. In Nepal, energy sector has a major share in the GHG emission among all other sectors (about 65% of the total emission of the year 2022 including removals from the land use sector). Of 25.014 Gg CO_2 equivalent GHG emissions from the energy sector, 19.04% is contributed by transport sub-sector [12]. Thus, to check the adverse environmental impacts and to help the country achieve net zero emission goals, transportation sector which contributes significantly to Nepal's GHGs emission, should be given due consideration. Reducing the environmental impact of the road sector has become international as well as national concern.

The construction sector is recognized as one of the leading contributors to environmental pollution. Traditional construction practices and management struggle to address emerging challenges including carbon emissions. These challenges underscore the necessity for professionals to reevaluate and enhance construction processes and technologies. This highlights the significant potential of the construction sector in advancing sustainable development, addressing economic, social, and environmental concerns. Embracing sustainable construction practices offers the opportunity to reduce overall energy consumption, maximize the utilization of renewable energy sources, minimize waste generation, conserve water resources, reduce vulnerability to flooding, decrease harmful emissions into water,

air, and soil, and mitigate noise and light pollution[13]. While there has been considerable focus on new construction materials and technologies, there has been relatively little attention given to the examination of the construction phase itself. This phase warrants closer examination to determine if improved construction process management can indeed result in reduced GHG emissions from projects. Upon close monitoring of several highway construction projects, it becomes evident that inadequate management practices during the construction phase are causing a notable increase in GHG emissions associated with these projects [14].The essential goal for achieving sustainable infrastructure project construction lies in finding a crucial balance between economic considerations and the potential for emissions reduction [15].

2. Literature Review

2.1. **Global Warming Potential.** Greenhouse gas emissions are quantified using the unit of carbon dioxide equivalents (CO_2e) [16]. A key impact category to consider in these analyses is the Global Warming Potential (GWP). The GWP outlined by the IPCC in the 2014 Climate Change Comprehensive Report was used to determine the ratio of various greenhouse gases to equivalent carbon dioxide. According to this report, the GWP of CO_2 is 1, CH_4 (methane) is 25, and N_2O (nitrous oxide) is 298 [17].

2.2. **Carbon Emission Factors.** As defined by Environmental Protection Agency (EPA) AP-42 (Compilation of Air Pollutant Emission Factors), an emission factor represents a value that correlates the quantity of a pollutant released into the atmosphere with the activity that generates it [18]. Emission factors translate activity data, such as material usage, production volumes, or energy consumption, into corresponding emission estimates. The list of carbon emission factor as obtained from various literature are shown in Table 1.

Table 1. CO2 Emission Factors for Different Construction Materials and Fuel

Component	Value	Unit	Source
Sand	0.0025	$kgCO_2/kg$	[19]
Aggregate	0.0028	$kgCO_2e/kg$	[19]
Bitumen	0.426	$kgCO_2e/kg$	[19]
Cement	0.8207	$kgCO_2e/kg$	[19]
Fuel (Diesel)	2.71	$kgCO_2e/liter$	[20]

2.3. **LCA in Evaluating Environmental Impact.** Given the importance of carbon footprint due to global warming, it's crucial to understand that a lower carbon footprint doesn't necessarily mean better environmental performance. Therefore, it's recommended to conduct carbon footprint studies alongside broader tools like LCA (Life Cycle Assessment) for a more comprehensive evaluation [21]. LCA and CF may appear similar, but the key difference is that CF evaluates using a single indicator, whereas LCA considers multiple indicators to assess environmental impacts [22]. LCA is gaining popularity as a tool to analyze the environmental effects of construction activities and identify strategies for impact reduction [23].

LCA in the field of transportation offers a thorough method for assessing the full environmental impact of a specific product (like a ton of aggregate) or more intricate systems (such as a transportation facility). It evaluates key environmental inputs and outputs

throughout the product's life cycle, from the production of raw materials to its eventual disposal [24]. The life cycle of the product begins with the acquisition of raw materials, progresses through various distinct phases (such as material processing, production, and usage), and ends at the end-of-life (EOL) stage.

2.4. **Relevant Studies.** Several studies have focused on methods for calculating carbon emissions in road construction and have explored various measures to mitigate these emissions. The GHGs emissions related to transportation infrastructure are calculated widely using the LCA method [25]. Horvath et al. [26] studied the environmental consequences of asphalt and steel-reinforced pavements in United States. LCA conducted in this study suggested that asphalt pavements can be a more environmentally sustainable option when they are effectively recycled. White et al. [19] examined various pavement types' carbon emissions throughout road material production and construction; and developed a carbon emission calculation model that took into account calculation parameters such as road width, material properties, road thickness, and service life. Santos et al. [27] used LCA model to investigate the effects of in-place recycling procedures on the construction and repair of pavement. And found a 75% reduction in environmental impacts during raw material extraction and mixture production was achieved by opting for recycling-based maintenance and rehabilitation (M&R) activities instead of traditional reconstruction methods. Barandica et al. [28] evaluated the GHG emissions of Spanish road constructions throughout the entire life cycle. Their results showed emissions range from 8,880 to 50,300 t CO_2e/km, mainly from construction activities, with the maintenance stage playing a minor role. Earthworks dominate emission in construction stage (60–85%), driven primarily by off-road machinery (61.5–84.9%), followed by material-related emissions (9.5–32.9%). Kim et al. [29] calculated the GHG emissions from the production of the materials used in road construction. Wang et al. [30] described that the majority of CO_2 emissions from highway construction comes from the production of raw materials. Results indicated that, mixture mixing phase generates the highest GHG emissions, contributing approximately 54% of the total, while the production of raw material is the second highest. In asphalt course construction, 95.04% of emissions came from mixture mixing, and 2.38% from raw material and mixture transportation, excluding raw material manufacturing. Peng et al. [31] calculated the GHG emissions from asphalt roadways, using LCA method. The results showed that road length, type, material use, and technology are key factors in high GHG emissions. Asphalt roads emit 39–63% less GHG than cement roads. Ma et al. [32] studied the construction of asphalt-paved highways into three layers asphalt course, cement stabilized aggregate base and cement stabilized gravel sub base based on the life cycle inventory method. The results indicate that the mixture mixing phase generates the highest greenhouse gas emissions, accounting for approximately 54% of the total, followed by the raw material production phase as the second largest contributor.

Noland and Hanson (2015) carried out an in-depth life-cycle assessment of greenhouse gas emissions for highway re-construction project in New Jersey. Their study took into account the emissions from material extraction, construction, and maintenance phases [33]. A study by Gulotta et al. [34] in Italy, which analyzed the life cycle of various pavement technologies for urban roads, found that material production is responsible for more than 60% of the total carbon emissions. This analysis considered all stages; extraction of material, construction, maintenance, and end-of-life. Huang et al. [35] developed a life cycle assessment tool specifically for evaluating the construction and maintenance of asphalt pavements in UK. Their study utilized this tool to assess the environmental consequences

of asphalt pavement construction. A study considering the key impact categories – human health, ecosystem quality, and resource consumption – found that the total impact value for rigid pavement is 78.90 kPt, which is 45% of the 175.50 kPt impact for flexible pavement. This indicated that rigid pavement is more sustainable in long term [36].

A study in [37] found that bitumen contributed between 38% and 39% of the total GHG emissions, taking into account the stages of raw material extraction and the construction and the operation of the Hot Mix Asphalt (HMA) plant was the largest contributor to GHG emissions; also, the study found that the energy used to operate the plant was insignificant, primarily due to the use of renewable energy. A study in [38] found that asphalt production at the plant is the most energy-intensive process. A study conducted in expressway construction in China found that the aggregate and asphalt heating are the main sources of energy consumption and can be lowered by utilizing natural gas [4]. A case study in China by [15] examined seven stages of road construction, finding that subgrade construction contributed the most emissions than pavement construction.

As discussed in [39], the carbon emission from asphalt pavement on a second-class road considering the material usage, construction, maintenance, and renovation phases was found to be 1,754 tons per kilometer. As discussed in [40], four different pavement structures were responsible for 121.86, 116.66, 104.54, and 100.59 tons of CO_2e emission from 1 km of road, during the stages of extraction, production, transportation, and construction. The different pavement structures constituted: aggregates, bitumen, and cement; aggregates, bitumen, and polymer-modified asphalt; aggregates and bitumen; and aggregates with recycled asphalt, respectively. Similarly, a study in [32] assessed and calculated emissions, considering various phases such as raw material production, mixing, transportation, laying, compacting, and curing. The total CO_2e emissions for the 20 km asphalt pavement construction was found to be 52,264,916.06 kg.

A study [41] found that the construction management plan is the most critical criterion for achieving green highway development, followed by quality management. According to [42], emission reduction technologies for materials include using recycled materials like rubber asphalt and reclaimed asphalt pavement, and replacing traditional materials with alternatives like bio-bitumen. For the construction phase, emissions can be reduced by adopting warm, half-warm, or cold asphalt manufacturing techniques, substituting energy sources such as using natural gas as fuel for asphalt plants, and using biodiesel or hybrid and electric-powered construction equipment. Recycling technologies like hot-in-place and cold-in-place recycling also contribute to emission reduction. As discussed in [43] use of Reclaimed Asphalt Pavement (RAP) and recycled concrete as alternative materials are acceptable in various pavement systems and applications. Incorporating RAP in asphalt base and sub-base layer construction can significantly lower environmental impacts, including a 20% reduction in global warming potential and 16% in energy use [44]. Also, a study [45] found that asphalt mixed with 18% crumb rubber using wet technology showed a carbon emission reduction of 36% to 44% compared to standard asphalt mixtures. Another study [46] demonstrated that incorporating RAP with HMA could lower CO_2 emissions by 6.8%. As discussed in [47] the Hot Mix Asphalt (HMA) requires high production temperatures (155–165°C), leading to increased greenhouse gas emissions, which contribute to global warming and harm workers' respiratory health. Warm Mix Asphalt (WMA) technology lowers the mixing and compaction temperature by about 30°C compared to HMA, offering benefits such as fuel savings. Another study [48] showed that WMA can reduce GHG

emissions by 20% compared to HMA. Also, study [49] found that using biomass-based fuel for construction equipment can reduce carbon emissions by 36% to 90%, while electrified construction equipment can achieve a 67% to 95% reduction in GHG emissions.

3. Methodology

3.1. **Study Area.** The Pokhara-Mugling Road, chosen for this study, is a section of the Prithvi Highway, classified as National Highway H04 according to Department of Roads (DoR)(see FIGURE 1). The road plays a crucial role in enhancing tourism in the western regions of Nepal. This route starts at the right bank of the Trishuli River, near the new bridge site in Mugling, Tanahun District, and extends approximately 88.810 kilometers to Sahid Chowk in Pokhara Bazar, Kaski District. However, for this study two sections of road were considered from Ch. 8+250 to Ch. 49+700 (section-01) and from Ch. 49+700 to Ch. 88+583 (section-02), totaling 80.333 km. The geometric design standard for this road generally has been followed as for the Class II Road under Nepal Road Standard (NRS) 2070. This road is being designed for a speed of 60 kilometers per hour (kmph) based on the terrain. Road is a four-lane highway. The pavement material is asphalt concrete.

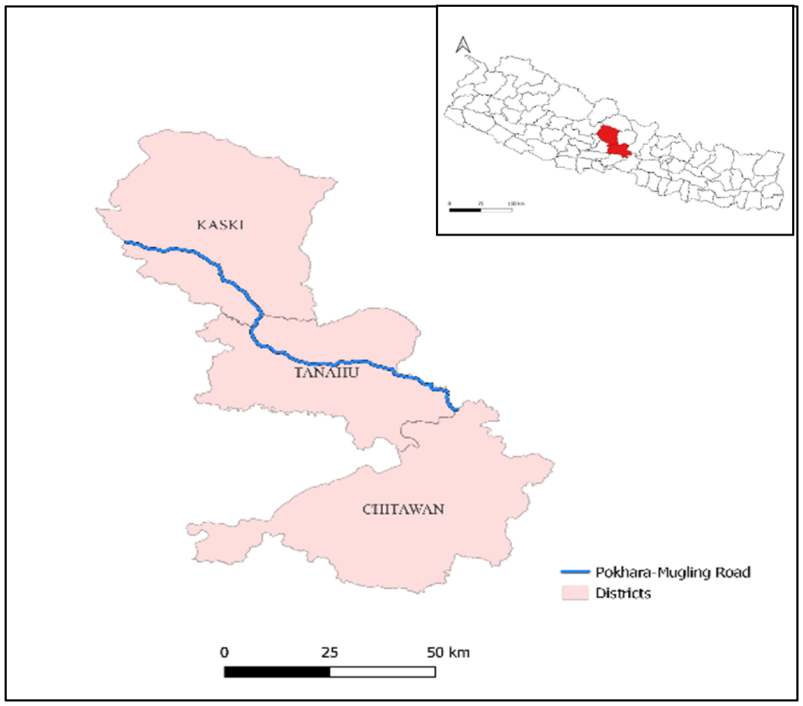

FIGURE 1. Pokhara-Mugling Road.

3.2. **Data Analysis.** LCA method was employed to analyze and quantify GHG emissions associated with the road construction project. LCA provides a detailed framework for assessing the environmental impacts of the project by considering relevant stages from material extraction to construction. The analysis focuses on the gate-to-gate system boundary, which encompasses emissions related to material use and construction activities. Emissions from the material extraction and transportation from the extraction to

the construction sites are not considered for this study. LCA includes the following stages:

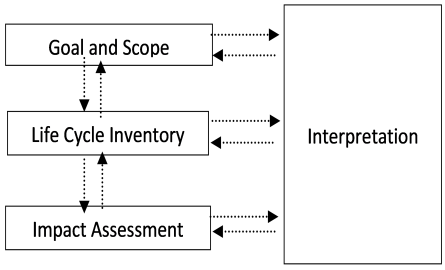

FIGURE 2. Life cycle assessment frame work [50]

3.2.1. *Goal and Scope Definition.* In the case study, GHG emissions were regarded as the primary environmental indicator. Therefore, the scope of the study has been designed to incorporate GHG emissions as the environmental indicator. For this stage of the Pokhara-Mugling road project, the LCA method will focus exclusively on the construction phase. To align with the objective of evaluating the environmental impacts of highway construction, the study considers GHG emissions within a gate-to-gate system boundary. Within this system boundary, the case study takes into account GHG emissions related to materials and construction machinery. The gate-to-gate LCA approach focuses specifically on the construction stage, capturing emissions generated from the production, as well as the energy consumed by construction equipment. In this study, lane-kilometer was chosen as the functional unit, and the total greenhouse gas emissions were quantified in tons of CO2e per lane-kilometer.

3.2.2. *Life Cycle Inventory Analysis.* The Life Cycle Inventory (LCI) stage of an LCA for the Pokhara-Mugling road involves a comprehensive identification and quantification of all environmentally relevant inputs and outputs throughout the construction process using mass and energy balance approaches. This phase includes a detailed collection of data on material inputs (such as aggregates, bitumen, and fillers), energy use (including fuel consumption for machinery and electricity for operations), and outputs like air emissions. The inventory captures data specifically during the construction stage of the road's life cycle that is it includes on-site activities.

3.2.3. *Impact Assessment.* In LCA study of carbon emissions for the Pokhara-Mugling road construction, the impact assessment is limited to environmental aspects. The evaluation specifically targets the GWP, which measures the road's contribution to climate change by assessing the greenhouse gas emissions associated with various construction stages and materials used.

3.3. **Calculation Formula.** The standard method for estimating GHG emissions used in this inventory involves applying the formula provided by the IPCC in its 2006 guidelines [51]:

$$\text{Emission} = \sum_{i=1}^{n} (Ac \times EF)_i, \tag{1}$$

Where,
EF = emission factor

Ac denotes the activity i, with i indicating various activity types (1, 2, 3, . . . , n).
EF represents the amount of GHG emissions generated per unit of activity.
Ac represents the activity level measured in units that match the emission factor. Activity data indicates the extent of human activity that leads to emissions or removals over a specific period.

3.4. **Relative Importance Index.** This approach facilitates the identification of the most suitable options for minimizing greenhouse gas emissions in road construction by systematically assessing the relative significance of each alternative. The Relative Importance Index (RII) was employed to evaluate and prioritize various methods, techniques, and alternatives that can effectively reduce emissions in road construction. For the RII analysis, a questionnaire was sent to experts selected based on their experience in road construction, construction management, and environmental sustainability. The respondents included environmental specialists, highway engineers and consultants, with some directly involved in the Pokhara–Mugling road project. Responses were received from 15 respondents and used for RII analysis. The formula for calculating RII is outlined by [52, 53] as follows:

$$\mathrm{RII} = \frac{\sum W}{A \times N} = \frac{5N_5 + 4N_4 + 3N_3 + 2N_2 + 1N_1}{5N}, \tag{2}$$

Where,
W represents the weight assigned to each variable by respondents, on a scale ranging from 1 to 5.
N_1, N_2, N_3, N_4, and N_5 represent the number of respondents for strongly disagree, disagree, neutral, agree, and strongly agree, respectively.
A is the maximum weight assigned, which is 5.
N represents the total number of respondents.

4. Results and Discussion

4.1. Carbon Emission During the Construction of Road.

4.1.1. *Material Specific Emission.* Among primary materials used in asphalt road construction, aggregate was the most extensively used, with a total consumption of 3,115.88 kilotons, followed by bitumen, which amounted to 27.61 kilotons. Filler materials were utilized in the smallest quantity, totaling only 5.39 kilotons. The analysis demonstrated that aggregate constituted approximately 99% of the total weight of the materials used in pavement construction. However, despite its dominant presence by weight, aggregate was responsible for only 42.50% of the total greenhouse gas (GHG) emissions associated with these materials. In contrast, bitumen, which represented just 1% of the total weight, accounted for a substantial 57.40% of the total GHG emissions, as presented in Table 2. This disparity highlighted the significant environmental impact of bitumen relative to its weight in the asphalt mix. It is crucial to note that this study does not include considerations for the use phase, maintenance phase, or end-of-life stage of the pavement.

4.1.2. *Emission from Use of Plants and Equipment.* **The figure** shows the fuel consumption for hot mix asphalt plants and other equipment as well as total fuel consumption by plants and equipment for Pokhara - Mugling road construction. Hot mix asphalt plants consumed the largest portion of the total fuel usage (hot mix asphalt plant consumed a

TABLE 2. GHG emission from the materials based on their consumption for pavement construction.

S.N.	Materials	GHG Emission ($ktCO_2e$)	Percentage Contribution
1	Aggregate	8.724	42.50%
2	Bitumen	11.76	57.40%
3	Filler	0.015	0.10%
	Total	**20.499**	

TABLE 3. GHG emission from plants and equipment used in pavement construction.

S.N.	Plants and Equipment	Total GHG Emission ($ktCO_2e$)	Percentage
1	Hot mix asphalt	9.28	70%
2	Other equipment	3.95	30%
	Total	**13.23**	

total of 3425.42 kilolitres of fuel). This significant consumption highlighted the energy-intensive nature of asphalt production, where fuel was required for heating and mixing materials. In comparison, all other construction equipment collectively consumed 1,457.15 kilolitres of fuel. Among these, rollers (vibratory, pneumatic, and smooth-wheeled) were the dominant consumers at 552.27 kl, followed by motor graders (281.75 kl), loaders (174.21 kl), and paver finishers (132 kl). Other machinery, including generators, tractors with rippers, bitumen distributors, air compressors, boilers, mechanical broomers, and tippers, contributed comparatively smaller amounts. Notably, the hot mix asphalt plant was responsible for 70% of the total emissions from plant and equipment operation. In contrast, all other equipment involved in asphalt pavement construction collectively contributed for the remaining 30% of the emissions (Table 3). These findings highlighted the substantial impact of the hot mix asphalt plant on the overall carbon footprint of the construction process.

4.1.3. *Total Carbon Emission.* The emissions from material usage were found higher than those generated by the operation of plants and equipment during construction. The total emission from the pavement construction was found to be 33.73 kilotons of CO_2 equivalent ($ktCO_2e$) as shown in Figure III. A substantial portion of these emissions, 20.50 $ktCO_2e$ (accounting 60.78% of total emission), originated from the materials used, underscoring their considerable impact on the overall carbon footprint. In contrast, the emissions resulting from the use of plants and equipment were found to be 13.23 $ktCO_2e$; accounting for about 39.22% of the total emission during pavement construction. The results show that the material consumption contributes significant GHG emission in total for pavement construction compared to the emissions from the use of plants and equipment.

The gate-to-gate analysis for the Pokhara-Mugling road construction revealed that the total emissions amounted to 419.9 tonnes of CO_2e per kilometer of road. This assessment considers the emissions generated from the material use and operation of plants and equipment during the pavement construction but excludes any emissions from the use phase, maintenance activities, and the road's end-of-life stage. The per km emission from Pokhara-Mugling road compared to the study conducted by Araújo et al. [40] is relatively higher even without considering the material extraction, production and transportation

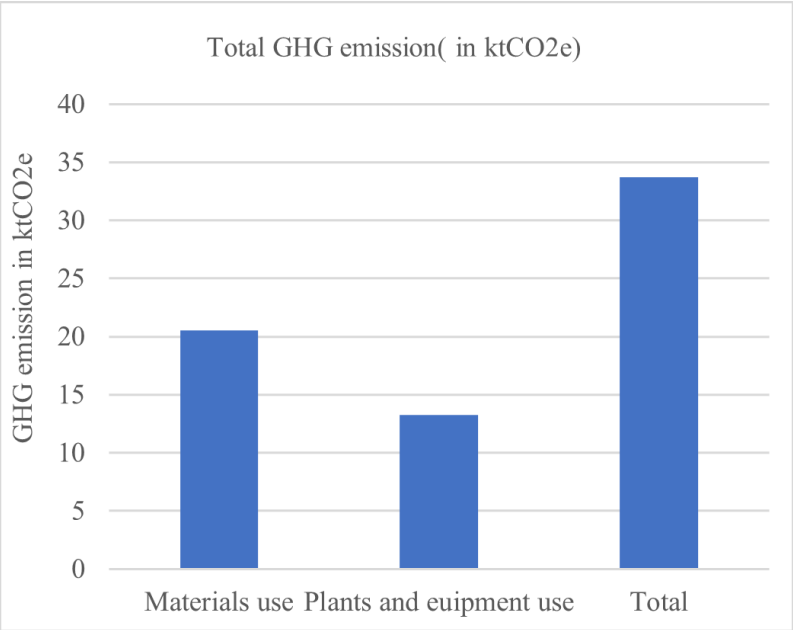

FIGURE 3. Total GHG emission from pavement construction of Pokhara Mugling Road.

TABLE 4. Carbon emission in different phases of asphalt surface construction

Phase	**Mixing Phase**	**Laying Down Phase**	**Compacting Phase**
CO_2e Emissions (kg)	22,668,564.44	588,189.39	641,448.20

stages.

4.2. **Emission from the Different Stages of Pavement Construction.** The total greenhouse gas emissions, measured across different stages of road construction, showed that the emissions from subgrade preparation amounted to 2.84 KtCO_2e, making it the stage with the lowest emissions. The sub-base and base stage followed with emissions of 6.99 KtCO_2e. However, the binder and wearing course stages contributed the highest emissions at 23.90 KtCO_2e. This indicates that binder and wearing courses, particularly due to the use of HMA plants and bitumen, have the most significant impact on the overall carbon footprint of road construction. In the construction of asphalt binder and wearing course, however, the largest CO_2e emission was found during the mixing phase, followed by the compacting phase and least during the laying phase, as shown in Table 4. This high emission level during the mixing phase is largely attributed to the energy-intensive processes involved in heating and mixing the materials (aggregates and binder). The machinery and fuel consumption needed for this stage are considerable, leading to its large environmental impact. The compacting phase comes second in terms of emissions, while the laying down phase has the least environmental impact.

4.3. **Sensitivity Analysis.** Sensitivity analysis was conducted to assess how variations in bitumen and aggregate content affect total GHG emissions. The findings of this study indicate that a 10% reduction in bitumen percentage results in a 3.49% decrease in total

TABLE 5. Probable mitigating measures with RII value and their rank

Probable Mitigating Measures	**RII**	**Rank**
Optimizing construction and quality management plans is essential for reducing GHG emissions in road construction.	0.853	1
Using electricity as a fuel source for heating in asphalt production could substantially lower emissions compared to traditional fossil fuels.	0.813	2
Adopting warm mix or cold asphalt mix technologies in current road construction practices is practical and beneficial for reducing emissions.	0.747	3
The use of recycled materials like Reclaimed Asphalt Pavement (RAP) and crumb rubber in asphalt mixtures is feasible in Nepal's road construction projects.	0.747	3
Transitioning to low-emission equipment such as electric or biodiesel-powered machinery is achievable in large-scale projects like the Pokhara-Mugling road.	0.733	5
Using alternative energy sources, such as natural gas or biomass-based fuels, for asphalt plants could significantly reduce carbon emissions.	0.720	6

GHG emissions (33.73 $ktCO_2e$). Conversely, increasing the bitumen percentage by 10% and 20% leads to increases in total GHG emissions of 3.49% and 6.97%, respectively. Similarly, changes in the aggregate percentage were examined for their impact on GHG emissions. A 10% decrease in aggregate percentage corresponds to a 2.59% reduction in total GHG emissions. On the other hand, increasing the aggregate percentage by 10% and 20% results in increase in GHG emissions by 2.59% and 5.17%, respectively. Overall, the sensitivity analysis clearly demonstrates that variations in bitumen content have a significantly larger impact on total GHG emissions compared to changes in aggregate content, with bitumen adjustments causing nearly 1.35 times the percentage change in emissions. This finding highlights the critical role of bitumen in influencing the carbon footprint of road construction.

4.4. **Probable Mitigating Measures.** The RII analysis identified and ranked the most effective measures for reducing GHG emissions in the Pokhara-Mugling road project. Optimizing construction and quality management plans ranked highest, followed by using electricity for asphalt heating as a cleaner alternative to fossil fuels. Adopting warm or cold asphalt mix technologies and incorporating recycled materials such as RAP and crumb rubber were equally ranked in third place. Transitioning to low-emission equipment was placed fifth, while alternative energy sources like natural gas and biomass for asphalt plants ranked sixth. These results highlight that improving construction management, shifting to cleaner energy, and promoting material reuse are key strategies for minimizing emissions in road construction projects in Nepal.

5. Conclusion and Recommendations

5.1. **Conclusion.** The study reveals that materials contribute significantly more to GHG emissions compared to the plants and equipment used in the pavement construction process. Among the materials, bitumen emerges as the primary source of emissions compared to aggregate and filler materials. The analysis revealed that the total carbon emissions per lane km from the Pokhara-Mugling Road construction are higher compared to similar studies conducted in other countries where electricity was used as source of energy to heat asphalt or alternative pavement structures such as aggregates and recycled asphalt was used. The sensitivity analysis results emphasized the significant impact of bitumen on the carbon footprint of road construction, underscoring the importance of implementing targeted reduction strategies specifically aimed at minimizing bitumen usage. To address this, exploring alternative materials such as aggregate with recycled asphalt could be an effective strategy for lowering overall emissions. Additionally, the analysis indicates that the hot mix asphalt plant is the largest contributor to GHG emissions among all the equipment and plants involved in the construction process, as they consume more fuel. And the RII analysis indicated that the most effective measures are optimizing construction and quality management plans and using electricity for asphalt heating as a cleaner alternative to fossil fuels.

5.2. **Recommendations.** To mitigate the emissions from road construction, this study recommends exploring alternative energy sources, such as renewable energy, natural gases for the operation of hot mix plants or adopting WMA technology. Transitioning to low-emission construction equipment, such as biodiesel or electric-powered machines, might also contribute to emission reductions. Moreover, this study also finds effective construction and quality management plans as essential measures for minimizing environmental impacts. Implementing these approaches can be key to reducing the overall greenhouse gas emissions from road construction and promoting sustainable road infrastructure development in Nepal.
Future research should extend beyond construction phase to include the full life cycle of highways, encompassing maintenance, operation, and end-of-life phases. Likewise, the alternative construction such as rigid pavement should be explored in terms of their environmental impact in the future.

References

[1] N. Martinov-Bennie, "Greenhouse gas emissions reporting and assurance: Reflections on the current state," *Sustainability Accounting, Management and Policy Journal*, vol. 3, no. 2, pp. 244–251, 2012, doi: 10.1108/20408021211282340.

[2] L. E. Erickson, "Reducing greenhouse gas emissions and improving air quality: Two global challenges," John Wiley and Sons Inc., Jul. 1, 2017, doi: 10.1002/ep.12665.

[3] D. C. Quiros, J. Smith, A. Thiruvengadam, T. Huai, and S. Hu, "Greenhouse gas emissions from heavy-duty natural gas, hybrid, and conventional diesel on-road trucks during freight transport," *Atmos. Environ.*, vol. 168, pp. 36–45, 2017, doi: 10.1016/j.atmosenv.2017.08.066.

[4] B. Peng, X. Tong, S. Cao, W. Li, and G. Xu, "Carbon emission calculation method and low-carbon technology for use in expressway construction," *Sustainability*, vol. 12, no. 8, Apr. 2020, doi: 10.3390/SU12083219.

[5] E. M. Abdelkader, "Optimizing Construction Emissions for Sustainable Construction Projects." [Online]. Available: https://www.researchgate.net/publication/353259817

[6] G. Fernández-Sánchez and F. Rodríguez-López, "A methodology to identify sustainability indicators in construction project management - Application to infrastructure projects in Spain," *Ecol. Indic.*, vol. 10, no. 6, pp. 1193–1201, Nov. 2010, doi: 10.1016/j.ecolind.2010.04.009.

[7] N. J. Santero and A. Horvath, "Global warming potential of pavements," *Environmental Research Letters*, vol. 4, no. 3, 2009, doi: 10.1088/1748-9326/4/3/034011.
[8] W. F. Laurance *et al.*, "Corrigendum: A global strategy for road building," Nature Publishing Group, Oct. 9, 2014, doi: 10.1038/nature13876.
[9] "Financing Low Carbon Transport Solutions in Developing Countries," 2021.
[10] "Nepal's Long-term Strategy for Net-zero Emissions," Government of Nepal, Kathmandu, 2021.
[11] "Nationally Determined Contribution (NDC) 3.0," Government of Nepal, Kathmandu, 2025.
[12] "Nepal First Biennial Transparency Report," Ministry of Forests and Environment, Government of Nepal, 2025.
[13] J. M. Hussin, I. A. Rahman, and A. H. Memon, "The Way Forward in Sustainable Construction: Issues and Challenges," *International Journal of Advances in Applied Sciences*, vol. 2, no. 1, Mar. 2013, doi: 10.11591/ijaas.v2i1.1321.
[14] P. Tang, "Investigating the effect of construction management strategies on project greenhouse gas emissions using interactive simulation," Michigan Technological University, Houghton, MI, 2012, doi: 10.37099/mtu.dc.etds/510.
[15] W. Luo, M. Sandanayake, G. Zhang, and Y. Tan, "Construction cost and carbon emission assessment of a highway construction—a case towards sustainable transportation," *Sustainability*, vol. 13, no. 14, Jul. 2021, doi: 10.3390/su13147854.
[16] F. Ma, A. Sha, P. Yang, and Y. Huang, "The greenhouse gas emission from Portland cement concrete pavement construction in China," *Int. J. Environ. Res. Public Health*, vol. 13, no. 7, Jul. 2016, doi: 10.3390/ijerph13070632.
[17] Intergovernmental Panel on Climate Change, *Climate Change 2014: Synthesis Report. Longer Report.* 2015.
[18] "AP 42 EPA."
[19] P. White, J. S. Golden, K. P. Biligiri, and K. Kaloush, "Modeling climate change impacts of pavement production and construction," *Resour. Conserv. Recycl.*, vol. 54, no. 11, pp. 776–782, Sep. 2010, doi: 10.1016/j.resconrec.2009.12.007.
[20] Ministry for the Environment, *Measuring Emissions: A Guide for Organisations. 2020 Summary of Emission Factors* [R/OL], Wellington: New Zealand Government, 2020, p. 27.
[21] M. Ormazabal, C. Jaca, and R. Puga-Leal, "Analysis and comparison of life cycle assessment and carbon footprint software," in *Advances in Intelligent Systems and Computing*, Springer, 2014, pp. 1521–1530, doi: 10.1007/978-3-642-55122-2_131.
[22] B. P. Weidema, M. Thrane, P. Christensen, J. Schmidt, and S. Løkke, "Carbon footprint: A catalyst for life cycle assessment?," Feb. 2008, doi: 10.1111/j.1530-9290.2008.00005.x.
[23] T. D. Nguyen and P. Pishdad-Bozorgi, "A Review of Life Cycle Assessment Tools for Measuring the Environmental Impact of Building and a Decision Support Framework for Choosing Among Them."
[24] FHWA, "Pavement Life Cycle Assessment Framework."
[25] D. Cass and A. Mukherjee, "Calculation of greenhouse gas emissions associated with highway construction projects using an integrated life cycle assessment approach," in *Construction Research Congress 2010: Innovation for Reshaping Construction Practice*, 2010, pp. 1406–1415, doi: 10.1061/41109(373)141.
[26] A. Horvath and C. Hendrickson, "Comparison of environmental implications of asphalt and steel-reinforced concrete pavements," *Transp. Res. Rec.*, no. 1626, pp. 105–113, 1998, doi: 10.3141/1626-13.
[27] J. Santos, A. Ferreira, and G. Flintsch, "A life cycle assessment model for pavement management: Methodology and computational framework," *Int. J. Pavement Eng.*, vol. 16, no. 3, pp. 268–286, Mar. 2015, doi: 10.1080/10298436.2014.942861.
[28] J. M. Barandica, G. Fernández-Sánchez, Á. Berzosa, J. A. Delgado, and F. J. Acosta, "Applying life cycle thinking to reduce greenhouse gas emissions from road projects," *J. Clean. Prod.*, vol. 57, pp. 79–91, Oct. 2013, doi: 10.1016/j.jclepro.2013.05.036.
[29] B. Kim, H. Lee, H. Park, and H. Kim, "Framework for Estimating Greenhouse Gas Emissions Due to Asphalt Pavement Construction," 2012, doi: 10.1061/(ASCE)CO.1943-7862.
[30] X. Wang, Z. Duan, L. Wu, and D. Yang, "Estimation of carbon dioxide emission in highway construction: A case study in southwest region of China," *J. Clean. Prod.*, vol. 103, pp. 705–714, 2015, doi: 10.1016/j.jclepro.2014.10.030.
[31] B. Peng, C. Cai, G. Yin, W. Li, and Y. Zhan, "Evaluation system for CO2 emission of hot asphalt mixture," *Journal of Traffic and Transportation Engineering (English Edition)*, vol. 2, no. 2, pp. 116–124, Apr. 2015, doi: 10.1016/j.jtte.2015.02.005.

[32] F. Ma, A. Sha, R. Lin, Y. Huang, and C. Wang, "Greenhouse gas emissions from asphalt pavement construction: A case study in China," *Int. J. Environ. Res. Public Health*, vol. 13, no. 3, Mar. 2016, doi: 10.3390/ijerph13030351.

[33] R. B. Noland and C. S. Hanson, "Life-cycle greenhouse gas emissions associated with a highway reconstruction: A New Jersey case study," *J. Clean. Prod.*, vol. 107, pp. 731–740, Nov. 2015, doi: 10.1016/j.jclepro.2015.05.064.

[34] T. M. Gulotta, M. Mistretta, and F. G. Praticò, "A life cycle scenario analysis of different pavement technologies for urban roads," *Science of the Total Environment*, vol. 673, pp. 585–593, Jul. 2019, doi: 10.1016/j.scitotenv.2019.04.046.

[35] Y. Huang, R. Bird, and O. Heidrich, "Development of a life cycle assessment tool for construction and maintenance of asphalt pavements," *J. Clean. Prod.*, vol. 17, no. 2, pp. 283–296, Jan. 2009, doi: 10.1016/j.jclepro.2008.06.005.

[36] J. U. D. Hatmoko and L. Lendra, "How sustainable are flexible and rigid pavement? A Life Cycle Impact Assessment (LCIA) approach," *IOP Conf. Ser. Mater. Sci. Eng.*, vol. 1072, no. 1, p. 012071, Feb. 2021, doi: 10.1088/1757-899x/1072/1/012071.

[37] M. Espinoza *et al.*, "Carbon footprint estimation in road construction: La Abundancia-Florencia case study," *Sustainability*, vol. 11, no. 8, Apr. 2019, doi: 10.3390/su11082276.

[38] L. Thesis and A. A. Butt, *Life Cycle Assessment of Asphalt Pavements including the Feedstock Energy and Asphalt Additives*, 2012.

[39] R. Mao *et al.*, "Quantification of carbon footprint of urban roads via life cycle assessment: Case study of a megacity-Shenzhen, China," *J. Clean. Prod.*, vol. 166, pp. 40–48, Nov. 2017, doi: 10.1016/j.jclepro.2017.07.173.

[40] J. P. C. Araújo, J. R. M. Oliveira, and H. M. R. D. Silva, "The importance of the use phase on the LCA of environmentally friendly solutions for asphalt road pavements," *Transp. Res. D Transp. Environ.*, vol. 32, pp. 97–110, 2014, doi: 10.1016/j.trd.2014.07.006.

[41] R. R. R. M. Rooshdi, N. A. Rahman, N. Z. U. Baki, M. Z. A. Majid, and F. Ismail, "An Evaluation of Sustainable Design and Construction Criteria for Green Highway," *Procedia Environ. Sci.*, vol. 20, pp. 180–186, 2014, doi: 10.1016/j.proenv.2014.03.024.

[42] N. Liu *et al.*, "Road life-cycle carbon dioxide emissions and emission reduction technologies: A review," Chang'an University, Aug. 1, 2022, doi: 10.1016/j.jtte.2022.06.001.

[43] A. Jamshidi, "Use of recyclable materials in pavement construction for environmental sustainability," 2019. [Online]. Available: https://www.researchgate.net/publication/331465966

[44] J. C. Lee, T. B. Edil, J. M. Tinjum, and C. H. Benson, "Quantitative assessment of environmental and economic benefits of recycled materials in highway construction," *Transp. Res. Rec.*, no. 2158, pp. 138–142, Jan. 2010, doi: 10.3141/2158-17.

[45] A. Farina, M. C. Zanetti, E. Santagata, and G. A. Blengini, "Life cycle assessment applied to bituminous mixtures containing recycled materials: Crumb rubber and reclaimed asphalt pavement," *Resour. Conserv. Recycl.*, vol. 117, pp. 204–212, Feb. 2017, doi: 10.1016/j.resconrec.2016.10.015.

[46] M. I. Giani, G. Dotelli, N. Brandini, and L. Zampori, "Comparative life cycle assessment of asphalt pavements using reclaimed asphalt, warm mix technology and cold in-place recycling," *Resour. Conserv. Recycl.*, vol. 104, pp. 224–238, Nov. 2015, doi: 10.1016/j.resconrec.2015.08.006.

[47] A. Sharma, P. Kumar, and A. Walia, "Use of Recycled Material in WMA- Future of Greener Road Construction," in *Transportation Research Procedia*, Elsevier, 2020, pp. 3770–3778, doi: 10.1016/j.trpro.2020.08.042.

[48] A. M. Rodríguez-Alloza, A. Malik, M. Lenzen, and J. Gallego, "Hybrid input-output life cycle assessment of warm mix asphalt mixtures," *J. Clean. Prod.*, vol. 90, pp. 171–182, Mar. 2015, doi: 10.1016/j.jclepro.2014.11.035.

[49] I. Karlsson, J. Rootzén, and F. Johnsson, "Reaching net-zero carbon emissions in construction supply chains – Analysis of a Swedish road construction project," *Renew. Sustain. Energy Rev.*, vol. 120, Mar. 2020, doi: 10.1016/j.rser.2019.109651.

[50] "Environmental management—Life cycle assessment—Principles and framework," 2006.

[51] F. Wagner and M. P. Walsh, "Mobile combustion."

[52] D. W. M. Chan and M. M. Kumaraswamy, "A comparative study of causes of time overruns in Hong Kong construction projects," 1997.

[53] P. O. Olomolaiye, T. A. Wahab, and D. F. Price, "Problems Influencing Craftsmen's Productivity in Nigeria," 1987.

Everest Advances in Science and Technology (EAST), Vol. 1, No. 1, 2025
ISSN: 3102-0410(print), 3102-0429(online)

Decarbonizing Nepal's Cement Industry with Hydropower-Based Hydrogen

RISHAV KHANAL[1*]

Abstract. The cement industry is a significant global source of CO_2 emissions, with Nepal's clinker production contributing approximately 2.34 million metric tons annually through coal combustion. This study investigates the technical and economic feasibility of decarbonizing Nepal's cement sector by transitioning to green hydrogen fuel, leveraging the country's abundant hydropower resources. Through detailed energy balance calculations and techno-economic modeling, we demonstrate that complete coal replacement would require 227,743 metric tons of green hydrogen annually, necessitating 2,002 MW of dedicated hydropower capacity. Our projections indicate hydrogen production costs could decline to $2.15/kg by 2035, driven by electrolyzer efficiency improvements and Nepal's competitive industrial electricity tariffs. The analysis reveals this transition could eliminate up to 2.57 million metric tons of CO_2 emissions yearly, representing a 98% reduction in fuel combustion emissions. However, implementation challenges include seasonal hydropower variability, requiring 2,000 MW of reservoir projects, and substantial infrastructure investments estimated at $800 million. The study proposes a phased adoption pathway, with 30% hydrogen penetration by 2030 achieving 770,000 metric tons of annual emission reductions. We identify critical policy interventions including a $139/ton carbon price and targeted subsidies to bridge the current cost gap. A $139/ton carbon price and targeted subsidies are identified as key policy interventions to bridge the current cost gap.

Keywords: Cement clinker decarbonization, Green hydrogen, Industrial fuel switching, Nepal hydropower utilization, PEM electrolyzer economics.

[1]School of Engineering, Faculty of Science and Technology, Pokhara University, Pokhara, Nepal
E-mail: rishav.khanal@pu.edu.np
* Corresponding author
Manuscript received: 11 March, 2025; revised: 16 August 2025; accepted: 4 September, 2025.
Everest Advances in Science and Technology (EAST), Vol. 1, No. 1, 2025

1. Introduction

The global cement industry contributes around 5% to 10% of global carbon emissions, largely due to energy-intensive clinker production that relies heavily on fossil fuels like coal [1, 2, 3, 4]. Emissions range between 0.6 to 0.9 tons of CO_2 per ton of cement produced [5, 6]. Cement demand has surged due to rapid urban development, intensifying emissions. In Nepal, approximately 72 plants emit about 3.6 million metric tons (MT) of CO_2 annually [7].Global emissions from cement reached 1.57 gigatons (Gt) in 2019 [8], underlining the urgency for decarbonization. Nepal has substantial hydropower potential of around 42,000 MW [9] and generates most of its electricity from hydropower, with expansions underway [10]. This hydropower surplus can support green hydrogen production, which offers a carbon-free alternative to fossil fuels in cement manufacturing [7].

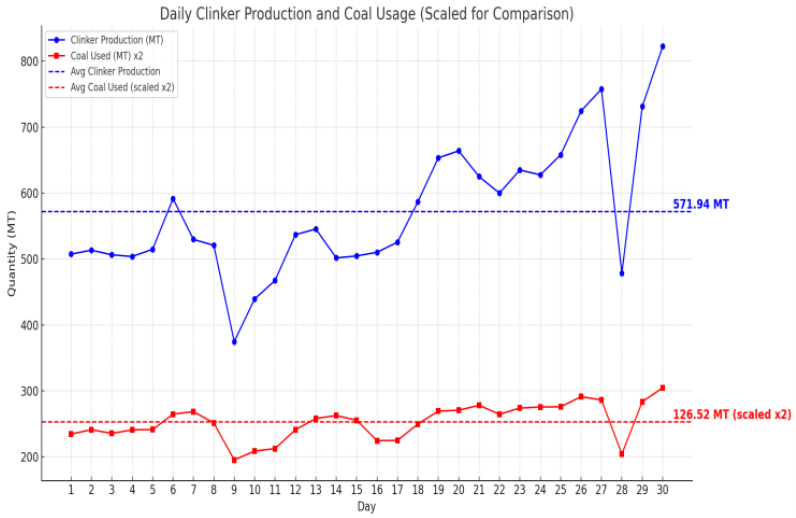

FIGURE 1. Illustration of the coal usage for clinker production in a Nepalese clinker factory.

From Figure 1, it is evident that 4.52 MT of clinker is produced from 1 MT of coal. With 5 million MT of clinker produced in Nepal in 2019/20 [11], this equates to 1.11 million MT of coal consumption, emitting 2.34 million MT of CO_2 from coal combustion alone [12]. These emissions are projected to increase with industry expansion. Green hydrogen could drastically reduce these emissions. Coal costs about \$121/MT in Nepal. Matching coal's energy content (7,000 kcal/kg) would require approximately 205.88 kg of hydrogen (LCV $\sim$ 34,000 kcal/kg) [13, 14]. At \$4–\$6/kg [15], equivalent hydrogen energy costs \$1,235/MT-10 times more than coal. However, hydrogen costs are expected to drop due to improved electrolyzers and renewables. Global carbon regulations and rising coal prices (3–5% annually) further diminish coal's cost advantage [16]. Hydrogen, with no direct greenhouse gas emissions, could replace fossil fuels in clinker kilns [17, 18, 19, 20]. Green hydrogen's viability depends on electrolyzer cost and efficiency [21, 22]. Technology advancements are lowering costs, and coupling these systems with Nepal's hydropower could make hydrogen competitive [23].

This study investigates the potential for replacing coal with green hydrogen in Nepal's cement industry. It evaluates energy and cost feasibility, hydropower capacity, and emissions impact through 2035. By integrating carbon pricing and investment planning [24], it offers a practical decarbonization roadmap for Nepal's cement sector.

2. Methodology

This study adopts a comprehensive analytical framework to evaluate the technical and economic feasibility of replacing coal with green hydrogen in Nepal's cement industry, with a specific focus on clinker production. The approach integrates mass and energy balance calculations, hydrogen substitution modeling, hydropower capacity assessment, and techno-economic analysis. A 2035 projection horizon is used to reflect evolving costs of electrolyzers and hydrogen production technologies. The system boundary considers Nepal's grid emissions, local hydropower dynamics, and industry-specific emission factors. Each stage of the methodology is designed to quantify the hydrogen requirements, assess renewable energy integration potential.

2.1. System Boundary and Baseline Establishment.

- Temporal Scope: 2024 (baseline) to 2035 (projection)
- Functional Unit: 1 metric ton (MT) of clinker produced.
- Key Assumptions:
  - Bituminous coal LHV: 7,000 kcal/kg (±2% variability)
  - Hydrogen LHV: 33.33 kWh/kg (34,000 kcal/kg)
  - Electrolyzer efficiency: 65% (PEM systems)
  - Grid emission factor: 0.012 kg CO_2/kWh (Nepalese grid)

PEM electrolyzers were considered due to their high current density and suitability for variable renewable inputs (reference).

2.2. Core Calculations With Enhanced Detail.

2.2.1. *Energy and Mass Balance Calculations.* Coal-to-Clinker Ratio is derived from plant operational data (Figure 1):

$$\text{Ratio} = \frac{\sum \text{Daily Clinker}}{\sum \text{Daily Coal}} \tag{1}$$

Annual Coal Consumption for 5 million MT clinker (2019/20) is:

$$\text{Coal} = \frac{\text{Clinker Production}}{\text{Clinker to Coal Ratio}} \tag{2}$$

CO_2 Emissions (EPA Tier 2) is:

$$CO_2 = \text{Coal Consumed (MT)} \times \text{Emission Factor} \quad (2.32 \text{ tons } CO_2/\text{ton coal}) \tag{3}$$

2.2.2. *Hydrogen Substitution Framework.* The energy equivalence is:

$$H_2 \text{ Required} = \frac{\text{Calorific Value of Coal (kcal/kg)}}{\text{Calorific Value of Hydrogen (kcal/kg)}} \tag{4}$$

Total Hydrogen Demand for 100% substitution is:

$$= \text{Coal Required} \times \text{Energy Equivalence} \tag{5}$$

2.2.3. *Renewable Energy Integration.* Hydropower Requirement (65% capacity factor):

$$\text{Energy Needed} = \frac{\text{Total Hydrogen needed (kg)} \times \text{Energy required to produce 1 kg of hydrogen (50 kWh/kg)}}{\text{Capacity factor of hydropower (0.65)} \times \text{Hours in a year (8760 hours)}} \quad (6)$$

$$= 2,002 \text{ MW}$$

Surplus Verification: Nepal's Hydropower Capacity vs. Green Hydrogen Requirements (2024) is shown in Table 1.

Table 1. Current Hydropower Status

Parameter	**Values**	**Notes**
Total Installed Hydropower	3,329.54 MW [25]	90.4% of Nepal's grid capacity
Peak Domestic Demand (2024)	2,316 MW [26]	10% annual growth
Monsoon Export (2023)	1.7B units [27]	≈ 1,940 MW continuous for 4 months
Dry Season Generation	≈ 1,085 MW	Drops to 1/3 of installed capacity [28]
Under Construction	7,000 MW [29]	Phased completion through 2030

Green Hydrogen Requirement

- Required Capacity: 2,000 MW (continuous, 65% capacity factor)
- Equivalent to: 61.4% of current hydropower capacity

Table 2. Feasibility Analysis

Scenario	**2024 Reality**	**2030 Projections**
Monsoon Availability	Total: ≈ 3,300 MW After demand: 984 MW surplus	Total: ≈ 10,255 MW After demand: 6,155 MW surplus
Dry Season Availability	Total: ≈ 1,085 MW Deficit: 917 MW	Total: ≈ 3,418 MW Marginal surplus: 18 MW
Hydrogen Feasibility	Impossible	Possible with new capacity

Critical Requirements

- Reservoir Projects: Minimum 2,000 MW needed for dry-season reliability
- Investment: $4–5 billion for dedicated hydrogen infrastructure
- Policy: Fast-track approvals for hydrogen-dedicated projects

Table 3. Cost Projections (2024 vs. 2035)

Parameter	**2024 Value**	**2035 Projection**	**Calculation Basis**
Electrolyzer CAPEX	$1,200/kW	$400/kW	12% annual reduction (Yang et al., 2023)
H_2 Production Cost	$5.00/kg	$2.15/kg	Learning curve (18% reduction/year)

2.2.4. *Techno-Economic Assessment.* These cost projections are primarily based on global learning curves; however, in the Nepalese context, electricity tariffs for industrial hydropower are lower. According to Nepal Electricity Authority (NEA), off-peak industrial tariffs range from 4.74 to 7.14 NPR/kWh, which equals $0.035 to $0.053 per kWh at 135 NPR/USD, depending on voltage level and time-of-use pricing [30]. To validate global hydrogen cost projections under Nepal-specific conditions, a Levelized Cost of Hydrogen (LCOH) calculation was performed based on domestic electricity pricing and electrolyzer characteristics.

As previously noted, Nepal's industrial tariffs provide a competitive electricity cost advantage for hydrogen production. Green hydrogen production via PEM electrolyzers requires approximately 50 kWh of electricity per kilogram of hydrogen, assuming 65% efficiency. Using these values, the electricity input cost per kg of hydrogen is calculated as follows:

Table 4. Input Cost per kg of Hydrogen

Electricity Price (USD/kWh)	**Electricity Cost per kg H_2 (USD)**
0.035	1.75
0.040	2.00
0.045	2.25
0.050	2.50
0.053	2.65

The Levelized Cost of Hydrogen (LCOH) is given by:

$$\text{LCOH} = \text{Electricity Cost} + \text{CAPEX Recovery} + \text{O\&M Cost}$$

$$= (C_e \times E) + \left(\frac{C_{\text{capex}} \times \text{CRF}}{8760 \times \text{CF} \times \eta}\right) + \left(\frac{C_{\text{O\&M}}}{8760 \times \text{CF} \times \eta}\right) \tag{7}$$

Where:

- C_e = Electricity price (USD/kWh)
- E = Energy per kg H_2 = 50 kWh
- C_{capex} = Electrolyzer cost (USD/kW)
- CRF = Capital Recovery Factor
- CF = Capacity Factor
- η = Efficiency (kg H_2/kWh input)
- $C_{\text{O\&M}}$ = Annual O&M cost (USD/kW/year)

Table 5. Input Parameters (2035 Projections)

Parameter	**Value**	**Unit**	**Notes**
Electrolyzer CAPEX	$400	/kW	PEM electrolyzer, 2035 projection
Electricity consumption	50	kWh/kg H_2	Industry standard for PEM electrolysis
Capacity factor (CF)	65%	–	Based on Nepal's hydropower variability
Fixed O&M cost	$15	/kW-year	3.75% of CAPEX
Discount rate	8%	–	Standard project financing rate
System lifetime	20	years	Typical electrolyzer lifespan

Using a simplified LCOH model (based on IEA/IRENA methodology):

$$\text{CAPEX Recovery} = \frac{\text{Electrolyzer CAPEX} \times \text{CRF}}{\text{Capacity factor (CF)} \times \text{hours in a year}} \tag{8}$$

Where:

$$\text{CRF (Capital Recovery Factor at 8\% for 20 years)} \approx 0.1019$$

$$\text{CAPEX contribution per kg } H_2 = \text{CAPEX Recovery} \times 50 \text{ kWh}$$

$$\text{Fixed O\&M contribution per kg } H_2 = \frac{\text{Fixed O\&M cost}}{\text{CF} \times \text{hours in a year}} \times 50 \tag{9}$$

TABLE 6. Total LCOH Range

Electricity Price (USD/kWh)	Electricity	CAPEX	O&M	Total LCOH (USD/kg)
0.035	1.75	0.36	0.13	2.24
0.040	2.00	0.36	0.13	2.49
0.045	2.25	0.36	0.13	2.74
0.050	2.50	0.36	0.13	2.99
0.053	2.65	0.36	0.13	3.14

These values show that, under Nepal's industrial electricity tariffs and projected electrolyzer costs by 2035, the levelized cost of green hydrogen could fall within the range of \$2.24 to \$3.14 per kg. This aligns closely with the IEA's global LCOH forecast for green hydrogen and demonstrates competitive feasibility in Nepal's context [23, 30, 31].

2.2.5. *Break-Even Analysis.*

(1) **Cost Comparison:**

$$\text{Coal Energy Cost} = \text{Cost of coal in Nepal/MT} + (\text{CO}_2 \text{ Emission Factor} \times \$50 \text{ carbon tax}) \tag{10}$$

$$\text{H}_2 \text{ Energy Cost} = \text{H}_2 \text{ required} \times \text{H}_2 \text{ Production Cost} \tag{11}$$

(2) **Subsidy Requirement:**

$$\text{Gap} = \text{H}_2 \text{ Energy Cost} - \text{Coal Energy Cost} \tag{12}$$

2.2.6. *Emission Reduction Potential.*

(1) **Direct Fuel Combustion:**

$$\Delta\text{CO}_2 = \text{CO}_2 \text{ Emissions MT/year} \times \text{Substitution Ratio} \tag{13}$$

(2) **Process Emissions (Le Chatelier's principle):**

$$\text{CaCO}_3 \rightarrow \text{CaO} + \text{CO}_2 \implies 0.52 \text{ MT CO}_2\text{/MT clinker} \tag{14}$$

(3) **Net Reduction (100% H_2 scenario):**

$$= \text{CO}_2 \text{ Emissions MT/year} - \big(5 \text{ million MT clinker} \times \text{Process Emissions}\big) \tag{15}$$

2.2.7. *Validation Protocol.*

(1) **Cross-Method Verification:**
- Coal calculations compared with CSI Cement CO_2 Protocol
- Hydrogen yields verified against IEA H_2 Technical Report (2023)

(2) **Sensitivity Testing:**
Key Variable: Electrolyzer efficiency (±5%)

$$\text{Revised H}_2 = \frac{\text{Total Hydrogen Demand for 100\% substitution}}{0.60} \quad \text{to} \quad \frac{\text{Total Hydrogen Demand for 100\% substitution}}{0.70} \tag{16}$$

(3) **Uncertainty Propagation:**

$$\text{Total Uncertainty} = \sqrt{(\text{Operational Cost}_{\text{Coal}})^2 + (\text{Operational Cost}_{\text{H}_2})^2} \tag{17}$$

2.2.8. *Policy Implications Framework.*

(1) **Incentive Structures:**

$$\text{Required Carbon Price} = \frac{\text{H}_2 \text{ Energy Cost} - \text{Coal Energy Cost}}{\text{Emission Factor}} \tag{18}$$

(2) **Infrastructure Investment:**

$$\text{Investment} = \frac{\text{Energy Needed (MW)}}{\text{2035 Projected Electrolyzer Cost}} \tag{19}$$

3. Results and Discussions

This section presents the core findings of the study by quantitatively analyzing the technical, environmental, and economic implications of replacing coal with green hydrogen in Nepal's cement industry. Key outcomes are derived from the previously discussed methodology and supported by real-world plant data, techno-economic assumptions, and national hydropower capacity insights.

3.1. **Clinker-to-Coal Dependency and Baseline Emissions.** Nepal's clinker production is heavily reliant on coal as its primary thermal energy source. Based on the operational clinker-to-coal ratio of 4.52 (from Figure 1), the annual production of 5 million metric tons (MT) of clinker requires approximately 1.106 million MT of coal. Using the Tier 2 emission factor of 2.32 tons CO_2 per ton of bituminous coal [12], the corresponding CO_2 emissions from coal combustion total approximately 2.57 million tons/year. This emission estimate establishes the baseline fossil carbon footprint for thermal energy input in the cement manufacturing process and provides the foundation for assessing hydrogen-based decarbonization.

3.2. **Hydrogen Substitution Requirement.** To replace coal with green hydrogen thermally, energy equivalence must be ensured. Given a hydrogen lower heating value (LHV) of 33.33 kWh/kg and bituminous coal LHV of 7,000 kcal/kg ($\approx$ 8.14 kWh/kg), the thermal equivalence factor becomes 205.88 kg of H_2 per ton of coal. For 1.106 million tons of annual coal consumption, the total hydrogen requirement is calculated to be 227,743 MT per year. Assuming 65% electrolyzer efficiency (based on the average performance of modern PEM systems, IEA, 2023), the electrical energy required for hydrogen production amounts to approximately 11.39 billion kWh/year, translating to a continuous power requirement of 2,002 MW. This forms the cornerstone for integrating hydropower and hydrogen strategies in Nepal.

3.3. **Hydropower Feasibility in Nepal and Capacity Factor Justification.** Nepal's total installed hydropower capacity as of 2024 stands at 3,255.8 MW, with over 7,000 MW under construction. The average net capacity factor for hydropower projects in Nepal is approximately 65%, supported by operational reports of peaking run-of-river and reservoir plants [32]. This figure was adopted as a representative national average to estimate annual usable energy for hydrogen production. Based on this assumption, the continuous demand of 2,002 MW for hydrogen production exceeds dry-season generation, which falls to 1,085 MW. During monsoon months, however, surplus capacity of nearly 1,884 MW becomes available. Nepal's dry season hydropower generation drops to one-third of installed capacity ($\approx 1,085$ MW), creating a seasonal deficit. During the monsoon, however, up to 1,884 MW of surplus capacity is available. By 2030, this gap is expected to narrow significantly due to ongoing hydropower expansions. A summary of seasonal capacity and hydrogen demand alignment is provided in Figure 2.

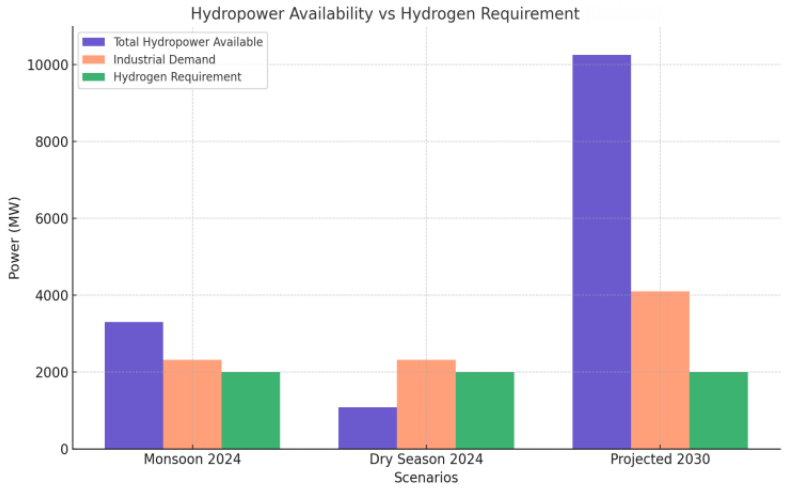

FIGURE 2. Seasonal Hydropower Availability vs. Hydrogen Demand.

3.4. **Emission Reduction Potential.** Full substitution of coal with green hydrogen would eliminate the 2.57 million tons of CO_2 emissions arising from fossil fuel combustion. However, process emissions from calcination of limestone ($CaCO_3 \rightarrow CaO + CO_2$) remain a challenge. With a process emission rate of 0.52 tons CO_2 per ton of clinker, total non-combustion emissions from producing 5 million tons of clinker amount to 2.6 million tons CO_2/year. Thus, net emissions under a 100% hydrogen scenario reduce to 66,370 tons/year, representing a 97.4% reduction in total CO_2 emissions from the cement plant. These values are summarized in Figure 2, which also compares partial substitution under a 30% hydrogen adoption scenario.

Figure 3 shows the stark contrast between current coal-based emissions and the near-zero emissions scenario with hydrogen adoption, while highlighting persistent process emissions from limestone calcination. The geographical concentration of clinker plants in specific regions (notably Province Koshi, Bagmati, and Lumbini) could enable targeted hydrogen infrastructure development.

3.5. **Economic Assessment and Break-Even Analysis.** The cost comparison indicates that the effective cost of coal, including a projected carbon tax of \$50/ton CO_2, amounts to \$237 per MT coal equivalent. On the other hand, with hydrogen projected at \$2.15/kg by 2035 (based on cost learning curves), the energy-equivalent cost reaches \$443 per MT-resulting in a cost premium of \$206 per MT. This would still represent an 87% cost premium compared to coal on an energy-equivalent basis, even with a \$50/ton carbon tax on coal.

Figure 4 demonstrates the sensitivity of hydrogen costs to electricity prices, showing how Nepal's low industrial tariffs (\$0.035–\$0.053/kWh) could make green hydrogen more competitive by 2035. Globally, hydrogen costs are projected to reach \$2–\$3/kg in Europe and the Middle East by 2035, with India aiming for sub-\$2/kg hydrogen through solar-based electrolysis. Compared to these benchmarks, Nepal's hydropower advantage and low industrial tariffs position it competitively, though seasonal generation challenges must be addressed through reservoir-backed capacity and grid management strategies.

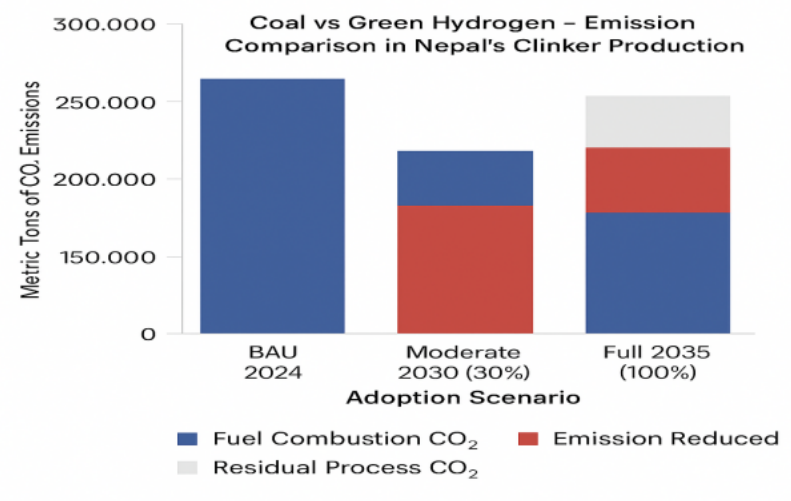

FIGURE 3. CO_2 Emission Comparison - Coal vs. Green Hydrogen

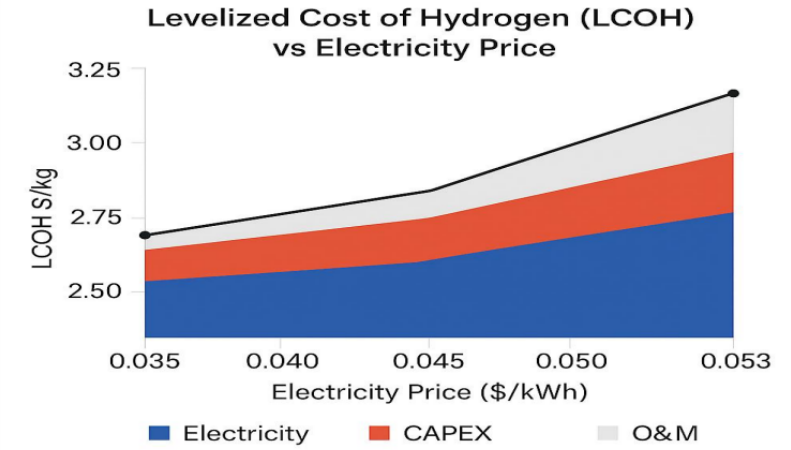

FIGURE 4. Levelized Cost of Hydrogen (LCOH) vs. Electricity Price.

3.6. **Strategic Adoption Pathways and Policy Recommendations.** A phased adoption strategy offers the most pragmatic approach to balancing environmental goals with infrastructure and economic constraints. By 2030, a 30% hydrogen penetration could displace 331,858 MT of coal annually while requiring manageable investments in 600 MW of hydropower capacity and $240 million for electrolyzers. Full adoption by 2035 would demand more substantial infrastructure-2,000 MW of reservoir projects ($4–5 billion) and $800 million for electrolyzers-but could achieve near-total elimination of combustion-related emissions.

Critical policy interventions include:

- Carbon pricing at $139/ton CO_2 to internalize coal's environmental costs,
- Subsidies for electrolyzer deployment and renewable integration,
- Fast-track approvals for hydrogen-dedicated hydropower projects,
- Industrial partnerships to pilot hydrogen-based clinker production.

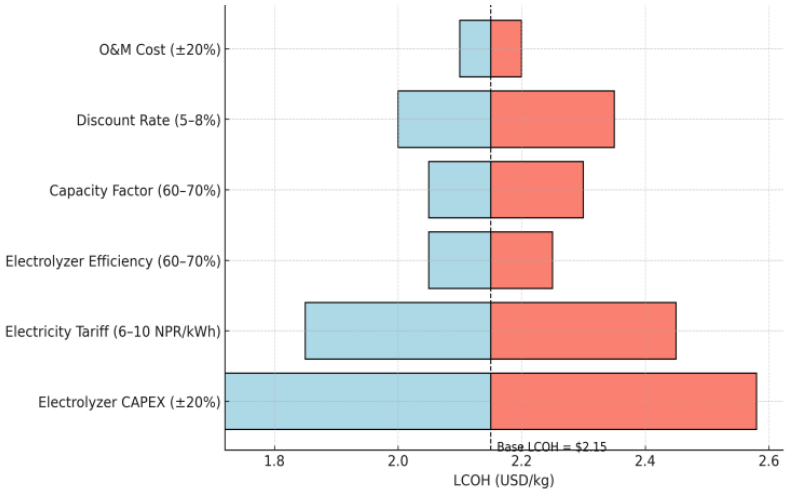

FIGURE 5. Sensitivity analysis (Tornado chart) of LCOH to key variables. Electrolyzer CAPEX and electricity tariffs have the strongest influence on hydrogen cost outcomes.

3.7. **Sensitivity and Scenario Analysis.** Sensitivity analysis shows that electrolyzer CAPEX and electricity prices have the strongest influence on hydrogen cost. A ±20% shift in CAPEX alters the Levelized Cost of Hydrogen (LCOH) between $1.72 and $2.58/kg under different electricity cost scenarios. A tornado chart illustrating the impact of key variables is shown in Figure 5.

TABLE 7. Scenario Modeling

Scenario	H_2 Penetration	Coal Displaced (MT)	CO_2 Reduction (MT)	Cost Premium
BAU (2024)	0%	0	0%	–
Moderate (2030)	30%	331,858	769,909	+72%
Full (2035)	100%	1,106,194	2,566,370	+87%

3.8. **Infrastructure and Policy Implications.** To enable large-scale adoption of green hydrogen in the cement sector, Nepal must invest in at least 2,000 MW of dedicated hydropower, preferably via reservoir-based or pumped storage projects to manage seasonal variability. Estimated capital requirements are between $4–5 billion, depending on location and integration cost. Policy recommendations include:

- Introduction of a carbon price floor (approximately $139/ton CO_2),
- Concessional financing mechanisms for electrolyzer infrastructure,
- Time-bound regulatory approvals for hydrogen-linked projects,
- Strategic co-location of cement kilns and hydropower plants to reduce transmission losses and support clustered green industrial zones.

4. Conclusion and Recommendations

This study presents a comprehensive analysis of the potential for green hydrogen to decarbonize Nepal's cement industry, highlighting both the transformative opportunities and significant challenges of such a transition. While replacing coal with green hydrogen is technically feasible, the path to implementation requires strategic planning, robust policy

support, and substantial infrastructure investments.

Nepal's cement sector currently emits approximately 2.34 million metric tons of CO_2 annually from clinker production. Green hydrogen could eliminate nearly all combustion-related emissions, reducing them by 98%, but achieving this would require 227,743 metric tons of hydrogen annually and 2,002 MW of dedicated hydropower, with a deficit of 18 MW. However, 2,000 MW of reservoir projects would still be essential to ensure year-round hydrogen reliability.

Nepal's 72 clinker plants, with an average capacity of 69,444 MT, present both challenges and opportunities for phased hydrogen adoption, particularly near hydropower sites using modular electrolyzers. Economically, hydrogen production costs are projected to decline to \$2.15–\$3.14/kg by 2035 due to improvements in electrolyzer efficiency and low industrial electricity tariffs. Even then, hydrogen would remain 87% more expensive than coal on an energy-equivalent basis, despite a \$50/ton carbon tax. Bridging this gap would require a carbon price of \$139/ton CO_2 and subsidies to offset the \$206/MT coal-equivalent premium. Time-of-use pricing could help optimize hydrogen production during power surpluses and improve economics.

A phased approach is recommended. By 2030, 30% hydrogen penetration could displace 331,858 MT of coal annually, reduce emissions by 769,909 MT CO_2, and require 600 MW of hydropower and \$240 million in electrolyzers. This would build operational experience toward full-scale implementation by 2035. Full adoption would require \$4–5 billion in hydropower reservoirs and \$800 million for electrolyzers, but could nearly eliminate all combustion-related CO_2 emissions.

Policy interventions are vital. Three key recommendations include: providing financial incentives to first-mover plants near hydropower hubs to enable pilot demonstrations; offering technical assistance for retrofitting coal kilns, including workforce training; and coordinating hydrogen infrastructure development aligned with current and future plant locations, especially in regions like the Terai, where 58% of clinker plants are concentrated. These approaches are essential to addressing the limitations of Nepal's distributed production system while capitalizing on geographic advantages.

This study is based on national-level modeling assumptions and does not capture plant-level differences or real-time hydropower dynamics. Spatial variations, grid integration challenges, and plant-specific retrofitting costs were beyond its scope. Cost projections assume linear technological progress. Future research should involve pilot-scale demonstrations, dynamic seasonal system modeling, and integration of green hydrogen with CCS and alternative cement chemistries to mitigate residual process emissions[17, 33, 34, 35]. Hybrid strategies combining hydrogen, CCS, and alternative clinker materials offer a promising route to full decarbonization.

In conclusion, the shift to green hydrogen in Nepal's cement industry is technically achievable and environmentally impactful but demands coordinated effort across policy, infrastructure, and industry. By aligning with global climate goals and utilizing its hydropower potential, Nepal can position itself as a leader in low-carbon cement among developing countries. The insights from this study also serve as a reference for other hydropower-rich

developing nations aiming to decarbonize hard-to-abate sectors. The pathway is challenging, but with phased execution and focused support, it is within reach.

References

[1] A. A. Jhatial, W. I. Goh, K. H. Mo, S. Sohu, and I. A. Bhatti, "Green and sustainable concrete: The potential utilization of rice husk ash and egg shells," *Civil Engineering Journal*, vol. 5, no. 1, pp. 74–81, 2019. doi: 10.28991/cej-2019-03091226.

[2] V. D. Pinheiro, J. Alexandre, G. D. C. Xavier, M. T. Marvila, S. N. Monteiro, and A. R. G. de Azevedo, "Methods for evaluating pozzolanic reactivity in calcined clays: A review," *Materials*, vol. 16, no. 13, p. 4778, 2023. doi: 10.3390/ma16134778.

[3] N. Bheel, R. A. Abbasi, S. Sohu, S. A. Abbasi, A. W. Abro, and Z. H. Shaikh, "Effect of tile powder used as a cementitious material on the mechanical properties of concrete," *Engineering, Technology & Applied Science Research*, vol. 9, no. 5, pp. 4596–4599, 2019. doi: 10.48084/etasr.2994.

[4] S. Patil, D. Joshi, R. Menon, and L. Wadhwa, "Environmental impact assessment of fly ash and GGBS-based geopolymer concrete in road construction," *E3S Web of Conferences*, vol. 405, p. 03021, 2023. doi: 10.1051/e3sconf/202340503021.

[5] J. Pokorný, "The effect of biomass-based fly ash on properties of cement pastes," *Journal of Physics: Conference Series*, vol. 2911, no. 1, p. 012018, 2024. doi: 10.1088/1742-6596/2911/1/012018.

[6] B. S. Reddy and R. Siempu, "Studies on the mechanical properties of ternary blended geopolymer concrete using fly ash, GGBS and alccofine," *Journal of Physics: Conference Series*, vol. 2779, no. 1, p. 012072, 2024. doi: 10.1088/1742-6596/2779/1/012072.

[7] B. S. Thapa, B. Pandey, and R. Ghimire, "Economy of scale for green hydrogen-derived fuel production in Nepal," *Frontiers in Chemistry*, vol. 12, 2024. doi: 10.3389/fchem.2024.1347255.

[8] C. Chen et al., "A striking growth of CO_2 emissions from the global cement industry driven by new facilities in emerging countries," *Environmental Research Letters*, vol. 17, no. 4, p. 044007, 2022. doi: 10.1088/1748-9326/ac48b5.

[9] R. Bhandari and S. Subedi, "Evaluation of surplus hydroelectricity potential in Nepal until 2040 and its use for hydrogen production via electrolysis," *Renewable Energy*, vol. 212, pp. 403–414, 2023. doi: 10.1016/j.renene.2023.05.062.

[10] C. Schulz and U. Saklani, "The future of hydropower development in Nepal: Views from the private sector," *Renewable Energy*, vol. 179, pp. 1578–1588, 2021. doi: 10.1016/j.renene.2021.07.138.

[11] S. Thakuri, S. B. Khatri, and S. Thapa, "Enflamed CO_2 emissions from cement production in Nepal," *Environmental Science and Pollution Research*, vol. 28, pp. 68762–68772, 2021. doi: 10.1007/s11356-021-15347-7.

[12] U.S. Energy Information Administration, "Carbon dioxide emissions coefficients," 2025. [Online]. Available: https://www.eia.gov/environment/emissions/co2_vol_mass.php

[13] Vedantu, "Bituminous coal," 2025. [Online]. Available: https://www.vedantu.com/geography/bituminous-coal

[14] D. Woodyard, "Fuels and lubes: Chemistry and treatment," in *Pounder's Marine Diesel Engines and Gas Turbines*, 9th ed. Butterworth-Heinemann, 2009, pp. 87–142. doi: 10.1016/B978-0-7506-8984-7.00004-7.

[15] International Renewable Energy Agency, *Green Hydrogen: A Guide to Policy Making*, 2021. [Online]. Available: https://www.irena.org

[16] R. Poudyal et al., "Mitigating the current energy crisis in Nepal with renewable energy sources," *Renewable and Sustainable Energy Reviews*, vol. 116, p. 109388, 2019. doi: 10.1016/j.rser.2019.109388.

[17] P. S. Fennell, S. J. Davis, and A. M. Mohammed, "Decarbonizing cement production," *Joule*, vol. 5, no. 6, pp. 1305–1311, 2021. doi: 10.1016/j.joule.2021.04.011.

[18] D. R. Nhuchhen, S. P. Sit, and D. B. Layzell, "Decarbonization of cement production in a hydrogen economy," *Applied Energy*, vol. 317, p. 119180, 2022. doi: 10.1016/j.apenergy.2022.119180.

[19] J. A. Jibran and C. Mahat, "Application of green hydrogen for decarbonization of cement manufacturing process," *Journal of Physics: Conference Series*, vol. 2629, no. 1, p. 012027, 2023. doi: 10.1088/1742-6596/2629/1/012027.

[20] C. T. Altaf, O. Demir, T. O. Colak, E. Karagöz, M. Kurt, N. D. Sankir, and M. Sankir, "Decarbonizing the industry with green hydrogen," in *Towards Green Hydrogen Generation*, 2024, pp. 1–48. doi: 10.1002/9781394234110.ch1.

[21] Y. Astriani, W. Tushar, and M. Nadarajah, "Optimal planning of renewable energy park for green hydrogen production using detailed cost and efficiency curves of PEM electrolyzer," *International Journal of Hydrogen Energy*, vol. 79, pp. 1331–1346, 2024. doi: 10.1016/j.ijhydene.2024.07.107.

[22] E. Taibi, R. Miranda, M. Carmo, and H. Blanco, *Green Hydrogen Cost Reduction*, IRENA, 2020. [Online]. Available: https://www.irena.org/publications

[23] B. Yang, R. Zhang, Z. Shao, and C. Zhang, "The economic analysis for hydrogen production cost towards electrolyzer technologies," *International Journal of Hydrogen Energy*, vol. 48, no. 37, pp. 13767–13779, 2023. doi: 10.1016/j.ijhydene.2022.12.204.

[24] S. Barbhuiya, B. B. Das, and D. Adak, "Roadmap to a net-zero carbon cement sector," *Journal of Environmental Management*, vol. 359, p. 121052, 2024. doi: 10.1016/j.jenvman.2024.121052.

[25] Department of Electricity Development, "License details," Government of Nepal. [Online]. Available: https://doed.gov.np/license/54

[26] MyRepublica, "Peak domestic demand for electricity posts record high of 2,316 MW on Sunday," *Nagarik Network*, Jun. 23, 2024. [Online]. Available: https://myrepublica.nagariknetwork.com/news/peak-domestic-demand-for-electricity-posts-record-high-of-2-316-mw-on-sunday

[27] The Himalayan Times, "NEA sells Rs 15.4 billion worth of power to India during monsoon this year," Dec. 8, 2023. [Online]. Available: https://thehimalayantimes.com/business/nea-sells-rs-154-billion-worth-of-power-to-india-during-monsoon-this-year

[28] S. Aryal et al., "Evolution and future prospects of hydropower sector in Nepal: A review," *Heliyon*, 2024. doi: 10.1016/j.heliyon.2024.e31139.

[29] Investment Board of Nepal, *Energy Demand Projection 2030*, Government of Nepal, 2012.

[30] Nepal Electricity Authority, "Electricity Tariff," 2024. [Online]. Available: https://www.nea.org.np

[31] International Energy Agency, *IEA H_2 Technical Report*, 2023.

[32] S. Joshi and R. Shrestha, "Performance evaluation of runoff river type hydropower plants operating in Nepal," *Journal of the Institute of Engineering*, vol. 10, no. 1, pp. 104–120, 2014. doi: 10.3126/jie.v10i1.10886.

[33] H. Ostovari, L. J. Müller, J. Skoček, and A. Bardow, "From unavoidable CO_2 source to CO_2 sink? A cement industry based on CO_2 mineralization," *Environmental Science & Technology*, vol. 55, no. 8, pp. 5212–5223, 2021. doi: 10.1021/acs.est.0c07599.

[34] J. Dengler, X. Li, H. Grassl, and C. Hesse, "Unlock the full potential of ordinary Portland cement with hydration control additive enabling low-carbon building material," 2023. doi: 10.21203/rs.3.rs-3146079/v1.

[35] M. Bacatelo et al., "Carbon-neutral cement: The role of green hydrogen," *International Journal of Hydrogen Energy*, pp. 382–395, 2024. doi: 10.1016/j.ijhydene.2024.03.028.

Everest Advances in Science and Technology (EAST), Vol. 1, No. 1, 2025
ISSN: 3102-0410(print), 3102-0429(online)

Experimental Study on Compressive and Tensile Strength of Plain Concrete With Polyethylene Terephthalate (PET) Powder

NEHA KUMARI KARNA[1*], NITESH SHRESTHA[2]

Abstract. This study examines the compressive strength and split tensile strength of concrete with polyethylene terephthalate (PET) powder as a partial replacement for sand in varying proportions. PET is a polymer commonly used in the food packaging industry, including cold drink and water bottles, and is considered a waste material. In this research, PET powder derived from recycled plastic bottles collected by a recycling plant in Itahari, Nepal, was utilized. Concrete specimens incorporating PET powder at proportions of 3.8%, 4.0%, and 4.2% by weight of sand were cast and tested for strength development at 7, 21, and 28 days. Cube and cylinder specimens were prepared using a water-to-cement ratio of 0.5. Results indicated that the inclusion of PET powder enhanced early-age compressive strength. At 7 days, concrete mixes with 3.8%, 4.0%, and 4.2% PET exhibited compressive strength increases of 26.44%, 40.53%, and 12.43%, respectively, over the M20 control mix, indicating accelerated early strength gain. However, all PET-modified mixes showed lower compressive strengths compared to the control mix at 21 and 28 days, with the reduction becoming more significant at higher PET concentrations. Notably, at 28 days, the mix with 4.2% PET showed a decrease in compressive strength of over 31.06% relative to the control mix. In contrast, split tensile strength increased consistently across all curing periods. The 4.0% PET mix achieved a 35.86% increase at 7 days, while the 3.8% PET mix showed the highest increase of 62.84% at 21 days. At 28 days, the 4.0% PET mix again showed the highest improvement, with a 45.35% increase in split tensile strength. These findings suggest that while a higher PET content may negatively impact long-term compressive strength, optimal PET incorporation can substantially enhance split tensile capacity, crack resistance, and ductility. Overall, the study demonstrates the sustainable utility of PET waste as a partial sand replacement in concrete, improving specific mechanical properties and promoting environmental sustainability. The results further confirm that compressive and tensile strengths tend to decrease with increasing PET content beyond optimal levels.

Keywords: Compressive strength, PET powder, Partial Replacement, Split tensile strength.

[1]Department of Civil Engineering, Everest Engineering College, Sanepa, Lalitpur, Nepal
E-mail: nehakumari.karna@eemc.edu.np
[2]Department of Civil Engineering, Everest Engineering College, Sanepa, Lalitpur, Nepal
E-mail: nitesh.shrestha@eemc.edu.np
* Corresponding author
Manuscript received: 15 April, 2025; revised: 25 May 2025; accepted: 5 September, 2025.
Everest Advances in Science and Technology (EAST), Vol. 1, No. 1, 2025

1. Introduction

Despite its apparently insignificant nature, sand is an essential component of our existence. It is the main component used to build contemporary cities. Sand and gravel are combined to create the concrete required to build office buildings, shopping centers and residential complexes, as well as the pavement used to build highways that connect them. Sand that has melted is used to make the glass in all windows, windscreens, and smartphone screens. Additionally, almost every piece of electronic equipment in your home, including the silicon chips found in our phones and laptops, is composed of sand [1]. The last 20 years have seen the production of half of all polymers ever produced. From 2.3 million tons in 1950 to 448 million tons in 2015, production grew at an exponential rate. By 2050, production is predicted to double. Approximately eight million tons of plastic debris from coastal countries end up in the oceans each year. It would be the same as filling five garbage bags with trash on every foot of the world's shoreline. Additives are often employed in plastics to increase their strength, flexibility, and durability. However, if a product ends up as litter, several of these chemicals can prolong its life; according to some forecasts, it will take at least 400 years for it to decompose [2]. According to studies, concrete's compressive strength decreases when recovered waste plastic is used in place of natural particles. For instance, the strength was reduced by 50% when PVC granules were used in place of up to 50% of the sand. Three primary causes contribute to the reduction in strength: increased air content, weakened cement paste-plastic aggregate binding, and decreased plastic aggregate strength and stiffness. Concrete is further weakened by the increased porosity in the interfacial transition zone caused by the low water absorption of plastic particles. The study shows that discarded plastic can be included into concrete to lessen trash going to landfills and possibly enhance the material's mechanical qualities. Waste plastic can be used to replace up to 10% of cement, fine, and coarse aggregates in concrete without changing the concrete's consistency or chemical composition, thereby providing a sustainable approach to resource use and waste management [3].

According to the slump test, batches containing recycled PET fibers had a slump of 472 mm, whereas control samples had a 22% higher slump. Higher dosages and ratios improved slump, probably because the fibers were more flexible, but the fiber dose and aspect ratio had little effect. Comparing 100 $\times$ 200 mm concrete cylinders to control samples, compressive testing revealed that adding recycled PET fiber had little impact on the final compressive strength. The stress-strain curves for varying fiber doses and dimensions, however, show that the addition of PET fibers improved the concrete's compressive toughness [4]. Higher replacement percentages lead to higher energy absorption; the reference specimens have the lowest absorption. At a replacement rate of 12.5%, the maximum energy absorption takes place, meaning it's 108.28% higher than the reference. Energy absorption is 50% greater than that of the reference specimens at a replacement rate of 5% [5]. Our initiative to partially substitute sand in building with waste PET plastic tackles a number of significant resource and environmental issues. Recycling PET plastic trash could lessen its environmental impact and encourage more sustainable waste management techniques. PET plastic waste is an important component of pollution and landfill accumulation. Important natural resources can also be maintained by substituting natural sand, whose mining destroys ecosystems and depletes riverbeds. In keeping with international initiatives to promote the use of waste materials, this strategy promotes sustainable development methods by providing an environmentally friendly substitute for

traditional building materials. Incorporating recycled plastic trash into concrete has become a viable way to improve material performance and reduce environmental issues.

The potential of waste polyethylene terephthalate (PET) and other plastic derivatives as aggregates, fibers, and reinforcements in concrete has been investigated in a number of research. Utilizing recycled PET [6] examined the time-temperature characteristics of polymer concrete, proving its feasibility for use in building applications. Similar to this, [7] investigated how plastic particles affected the durability and mechanical strength of concrete. The valorization of post-consumer waste plastic and PET bottle aggregates was the subject of studies by [8] and [9], respectively. The results showed encouraging results in terms of workability, density decrease, and impact resistance. Furthermore, [10] investigated the incorporation of certain waste components into concrete mixtures, indicating that plastic trash enhances sustainability in the building industry. Additionally, studies have shown that polymer-modified concrete reinforced with waste plastic fibers can increase durability and flexural strength [11]. Furthermore, studies by [12] and [13] examined how concrete compositions could be made tougher and more ductile by substituting scrap tire rubber and textile fibers, respectively, for conventional particles. The usage of fiber-reinforced polymer (FRP) encased rubberized concrete and the effects of recycling PET bottles in building materials were the subjects of other investigations, including those conducted by [14] and [15]. A thorough analysis of recycled plastic in concrete was presented by [16] confirming its viability for use in large-scale building. The mechanical characteristics of recycled PET fiber-reinforced mortar and concrete were further investigated by [17] and [18], respectively, and the results showed notable increases in structural integrity. Recent developments by [19] and [20] showed potential uses in load-bearing structures by successfully integrating plastic waste into fiber-reinforced concrete beams. The addition of waste plastic fibers to reinforced concrete beams has been shown to improve its ductility and shear strength [21]. Furthermore, research by [22] on the substitution of PET waste for fine aggregates demonstrated that it may be used to create lightweight and eco-friendly concrete composites. The mechanical behavior of PET-modified concrete was evaluated in other noteworthy research by [23] and [24], which showed how well it improved impact resistance and decreased shrinkage cracks. The performance of plastic-modified concrete is assessed using standardized testing techniques which guarantee adherence to industry standards. The use of recycled plastics in concrete offers a practical substitute for conventional materials, supporting the circular economy concepts and lowering dependency on non-renewable resources in light of the growing concerns over environmental sustainability and waste management.

The consequence of powdered PET on the microstructure, particle-cement bonding, and overall performance of concrete in contrast with shredded PET is one of the research gaps in our project. The long-term impact on characteristics including permeability, freeze-thaw resistance, and chemical attacks, as well as durability tests under various conditions in the environment require consideration. Additionally, the cost-effectiveness and adaptability of utilizing powdered PET are frequently disregarded, as are the environmental effects determined by lifecycle assessments. Investigating hybrid replacement using distinct industrial byproducts alongside particular uses for sustainable or lightweight building could also provide meaningful information and close knowledge gaps.

The study looks into using Polyethylene Terephthalate Waste Powder (PWP) in mortars as a partial substitute for sand. It finds that while higher PWP percentages reduce density and mechanical qualities, 5% PWP improves workability and strength. By increasing compressive strength and ductility, the ideal 5% PWP provides an environmentally beneficial way to control waste in building materials. It is advised to conduct more durability research [25]. The study investigates the utilization of waste Polyethylene Terephthalate (PET) in concrete by substituting 3%, 6%, and 9% PET by weight for fine particles. According to the study, adding PET to concrete weakens it, but a 3% PET component provides the optimal strength-to-sustainability ratio. Concrete's density barely changed, yet using 3.52% PET resulted in a 0.47% cost reduction. According to their results, PET aids in waste management and marginally lowers expenses, but if utilized in excess of what is necessary, strength is compromised. For real-world applications, the study suggests more research on maximizing PET content, environmental impact, and durability [26]. To lessen plastic waste and enhance material qualities, the study looks into replacing some of the sand in concrete with PET bottle fibers. PET fibers in concrete mixtures containing 1%–5% demonstrated the maximum flexural strength at 2.5% and the best compressive strength at 2%. Strength declined beyond these percentages.

According to the findings, replacing up to 2.5% of the PET fiber in concrete increases its strength and provides a sustainable way to reduce waste and improve material quality. Research on additives may be necessary to further improve performance [27]. For two main reasons, the percentages of 3.8%, 4%, and 4.2% were chosen to partially replace sand with plastic. The values were selected to examine performance just below (3.8%) and above (4.2%) this criterion since research showed that a 4% replacement is a commonly used and successful benchmark. This allowed for sensitivity analysis close to the predetermined range. Second, utilizing larger percentages was not feasible due to material availability limitations, therefore these small changes were both useful and scientifically significant for the study.

The objective of this study is to evaluate and compare the compressive and tensile strength between ordinary M20 grade plain concrete and PET mixed concrete. The scope of this study is comparison of compressive and tensile strength of plain concrete of M20 grade and concrete mixed with PET powder. Compressive strength and Tensile strength of plain concrete and PET mixed concrete comparison study has been studied for M20 grade of concrete only. The results and outputs may vary for other grades of concrete. The study is conducted using 3.8%, 4% and 4.2% PET replacement of fine aggregate. The fineness modulus analysis of natural sand and PET pouches were not conducted. Only one specimen per mix was evaluated for tensile strength. To guarantee statistical validity, future research should strive for a minimum of three specimens per test circumstances.

2. Methodology

This experiment investigates the effects of partially replacing fine aggregates in concrete with varying percentages of polyethylene terephthalate (PET) waste, which has been cut, shredded, and powdered by machinery. The optimal weight percentage of PET waste is determined by comparing concrete samples with different PET contents against reference samples containing only fine aggregates. The concrete mix used is a nominal M20 mix (1:1.5:3) with a water-to-cement ratio of 0.5, following Indian Standards. This water-to-cement ratio ensures adequate hydration, and the mixture meets the standard parameters

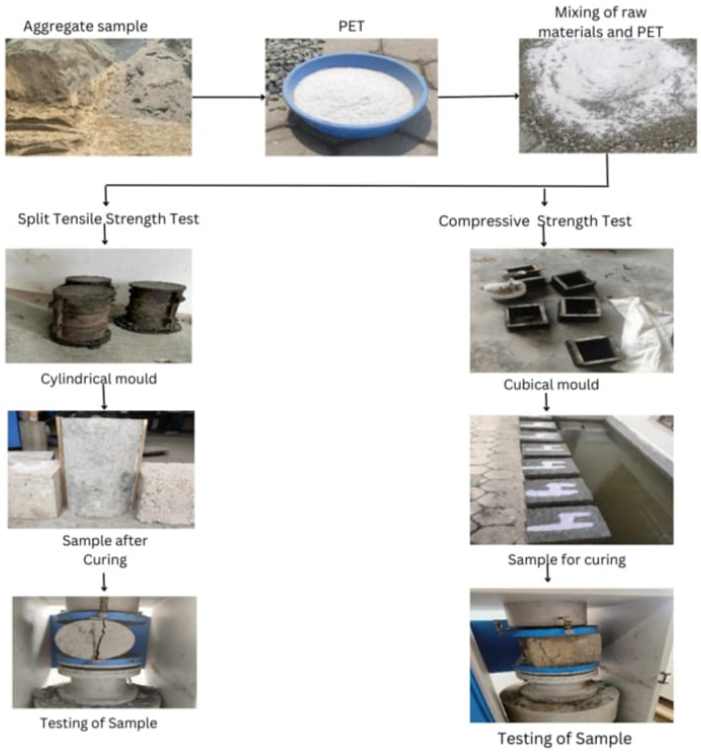

FIGURE 1. Chart showing Methodology.

for M20 concrete. Good quality potable water was used throughout the experiment. Fine and coarse aggregates were sourced with proper gradation and purity, and Ordinary Portland Cement (OPC) grade 43 was employed.

Concrete samples were prepared by replacing fine aggregates with PET powder at percentages of 0%, 3.8%, 4%, and 4.2% by weight. The materials were first dry-mixed to ensure uniform distribution of constituents. Water was then gradually added during mixing to prevent segregation and lump formation. Destructive strength tests, including compressive strength and split tensile strength tests, were conducted on the samples. Three specimens from each mix were tested at 7, 21, and 28 days to failure to determine their ultimate compressive strength. All tests were performed according to the relevant Indian Standard procedures. The methodology for this study is shown in Figure 1.

2.1. **Materials.**

2.1.1. *Cement.* In this study, ordinary Portland cement of grade 43 is utilized. In accordance with Indian Standard (IS) Code: 8112-1989, the cement's physical properties and chemical components are met. The cement utilized during the experiment was purchased from the commercial market, which guarantees that it satisfies standard quality and consistency requirements. The commercially available cement is widely used in a variety of construction applications, making it perfect for implementing real-world conditions in the experimental setup.

2.1.2. *Coarse Aggregates.* The coarse aggregates used in this study are crushed natural stones with a maximum size of 20 mm, while the fine aggregates consist of natural sand

with a maximum size of 4.75 mm. The grading and specifications for the fine aggregates conform to the Indian Standard Specification IS 383:2016. The aggregates were procured directly from the quarry, ensuring high quality and providing cost advantages. These aggregates exhibit suitable shapes, robust durability, and consistent particle sizes that contribute to superior bonding within the concrete matrix. Additionally, the controlled particle size distribution and moisture content of the aggregates enhance the overall performance of the concrete. Testing of key properties such as grading and absorption was carried out to optimize their application in the construction process.

2.1.3. *Fine Aggregates.* It was clean and free from any types of dust, clay, and chemicals. PET is added to the reference mixture in three different percentages (3.8%, 4%, and 4.2%) by weight of sand as a partial replacement.

2.1.4. *Pet.* In this investigation, PET bottles of various sizes were collected from nearby recycling plants and processed into a fine powder. The polyethylene terephthalate (PET) particles underwent sieve analysis to determine their suitability for use in concrete. Specifically, the powdered PET was sourced from a recycling facility in Itahari, Nepal, where plastic waste bottles are collected, shredded, and powdered. This recycled PET was incorporated into the concrete mix as a partial replacement for fine aggregate to evaluate its potential as a sustainable building material. Besides promoting reuse of plastic waste and supporting environmental sustainability, this approach provides valuable insight into how PET influences the durability and strength characteristics of concrete. The PET powder used was clean and free from contaminants such as dust, clay, and chemicals. The application of recycled PET in this experiment aims to develop innovative methods for utilizing waste plastic in construction, thereby improving both material efficiency and environmental performance.

FIGURE 2. Shredding Machine for Powdered PET.

FIGURE 3. PET Powder.

2.2. **Mixture Proportions.** In this study, a nominal mix for M20 concrete (1:1.5:3) was used. The water-to-cement ratio was maintained at 0.5.

TABLE 1. Material Quantities for Casting Specimens

Cement (kg)	Sand (kg)	Aggregate (kg)	Water (L)	PET (%)
6.41	10.21	22.05	3.21	3.8
6.41	10.19	22.05	3.21	4.0
6.41	10.17	22.05	3.21	4.2

2.3. **Preparation of the Test Specimens.** Prior to use, the fine and coarse aggregates are cleaned and washed. Before casting, all cube and cylinder molds are prepared, cleaned, and lubricated. To partially replace sand, the PET waste particles are first processed and combined according to the weight percentages mentioned above. The aggregates, including gravel and PET waste substitutes, are mixed in a mixer. Cement is then added to the concrete mixture. Finally, water is gradually added while mixing continuously for at least two minutes.

TABLE 2. Variation in Specimen Types Prepared

S.N	Specimen Type	Set 1	Set 2	Set 3	Total Specimens
1	Cube	12	12	12	36
2	Cylinder	4	4	4	12
Total Number of Specimens Prepared					48

FIGURE 4. Specimen Casted.

2.4. **Laboratory Tests.** Compressive strength tests were conducted using a compression testing machine with a capacity of 2000 kN, following the guidelines specified in IS 516:1959. For each substitution ratio, 36 concrete cubes measuring 150 × 150 × 150 mm were cast to evaluate compressive strength at curing ages of 7, 21, and 28 days. Similarly, split tensile strength tests were performed using the same 2000 kN capacity compression testing machine in accordance with IS 5816:1999. For this test, twelve cylindrical specimens measuring 150 mm in diameter and 300 mm in height were prepared—four specimens for each curing age.

FIGURE 5. Preparation of Compression Test Specimens.

FIGURE 6. Failure Modes of Specimens.

3. Results and Discussions

3.1. **Compressive Strength.** Concrete specimens were tested to assess their capacity to withstand axial loads applied uniformly along their length. This test is critical for evaluating the suitability of concrete for structural applications, as it provides essential data regarding the material's overall strength and durability. When compared to the standard M20 mix, the addition of PET demonstrated a significant influence on compressive strength. Mixes containing 3.80% and 4.00% PET exhibited notable increases in compressive strength at 7 days by 26.44% and 40.53%, respectively, indicating enhanced early-age performance. However, all PET-modified mixes displayed lower compressive strengths than the control M20 mix at 28 days, with the reduction becoming more pronounced as the PET content increased. These results suggest that while PET addition can improve early strength, excessive PET content may negatively impact long-term compressive strength.

TABLE 3. Variations of 7-days Compressive Strength

S.N	% Addition of PET	Failure Load (kN)	Compressive Strength (MPa)	Avg. Compressive Strength (MPa)	% Change in Compressive Strength
1	0%	292.5	13.00		
		289.8	12.88	12.97	–
		293.2	13.03		
2	3.80%	332.7	14.79		
		392.2	17.43	16.40	26.44
		382.1	16.98		
3	4%	396.9	17.64		
		468.2	20.81	18.23	40.53
		365.2	16.23		
4	4.20%	338.8	15.06		
		316.3	14.06	14.58	12.43
		329.2	14.63		

At 21 days, compressive strength for all PET-modified mixes was also lower than that of the control mix, with decreases of 5.54%, 11.19%, and 38.31% observed for the 3.80%,

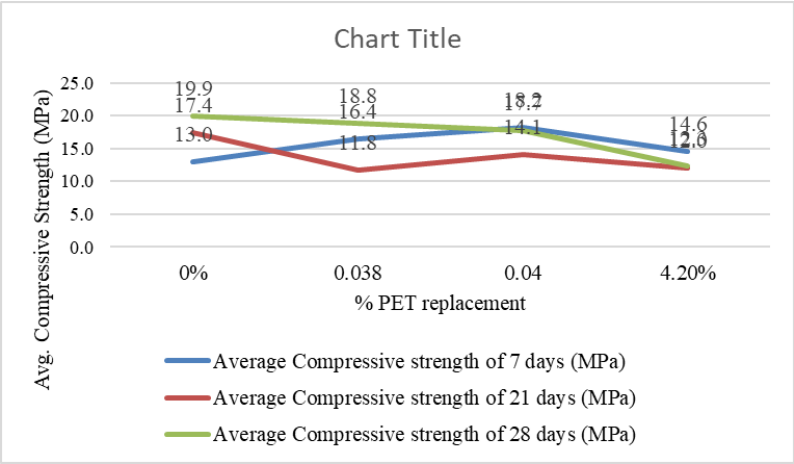

FIGURE 7. Compressive Strength Test of Samples Obtained After Curing for Respective Days.

TABLE 4. Variation of 21 Days Compressive Strength

S.N	% Addition of PET	Failure Load (kN)	Compressive Strength (MPa)	Avg. Compressive Strength(MPa)	% Change in Compressive Strength
1	0%	391.8	17.41		
		394.4	17.53	17.42	–
		389.9	17.33		
2	3.80%	306.5	13.62		
		211.1	9.38	11.78	-32.37
		277.8	12.35		
3	4%	335.7	14.92		
		335.6	14.92	14.07	-19.24
		278.5	12.38		
4	4.20%	277.3	12.32		
		245.4	10.91	12.01	-31.06
		288.1	12.80		

TABLE 5. Variations of 28 Days Compressive Strength

S.N	% Addition of PET	Failure Load (kN)	Compressive Strength(MPa)	Avg. Compressive Strength (MPa)	% Change in Compressive Strength
1	0%	449.2	19.96		
		447.9	19.91	19.89	–
		445.7	19.81		
2	3.80%	423.9	18.84		
		417.3	18.55	18.79	-5.54
		427.2	18.99		
3	4%	396.5	17.62		
		404.3	17.97	17.67	-11.19
		391.8	17.41		
4	4.20%	274.2	12.19		
		283.3	12.59	12.27	-38.31
		270.9	12.04		

4.00%, and 4.20% PET mixes, respectively. Despite the early strength gains observed at 7 days, these findings indicate that PET incorporation adversely affects medium-term strength development. None of the PET-containing mixes attained the target M20 compressive strength of 20 MPa at 28 days. Strength reductions of approximately 32.37%, 19.24%, and 31.06% were recorded for the 3.80%, 4.00%, and 4.20% PET mixes, respectively. This trend confirms that although PET can enhance early-age strength, higher replacement levels significantly impair compressive strength over extended curing periods. Overall, the results indicate that PET waste can effectively improve both compressive and tensile strengths of concrete when used in optimal amounts. The ideal dosage varies by strength parameter, with 3.80% PET being optimal for tensile strength and 4.00% PET for early-age compressive strength. This variation suggests that while PET contributes to densification and crack resistance at moderate levels, it may act as an inert filler beyond a

certain threshold, adversely affecting load distribution. These experimental findings support the sustainable reuse of PET plastic waste as a partial sand replacement, promoting environmental conservation while enhancing specific concrete properties. The strength development of the different concrete mixes over time is illustrated in Figure **??**.

3.2. **Split Tensile Strength.** Here, 12 cylindrical specimens were tested for their tensile strength. The highest split tensile strength was found to be 2.87 MPa with a 4% partial replacement of sand by PET plastic finer powder after 28 days of curing.The split tensile strength of various concrete mixes is shown in Figure 9 as it varies over 7, 21, and 28 days. When compared to the M20 control mix, the 7-day split tensile strength data show that the use of PET enhances early-age tensile performance. The mixes containing 3.80% and 4% PET showed the greatest improvement, with increases of 21.01% and 35.86%, respectively. A moderate 13.09% increase was seen even at 4.20% PET. PET has a beneficial influence on early-age tensile capacity, as seen by the control mix (0% PET).

TABLE 6. Variation of 7-Days Split Tensile Strength

S.N	% Addition of PET	Failure Load (kN)	Split Tensile Strength of 7 days (MPa)	% Change in Tensile Strength
1	0	90.9	1.29	–
2	3.8	110	1.56	21.01
3	4	123.5	1.75	35.86
4	4.2	102.8	1.45	13.09

FIGURE 8. Split Tensile Strength Test Specimens.

Split tensile strength at 21 days was considerably higher with PET incorporation than with the M20 objective of 1.74 MPa. The 3.80% PET concrete mix showed the greatest improvement at 62.84%, followed by 4.20% PET concrete mix (43.36%) and 4% PET concrete mix (24.61%). The target value was somewhat exceeded by the control mix. This demonstrates that, particularly at moderate contents, PET replacement improves medium-term tensile performance. With increases ranging from 23% to 44%, all PET-modified mixes performed better than the M20 tensile target of 1.98 MPa after 28 days.

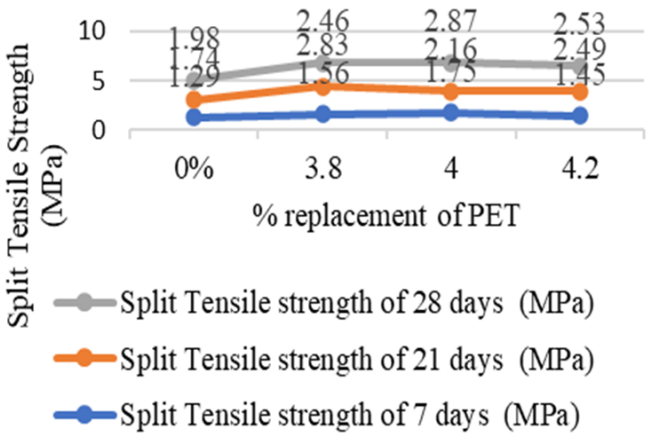

FIGURE 9. Comparison of Split Tensile Test Result.

The largest split tensile strength increase of 45.35% was attained by the 4% PET concrete mix, which was closely followed by the 4.20% PET concrete mix by 27.97% and 3.80% PET concrete mix by 24.32%. When applied in the right quantity, PET addition can improve long-term tensile capability, as demonstrated by the control mix.

TABLE 7. Variation of 21 Days Split Tensile Strength

S.N	% Addition of PET	Failure Load (kN)	Split Tensile Strength of 21 days (MPa)	% Change in Tensile Strength
1	0	122.7	1.74	–
2	3.8	199.8	2.83	62.84
3	4	152.9	2.16	24.61
4	4.2	175.9	2.49	43.36

TABLE 8. Variation of 28 Days Split Tensile Strength

S.N	% Addition of PET	Failure Load (kN)	Split Tensile Strength of 28 days (MPa)	% Change in Tensile Strength
1	0	139.8	1.98	–
2	3.8	173.8	2.46	24.32
3	4	203.2	2.87	45.35
4	4.2	178.9	2.53	27.97

The results of our examination correspond with an assortment of sources. Our usage of PET powder effectively addresses the requirement for sand substitutes, as highlighted by studies such as Beiser (2019). Similar to our findings at 3.8% replacement, research by Khajuria & Sharma and Khandelwal also revealed workability difficulties and strength benefits at optimal PET replacement levels. The ideal range indicated by Ahmed & Raju (2013) and OpenAI (2024) is 2–5%, which is quite comparable to our 3.8% outcome. According to research like Kumar & Kumar (2013) and Karthikeyan et al. (2019), our data aligns with the findings that lower PET replacement levels increase strength but higher amounts decrease it. The findings we found coincide with Meza et al. (2021) and Dawood et al. (2021), who further support the idea that PET waste enhances mechanical qualities and encourages sustainability.

4. Conclusion

This study demonstrates that PET powder from waste plastic bottles can be used to partially replace fine aggregate in concrete, providing a sustainable solution to environmental issues. PET in concrete promotes sustainable building practices by lowering dependency on natural resources and decreasing the amount of plastic waste that ends up in landfills. Future studies should examine performance in a range of environmental settings, long-term durability, and the possibility of large-scale implementation from an economic standpoint. The results of this study support sustainable development objectives by opening the door for creative and environmentally conscious solutions in the building sector.

Our research on using eliminated polyethylene terephthalate (PET) plastic to partially replace sand contains a number of gaps. First, little research has been done on the subject, especially within Nepal, and there is a lack of information about local aggregates, waste disposal methods, and environmental effects. The long-term environmental consequences of PET in building, including its effects on animals, water, and soil, are not widely understood. Furthermore, the financial viability and sustainability of substantial PET use have not been fully investigated, and further research is required in order to maximize the percentage of PET in different materials for construction.

References

[1] V. Beiser, "Why the world is running out of sand," *BBC Future*, Nov. 8, 2019. [Online]. Available: https://www.bbc.com/future/article/20191108-why-the-world-is-running-out-of-sand.

[2] National Geographic Society, "Plastic pollution," *National Geographic*. [Online]. Available: https://www.nationalgeographic.com/environment/article/plastic-pollution.

[3] A. K. R. A. Syed, "Utilization of Waste Plastic in Concrete," *ResearchGate*, Sep. 2019. [Online].

[4] A. Saikia and J. de Brito, "Use of plastic waste as aggregate in cement mortar and concrete preparation: A review," *Materials*, vol. 14, no. 2, p. 240, Jan. 2021. [Online]. Available: https://www.mdpi.com/1996-1944/14/2/240.

[5] M. Rahman, M. Imtiaz, M. Arulrajah, and H. Disfani, "Potential utilization of recycled plastic waste as construction materials: A review," *Case Studies in Construction Materials*, vol. 13, p. e00489, Jun. 2020. [Online]. Available: https://www.sciencedirect.com/science/article/pii/S2214509520301546.

[6] R. F. Zollo, "Fiber-reinforced concrete: An overview after 30 years of development," *Cement and Concrete Composites*, vol. 19, no. 2, pp. 107–122, Apr. 1997. [Online]. Available: https://www.sciencedirect.com/science/article/abs/pii/095894659400004I.

[7] A. A. Al-Manaseer and T. R. Dalal, "Concrete containing plastic aggregates," *Concrete International*, vol. 19, no. 8, pp. 47–52, Aug. 1997. [Online]. Available: https://www.semanticscholar.org/paper/Concrete-Containing-Plastic-Aggregates-Al-Manaseer-Dalal/3159475ef5fccb7607a0bbe37b866aaf6ad7bdfe.

[8] R. Siddique, J. Khatib, and K. Kaur, "Use of recycled plastic in concrete: A review," *Waste Management*, vol. 28, no. 10, pp. 1835–1852, Oct. 2008. [Online]. Available: https://www.sciencedirect.com/science/article/abs/pii/S0956053X06001048.

[9] C. Albano, N. Camacho, J. Reyes, J. L. Feliu, and M. Hernandez, "Influence of content and particle size of waste PET bottles on concrete behavior at different w/c ratios," *Cement and Concrete Research*, vol. 35, no. 5, pp. 891–897, May 2005. [Online]. Available: https://www.sciencedirect.com/science/article/abs/pii/S0008884604002169.

[10] R. Siddique, "Utilization of waste materials and by-products in producing controlled low-strength materials," *Resources, Conservation and Recycling*, vol. 50, no. 1, pp. 1–8, Mar. 2007. [Online]. Available: https://www.sciencedirect.com/science/article/abs/pii/S0956053X06002601.

[11] Z. Bayasi and J. Zeng, "Properties of polypropylene fiber reinforced concrete," *ACI Materials Journal*, vol. 90, no. 6, pp. 605–610, Nov.–Dec. 1993. [Online]. Available: https://www.semanticscholar.org/paper/PROPERTIES-OF-POLYPROPYLENE-FIBER-REINFORCED-Bayasi-Zeng/da1a4ed6b2c1ab5eb449bb1afb479cf298ee78c5.

[12] S. H. Choi, J. H. Lee, S. H. Kim, and Y. S. Choi, "Durability of waste polyethylene terephthalate plastic bottles fiber-reinforced concrete," *Construction and Building Materials*, vol. 23, no. 6, pp. 2269–2275, Jun. 2009. [Online]. Available: https://www.sciencedirect.com/science/article/abs/pii/S0950061808002869.

[13] S. M. Shaikh, M. N. Faruque, and M. M. S. Hossain, "Fiber and textile waste utilization in concrete: A review," *Materials and Design*, vol. 30, no. 4, pp. 1611–1620, Apr. 2009. [Online].

[14] A. P. de Souza, R. L. A. Silva, and L. F. M. da Silva, "Effect of polypropylene fiber on the mechanical properties of concrete," *Materials and Structures*, vol. 43, no. 5, pp. 649–659, Jun. 2010. [Online]. Available: https://link.springer.com/article/10.1617/s11527-010-9622-8.

[15] M. A. M. Al-Omran, H. M. Al-Athel, and A. I. Nasser, "Mechanical properties of concrete incorporating waste plastic as aggregate," *Cement and Concrete Composites*, vol. 33, no. 4, pp. 437–443, Apr. 2011. [Online]. Available: https://www.sciencedirect.com/science/article/abs/pii/S0921344911000656.

[16] R. Siddique, "Use of recycled plastics in concrete," *Waste Management*, vol. 28, no. 10, pp. 1835–1852, 2008.

[17] L. A. Oliveira, "Physical and mechanical behavior of recycled PET fibre reinforced mortar," *Construction and Building Materials*, vol. 25, no. 4, pp. 1712–1717, Apr. 2011.

[18] H. Wu, S. Lv, Y. He, and J.-P. Qu, "The study of the thermomechanical degradation and mechanical properties of PET recycled by industrial-scale elongational processing," *Construction and Building Materials*, vol. 77, p. 105882, Aug. 2019.

[19] F. S. Khalid, J. M. Irwan, M. H. Wan Ibrahim, N. Othman, and S. Shahidan, "Performance of plastic wastes in fiber-reinforced concrete beams," *Construction and Building Materials*, vol. 183, pp. 451–464, Sep. 2018.

[20] M. Guendouz, F. Debieb, O. Boukendakdji, and A. Kadri, "Use of plastic waste in sand concrete," *Construction and Building Materials*, Jan. 2016.

[21] M. Ahmed and A. I. Al-Hadithi, "The effects of adding waste plastic fibers on the mechanical properties and shear strength of reinforced concrete beams," *Iraqi Journal of Civil Engineering*, vol. 12, no. 1, Mar. 2018, doi: 10.37650/ijce.2018.142480.

[22] H. M. Adnan and A. O. Dawood, "Strength behavior of reinforced concrete beam using recycle of PET wastes as synthetic fibers," *Case Studies in Construction Materials*, vol. 13, p. e00367, Dec. 2020.

[23] M. Frigione, "Recycling of PET bottles as fine aggregate in concrete," *Waste Management*, vol. 30, no. 6, pp. 1101–1106, Jun. 2010.

[24] T. M. Joseph, S. Azat, Z. Ahmadi, O. M. Jazani, A. Esmaeili, E. Kianfar, J. Haponiuk, and S. Thomas, "Polyethylene terephthalate (PET) recycling: A review," *Case Studies in Chemical and Environmental Engineering*, vol. 9, p. 100673, Jun. 2024.

[25] S. Koirala, B. Hirachan, S. G. Chhetri, and T. R. Gyawali, "Utilizing residual waste particles from polyethylene terephthalate (PET) waste pellet production in cement mortar," *International Journal of Sustainable Engineering*, vol. 18, no. 1, pp. 1–13, 2025, doi: 10.1080/19397038.2024.2446755.

[26] N. Karki, "Compressive Strength Comparison Between Plain Concrete and Polyethylene Terephthalate (PET) Mixed Concrete," Kathmandu Engineering College, 2024. [Online]. Available: nimesh.karki@kecktm.edu.np.

[27] N. Bhattrai, "Experimental study on the properties of concrete with partial replacement of sand by plastic PET bottle fiber," *International Journal of Engineering and Applied Science*, vol. 7, no. 12, pp. 1–5, Dec. 2019.

Everest Advances in Science and Technology (EAST), Vol. 1, No. 1, 2025
ISSN: 3102-0410(print), 3102-0429(online)

A Study on Causes and Impacts of Disputes on Selected Road Construction Contracts under Department of Roads, Nepal

ANJU DHAKAL[1*]

Abstract. Construction projects, particularly road projects, are highly susceptible to disputes, leading to significant negative consequences. This research aimed to categorize road project disputes by severity, identify their root causes, analyze their impacts on contracts, and explore mitigation strategies. Data were collected through questionnaires distributed to 112 respondents, with an 82.14% response rate, and analyzed to determine major dispute causes, their effects, and potential solutions. Spearman's rank correlation was used to assess stakeholder (employer, consultant, contractor) perceptions. The study revealed that disputes primarily arise from land acquisition challenges, forest clearing delays, resettlement issues, mismanagement of contract terms, and fluctuations in labor, material, and equipment costs. These disputes severely impact road contracts, causing project delays, cost overruns, strained stakeholder relationships, reputational damage, and even project failure. To minimize such disputes, the study emphasizes fostering a trustworthy project environment, ensuring timely issue resolution, approving and delivering drawings promptly, and meeting other critical requirements. Proactive measures, such as clear contract documentation, effective communication, and stakeholder collaboration, are essential to reducing claims and disputes in future road projects. By addressing these key factors, construction stakeholders can enhance project efficiency, maintain harmonious relationships, and safeguard public image while ensuring successful project delivery. The findings underscore the importance of dispute prevention strategies to mitigate risks and improve overall project outcomes in the road construction sector.

Keywords: Road Projects, Contract, Disputes, Causes, Impacts, Minimization Measures.

[1]School of Engineering, Faculty of Science and Technology, Pokhara University, Pokhara, Nepal
E-mail: anzudhakal.er@gmail.com
* Corresponding author
Manuscript received: 17 March, 2025; revised: 26 August 2025; accepted: 5 September, 2025.
Everest Advances in Science and Technology (EAST), Vol. 1, No. 1, 2025

1. Introduction

The construction industry is inherently complex and prone to disputes, even among well-intentioned parties. Such disagreements often escalate into costly conflicts that negatively impact project budgets, timelines, and resource allocation. Nepal's rapidly expanding construction sector faces significant challenges, particularly in road infrastructure projects funded by agencies such as the Asian Development Bank (ADB) and the World Bank (WB). Several studies indicate that a significant proportion of road infrastructure projects in Nepal face disputes, resulting in delays, increased costs, and legal challenges despite growing investment in the sector. Disputes in construction projects arise from multiple factors, including delays in land acquisition, contractual ambiguities, and fluctuating costs. Several international reports focusing on construction disputes in various regions identify poor contract administration, design errors, and external factors such as adverse weather and regulatory changes as primary causes of dispute [1].

In the Nepalese context, disputes frequently originate from resettlement issues, utility relocations, and unrealistic contract terms, which further exacerbate project delays and cost overruns [2]. Additionally, common dispute types in construction projects include variations (adjustments), unforeseen site conditions, and delay [3]. The consequences of these disputes are severe, extending beyond direct financial losses to include strained stakeholder relationships, reputational damage, and even project failure. A study of seven road projects under Nepal's Department of Roads (DoR) found that approximately NRs 2.15 million was spent on Alternative Dispute Resolution (ADR), significantly higher than the typical cost of around NRs 370,000 [4]. This figure excludes intangible losses such as missed business opportunities, reduced workforce motivation, and property damage. Disputes have been identified as contributing factors to budget overruns, schedule delays, reduced productivity, quality deterioration, resource wastage, poor decision-making, increased costs, and elevated stress levels [4].

Effective dispute resolution mechanisms are therefore critical to mitigating these impacts. Nepal currently employs methods such as mutual negotiation, mediation, Dispute Resolution Boards (DRBs), and arbitration through the Nepal Council of Arbitration (NEPCA) [2]. However, several studies and reports reveal systemic inefficiencies, exemplified by prolonged disputes in infrastructure projects like the Pathlaiya-Birgunj road widening and the Narayanghat-Muglin improvement projects, underscoring the need for improvement in dispute resolution practices. Addressing these challenges requires proactive measures, including the development of clearer contractual terms, prompt decision-making, and enhanced collaboration among stakeholders. This study investigates the causes, impacts, and recommends mitigation measures for disputes in Nepal's road construction projects. Drawing on the perspectives of employers, contractors, and consultants, it identifies key dispute drivers and assesses their implications for cost and schedule performance. The findings are intended to inform more effective dispute prevention and resolution strategies, thereby enhancing project execution efficiency and minimizing financial losses.

2. Theory and Methods

This study utilized both primary and secondary data, incorporating quantitative and qualitative approaches to ensure comprehensive analysis. Primary data was collected through structured questionnaires and Key Informant Interviews (KIIs) to capture stakeholder

perceptions on construction disputes, their causes, impacts, and mitigation measures in Nepalese road projects. Respondents—including employers, consultants, and contractors—rated dispute-related factors on a 5-point Likert scale (1 = Strongly Disagree to 5 = Strongly Agree). Additionally, KIIs were conducted with arbitrators and road construction specialists to gather expert insights. Secondary data was sourced from legal dispute records of the Department of Roads (DoR), government reports (e.g., Public Procurement Monitoring Office, NEPCA), academic research, and policy documents. The study employed quantitative methods (Relative Importance Index, Spearman's rank correlation) to analyze survey data, while qualitative insights were derived from interviews. For analysis, nine road contracts under the Department of Roads (DoR), in which disputes arose and were registered in NEPCA for resolution during the fiscal year 2076/77, were selected to ensure targeted relevance to Nepal's road construction sector. The details of these contracts are as follows:

- Ghorahi-Holeri Section of Sahid Marg (Ghorahi-Ghartigaun)
  Contract No: RIP/337133/SM-02/2070-071
- Halesi–Diktel Road Contract No: SCRP/NCB/HD/02
- Narayanghat-Muglin Road
  Contract No: NIRTTP-DOR-W-ICB-2
- Black-topped Road (DBSD) at Hatiya-Burtibang Sector
  Contract No: MHHP/3371384/070-71/031
- Chandranigahpur–Gaur Road Project
  Contract No: RIP/EXIM/CG-07
- Dhading-Gorkha Road, Ghyampesal-Gorkha Section
  Contract No: EEAP/NCB/DG/03
- Rani–Biratnagar–Itahari–Dharan Road sector
  Contract No: TRIP/337312/RBID/071-72/01
- RCC Bridge Over Ghatte Khola
  Contract No: 58/067/068-650
- RCC Bridge for Dhankaul, along Naya Road Madhuwani Road, Sarlahi
  Contract No: HRP/3372244/071-72/BC-005

2.1. **Relative Importance Index (RII).** The relative importance of the causes, impacts, and minimization strategies of disputes in construction was obtained using the Relative Importance Index (RII). The respondents' scores were aggregated to determine the overall score for each factor. The RII was calculated using the following formula [5]:

$$\text{RII} = \frac{\sum W}{A \times N} = \frac{5n_5 + 4n_4 + 3n_3 + 2n_2 + 1n_1}{5N} \tag{1}$$

where:

- W = weighting given to each variable by the respondent (ranging from 1 to 5),
- n_1 = number of respondents for Strongly Disagree,
- n_2 = number of respondents for Disagree,
- n_3 = number of respondents for Neutral,
- n_4 = number of respondents for Agree,
- n_5 = number of respondents for Strongly Agree,
- A = highest weight (i.e., 5),
- N = total number of responses.

The RII ranges from 0 to 1 [6].

2.2. **Spearman's Rank Correlation.** Spearman's correlation coefficient (ρ) is a statistical measure of the strength and direction of association between two ranked variables [7]. It evaluates how well the relationship between two variables can be described using a monotonic function. The coefficient is bounded by $-1 \leq \rho \leq 1$. The formula is:

$$\rho = 1 - \frac{6 \sum d^2}{n(n^2 - 1)} \tag{2}$$

where:

- d = difference between the ranks of paired data,
- n = number of observations.

The interpretation of ρ is based on the strength of correlation:

- -1 = perfect negative correlation,
- 0 = no correlation,
- 0 to 0.19 = very weak,
- 0.20 to 0.39 = weak,
- 0.40 to 0.59 = moderate,
- 0.60 to 0.79 = strong,
- 0.80 to 1.00 = very strong,
- +1 = perfect positive correlation.

3. Results and Discussion

The findings of the study, derived from the analysis of nine selected road contracts and the responses collected through a structured research questionnaire, are presented in this section. The data provide insights into factors causing disputes and their impacts within Nepal's road construction sector.

3.1. **Qualitative Approach.** Based on a detailed case study of selected road contracts, Table 1 summarizes the primary causes and impacts of disputes that arose during the construction phase. The review identified that the most common causes were related to price adjustments and delays in the approval of extensions of time (EOT). Other notable factors included unresolved variation claims, unjust imposition of liquidated damages, delays in land acquisition, and perceived ill intent by the employer. These disputes resulted in increased project costs, schedule overruns, and cash flow difficulties for contractors. Additional consequences included rising administrative and legal expenses due to arbitration or litigation. Furthermore, the conflicts led to deteriorating relationships between employers and contractors, loss of trust, reputational damage to contractors, and adverse ripple effects on various project stakeholders—highlighting the need for better contract management and timely dispute resolution.

3.2. **Quantitative Approach.** The quantitative approach employed in this study involved the collection and systematic analysis of numerical data to assess the relative importance of various factors contributing to construction disputes. A structured questionnaire, developed based on an extensive literature review, was administered to professionals involved in nine selected road construction projects. Respondents included representatives from employers, contractors, and consultants. The questionnaire was distributed via hard copies and Google Forms. A total of 112 questionnaires were sent to stakeholders (45 employers, 32 consultants, and 35 contractors), yielding 92 responses (40, 27, and 25, respectively). The distribution of responses is illustrated in Figure 1.

TABLE 1. Summary of Dispute Causes and Impacts in Selected Road Projects

SN	Project	Contract No.	Causes of Disputes	Impacts of Disputes
1	Ghorahi-Holeri Section of Sahid Marg (Ghorahi-Ghartigaun)	RIP/337133/SM-02/2070-071	Delay in payments of IPC, variation issue, delay in approval of Extension of Time (EOT)	Increased contract price, overall project cost, and delay in project completion time.
2	Halesi – Diktel Road	SCRP/NCB/HD/02	Wrongful deduction of liquidated damage, claim for extended overhead	Additional managerial and administrative costs, increased overall project cost.
3	Narayanghat-Muglin Road	NIRTTP-DOR-W-ICB-2	Land acquisition issues, delay in payments, force majeure events (flood, earthquake), price adjustment on prolongation	Increased project cost, deterioration of employer-contractor relationship.
4	Black-topped Road (DBSD) at Hatiya-Burtibang Sector	MHHP/3371384/070-71/031	Price adjustment issues, delay in IPC payments, delay in EOT approval	Extra arbitration expenses, increased cost, delay in completion.
5	Chandranigahpur – Gaur Road Project	RIP/EXIM/CG-07	Price fluctuation of materials, labor and equipment; price adjustment issues, delayed payment	Increased project cost, strained relationships.
6	Dhading-Gorkha Road, Ghyampesal-Gorkha Section	EEAP/NCB/DG/03	Price adjustment, insurance payment issues, extra claims for equipment/materials, liquidated damages	Negative ripple effect, damaged contractor reputation.
7	Rani – Biratnagar – Itahari – Dharan Road Sector	TRIP/337312/RBID/071-72/01	Price adjustment issues, delay in EOT approval	Legal charges, increased costs, delay in completion.
8	RCC Bridge Over Ghatte Khola	58/067/068-650	Price adjustment issues, delay in EOT approval	Negative impact on stakeholders, reduced mutual respect.
9	RCC Bridge for Dhankaul, Naya Road, Madhuwani Road, Sarlahi	HRP/3372244/071-72/BC-005	Poor contract implementation, contract termination, price adjustment issues, employer's malintent	Damaged relationships, increased cost, delays, contractor cash flow problems.

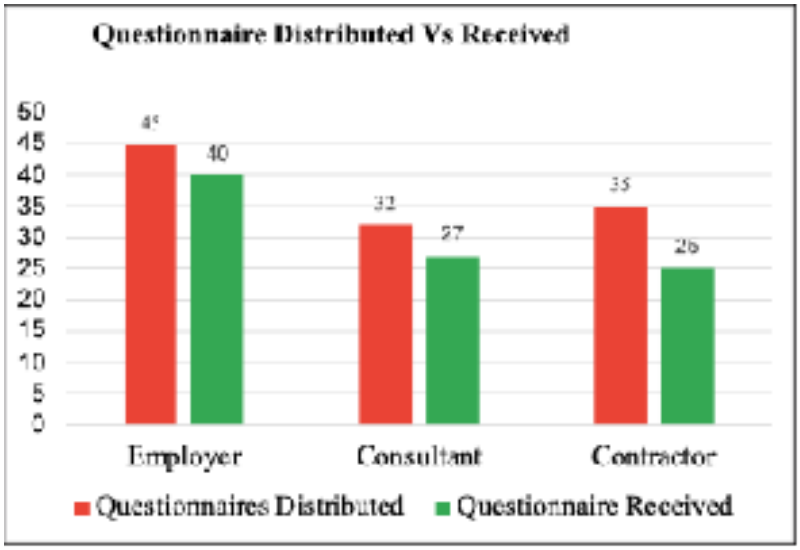

FIGURE 1. Questionnaire Distributed vs Received.

The data collected from the questionnaire survey were analyzed based on respondents' ratings, and the Relative Importance Index (RII) for each dispute-causing factor was calculated using Microsoft Excel. The identified factors were categorized into four thematic groups. Among all the factors, only the top five with the highest RII values are presented in the tables below, highlighting the most critical contributors to disputes in the studied construction projects.

3.3. **Thematic Analysis of Dispute Causes Across Stakeholder Perspectives.**

3.3.1. *Employer-related Dispute Factors.* The analysis of dispute causes revealed both consensus and divergence among stakeholders, as shown in Table 2. All groups identified delay in the approval of extensions of time (EOT) as the most critical employer-related factor, with a combined RII of 0.863. Similarly, land acquisition issues were consistently ranked second most critical (combined RII = 0.835) across all groups, confirming earlier findings [8, 9], who emphasized the impact of unresolved pre-construction challenges on dispute occurrence. However, a notable variation was observed in the perception of payment delays, where contractors assigned greater importance (RII = 0.808) than employers (RII = 0.780), reflecting differing financial priorities consistent with the observations of article [5]. Despite these differences, Spearman's rank correlation analysis demonstrated a strong overall agreement among stakeholders, as reflected in the results presented in Table 2.

TABLE 2. Employer-related dispute factors

Factors	Employer (RII)	Consultant (RII)	Contractor (RII)	Combined (RII)	Overall Rank
Delay in approval of extension of time (EOT)	0.840	0.896	0.864	0.863	1
Issue of land acquisition	0.810	0.867	0.840	0.835	2
Variation orders issue	0.735	0.815	0.789	0.813	3
Untimely delivery of design drawings	0.805	0.800	0.800	0.750	4
Payment delays	0.780	0.851	0.808	0.685	5

TABLE 3. Spearman's ρ for employer-related factors

Stakeholder Pair	ρ	p-value	Strength
Employer-Consultant	0.82	<0.001	very strong
Employer-Contractor	0.68	0.002	strong
Consultant-Contractor	0.84	<0.001	very strong

3.3.2. *Contractor-related Dispute Factors.* Contractor-related causes showed more variation between stakeholders, as presented in Table 4. While employers and contractors agreed that slow progress of work was the most problematic factor (RII = 0.860 and 0.808, respectively), consultants ranked poor quality work as the highest concern (RII = 0.867) [**?**].

TABLE 4. Contractor-related dispute factors

Factors	Employer (RII)	Consultant (RII)	Contractor (RII)	Combined (RII)	Overall Rank
Slow progress of work	0.860	0.852	0.808	0.841	1
Poor planning and management	0.769	0.844	0.733	0.826	2
Poor quality of work	0.840	0.867	0.748	0.817	3
Overcommitment	0.805	0.800	0.826	0.757	4
Contractor's financial problem	0.780	0.785	0.817	0.748	5

TABLE 5. Spearman's ρ for contractor-related factors

Stakeholder Pair	ρ	p-value	Strength
Employer-Consultant	0.78	<0.001	strong
Employer-Contractor	0.62	<0.001	moderate
Consultant-Contractor	0.58	<0.001	moderate

The Spearman's rank correlation results (Table 5) indicate a strong agreement between employers and consultants ($\rho = 0.78$), suggesting a high level of alignment in their perceptions of dispute factors. In contrast, the correlations between employers and contractors ($\rho = 0.62$) and between consultants and contractors ($\rho = 0.58$) were moderate, implying some differences in priorities and perspectives between these stakeholder groups.

3.3.3. *Contract-related Dispute Factors.* Contract-related issues consistently emerge as primary dispute drivers across all stakeholder groups. The data reveals particularly strong consensus regarding poor contract implementation as the most significant factor (combined RII = 0.859), with consultants expressing the highest concern (RII = 0.881). This suggests systemic challenges in applying contract terms consistently throughout project execution [9, 5].

TABLE 6. Contract-related dispute factors

Factors	Employer (RII)	Consultant (RII)	Contractor (RII)	Combined (RII)	Overall Rank
Poor contract implementation	0.835	0.881	0.872	0.859	1
Price fluctuation of construction materials, labor, etc.	0.880	0.770	0.864	0.843	2
Contract ambiguities	0.825	0.778	0.784	0.800	3
Price adjustment clause	0.785	0.741	0.752	0.763	4
Force majeure clause	0.690	0.748	0.800	0.737	5

TABLE 7. Spearman's ρ for contract-related factors

Stakeholder Pair	ρ	p-value	Strength
Employer-Consultant	0.85	<0.001	very strong
Employer-Contractor	0.77	<0.001	strong
Consultant-Contractor	0.88	<0.001	very strong

The high correlation coefficients ($\rho > 0.77$) with statistically significant p-values (< 0.001) indicate remarkable consistency in how different stakeholders prioritize contract-related problems. However, the slightly lower employer-contractor alignment ($\rho = 0.77$) reflects differing perspectives on risk allocation — employers often favor rigid terms while contractors emphasize flexibility for unforeseen conditions.

3.3.4. *Common Issues in Both Parties Causing Disputes.* Common issues represent shared problems that transcend traditional employer-contractor boundaries. The data shows remarkable consistency across stakeholders regarding lack of coordination and trust as the top concern (combined RII = 0.867), with consultants particularly emphasizing carelessness in dispute resolution (RII = 0.941). These interpersonal and systemic factors often amplify technical contract issues [8, 9, 10].

TABLE 8. Common issues causing disputes

Factors	Employer (RII)	Consultant (RII)	Contractor (RII)	Combined (RII)	Overall Rank
Lack of coordination/trust, etc.	0.850	0.881	0.880	0.867	1
Carelessness in dispute resolution	0.830	0.941	0.840	0.861	2
Late material supply	0.600	0.807	0.792	0.843	3
Issue of delay payment	0.820	0.837	0.846	0.822	4
Personal ego	0.800	0.719	0.688	0.695	5

TABLE 9. Spearman's ρ for common issues

Stakeholder Pair	ρ	p-value	Strength
Employer-Consultant	0.81	<0.001	very strong
Employer-Contractor	0.73	<0.001	strong
Consultant-Contractor	0.86	<0.001	very strong

The correlation analysis reveals particularly strong consultant-contractor alignment ($\rho = 0.86$) on common issues, suggesting field personnel share similar frustrations about collaboration challenges. The slightly lower employer-contractor correlation ($\rho = 0.73$) may reflect differing priorities between management and execution teams.

3.4. **Impacts of Disputes.** Table 10 summarizes the combined stakeholder assessment of dispute impacts, with project delays (RII = 0.933) and cost overruns (RII = 0.898) ranking as the most severe. Administrative burdens (RII = 0.865) and project failure risks (RII = 0.796) follow as significant secondary effects, while quality compromises (RII = 0.765) and reputational damage (RII = 0.722) emerge as persistent long-term concerns. This hierarchy reveals that, while immediate financial and schedule impacts dominate stakeholder perceptions, relational and operational consequences also substantially influence project outcomes. The consensus across employer, contractor, and consultant groups underscores the need for holistic dispute mitigation addressing both economic and collaborative dimensions of construction projects [8, 9, 10].

TABLE 10. Impacts of Disputes

Impacts of Disputes	**RII**	**Rank**
Delayed in project completion time	0.933	1
Increased Overall Project Cost	0.898	2
Additional expenses in management and administration of contract	0.865	3
Project Failure	0.796	4
Delay in getting benefit from project	0.795	5
High Arbitration and Litigation Cost	0.783	6
Low Quality of work	0.765	7
Poor site Safety	0.733	8
Loss of company/organization reputation	0.722	9
Deterioration of relationship between stakeholders (Employer, Contractor, Consultant)	0.698	10

3.5. **Proposed Strategies for Disputes Minimization.** Key Informant Interviews (KII) with experienced practitioners, including arbitrators and road construction specialists, identified several strategies for minimizing disputes in construction projects. Foremost among these was the timely issuance, approval, and delivery of drawings and other essential project requirements, as delays in these processes have been consistently cited as a major dispute trigger [11, 2]. Respondents also stressed that contracts should be awarded only after resolving land acquisition and socio-environmental issues, in line with the findings of articles [8, 9]. Regular progress meetings were recommended to address emerging issues before they escalate, a measure supported by previous studies highlighting proactive communication as an effective dispute prevention tool [3, 10]. Budget assurance and the establishment of a clear payment schedule prior to contract execution were emphasized as critical to preventing payment-related disputes, aligning with contractor-focused research from [5]. In addition, fostering teamwork and building a culture of trust among stakeholders were seen as essential, echoing [12] observations on collaborative practices in hydropower projects. Other recommended measures included the mandatory appointment of a contract manager or dispute manager in large-scale road projects, robust documentation practices [13], thorough site investigations prior to tendering, and the inclusion of explicit contract clauses relating to scheduling and time extensions. Together, these measures address both preventive and procedural dimensions of dispute management, targeting root causes while strengthening resolution mechanisms during road project execution.

4. Conclusion

The study identified delays in approving extensions of time (EOT) and land acquisition issues as the most significant drivers of construction disputes, with a strong consensus

among stakeholders. Payment delays were considered less critical overall, though contractors rated them higher, reflecting different financial priorities. Employers and consultants showed strong agreement in their views, while contractors' perspectives differed moderately. These disputes typically lead to project delays, cost escalations, and damaged stakeholder relationships, ultimately impacting project performance. To address these challenges, the study recommends both preventive and procedural measures, including early resolution of land and socio-environmental issues, timely delivery of design documents, securing budget availability, regular coordination meetings, appointment of dedicated dispute or contract managers, rigorous documentation, thorough site investigations before tendering, and clear contractual provisions on scheduling and time extensions. Together, these strategies aim to reduce conflicts, strengthen collaboration, and support successful project delivery in the road construction sector.

References

[1] M. Allen, "Global Construction Disputes," *International In-house Counsel Journal*, vol. 9, 2016.

[2] D. R. Aryal and S. Aryal, "A Review of Causes and Effects of Disputes in the Construction Projects of Nepal," *Journal of Steel Structure & Construction*, vol. 4, no. 2, 2018.

[3] I. M. C. S. Illankoon, V. W. Y. Tam, K. N. Le, and K. A. T. O. Ranadewa, "Causes of disputes, factors affecting dispute resolution and effective alternative dispute resolution for Sri Lankan construction industry," *International Journal of Construction Management*, vol. 22, no. 2, pp. 218–228, 2022, doi: 10.1080/15623599.2019.1616415.

[4] K. Mishra, "Dispute resolution practice of project management in Nepal," *SSRN*, 2022. [Online]. Available: https://ssrn.com/abstract=4182726

[5] M. T. Alqershy, M. T. Al-Qershi, and R. Kishore, "Claim Causes and Types in Indian Construction Industry—Contractor's Perspective," *American Journal of Civil Engineering and Architecture*, vol. 5, no. 5, pp. 196–203, 2017, doi: 10.12691/ajcea-5-5-3.

[6] K. T. Wong, Y. H. Shen, and S. O. Cheung, "Construction Negotiation Online," *Journal of Construction Engineering and Management*, vol. 130, no. 6, 2004.

[7] J. H. Zar, "Spearman rank correlation," *Encyclopedia of Biostatistics*, vol. 7, 2005.

[8] S. Khadka, "Analysis of Causes of Disputes and its Impacts on Selected Irrigation Projects under Department of Water Resources and Irrigation, Nepal," M.Sc. thesis, *Construction Management*, 2021.

[9] B. H. Hadikusumo and S. Tobgay, "Construction claim types and causes for a large-scale hydropower project in Bhutan," *Journal of Construction in Developing Countries*, vol. 20, no. 1, pp. 49–65, 2015.

[10] K. P. Kisi, J. K. Krishna, and N. L. R. Kumar, "Alternative Dispute Resolution Practices in International Road Construction Contracts," *Journal of Legal Affairs and Dispute Resolution in Engineering and Construction*, vol. 12, no. 2, 2020.

[11] N. K. Acharya, Y. D. Lee, and H. M. Im, "Conflicting factors in construction projects: Korean perspective," *Engineering, Construction and Architectural Management*, vol. 13, no. 6, pp. 543–566, 2006.

[12] G. P. Kayastha, "Common Causes of Disputes in Hydropower Projects of Nepal," M.Sc. thesis, *Nepal Engineering College - Center for Postgraduate Studies (nec-CPS), Pokhara University*, 2006.

[13] A. Enshassi and A. Abu Rass, "Dispute resolution practices in the construction industry in Palestine," in *International Conference on Multi-National Construction Projects*, China, Nov. 2008.

Everest Advances in Science and Technology (EAST), Vol. 1, No. 1, 2025
ISSN: 3102-0410(print), 3102-0429(online)

Analysis of the Factors Affecting Material Management in Selected Hydropower Construction Projects in Nepal

BINOD MAHARJAN[1*]

Abstract. The main goal of this research is to identify the most influencing factors that are affecting material management system in under construction hydropower projects in Nepal. Material management in hydropower construction projects is one of the important issues of Nepal with costing around NRs. 500 to 600 billion considering 50% to 60% of total cost of hydropower construction projects. As of fiscal year 2018-19, hydropower projects with total capacity of 4642 MW are already under construction. Material mismanagement in hydro projects could cause huge amount of nation's capital to be expensed on unproductive cost overrun caused due to delays. A total of 15 under construction hydropower projects are taken as the study area for data collection. The respondents are requested to rank their answers in five-point Likert scale. The responses for total numbers of 34 factors categorized into 10 headings viz. Planning, Supplier, Finance, Staff, Transport, Storage and Handling, Management, Contractual Issue, Governmental Interference and Environment / Weather are collected. The factors are then ranked using Relative Importance Index technique. Based upon the responses, material requirement planning under planning group is ranked as most influential factor affecting material management system. Based upon the study, it is concluded that most of the hydro projects are using Enterprise Resource Planning software viz. tally and other third-party software for material management and some of them are using Microsoft Excel. Most of the studied hydropower construction projects are located at remote areas where facilities of electricity from national power grid, internet facility is unavailable. Because of this, material requisition is still executed using phone conversation in some projects. Record keeping is still paper based rather than digital method.

Keywords: Material management, hydropower, low productivity, cost overrun, enterprise resource planning.

[1]Nepal Engineering College, Bhaktapur, Pokhara University, Nepal
E-mail: maharjan024@gmail.com
* Corresponding author
Manuscript received: 27 March, 2025; revised: 21 August 2025; accepted: 5 September, 2025.
Everest Advances in Science and Technology (EAST), Vol. 1, No. 1, 2025

1. Introduction

The material cost in a project can vary from 50% to 60% of the total project cost, so minimizing procurement cost improves opportunities for reducing the overall project cost. Improper material management can result in increased cost during construction. If materials are purchased too early, capital may be held up and interest charges incurred on the excess inventory of materials. Materials may deteriorate during storage or be stolen if proper care is not taken. In addition, if materials are purchased too late, it can lead to project delays. Ensuring the timely flow of materials in any construction project is one of the major challenges in material management [1]. The major characteristics of hydropower projects in the context of Nepal can be listed as multidisciplinary nature, relatively long duration, and remoteness. The hydropower projects are multidisciplinary in the sense that they comprise numerous sectors. Materials used in HCPs (Hydropower Construction Projects) can be categorized based on their use in different phases or sectors of construction. Generally, the materials used in different phases can be categorized as materials required for civil works, tunnel works, hydro-mechanical works, electro-mechanical works, and transmission line works. Management of numerous activities within these phases of HCPs is an important aspect and directly affects the project schedule. Effective material management in each construction phase is critical to ensuring timely execution and successful project delivery.

1.1. **Problem Statement.** Most hydropower projects in Nepal are experiencing cost overruns due to project delays, resulting in significant financial losses. Numerous factors can contribute to these delays. Among them, material management stands out as one of the most important, given its significant share in the total project cost. Therefore, it is essential to conduct a study on the factors affecting material management in hydropower construction projects in Nepal.

2. Literature Review

As of 2018–19, the total installed electricity generation capacity in Nepal was only 1,182 megawatts (MW), including 621 MW owned by the Nepal Electricity Authority and 560 MW owned by private investors, whereas the peak electricity demand was 1,320 MW [3]. Among numerous feasible hydropower projects, a total of 302 projects had already received survey licenses, and 172 projects had secured generation licenses. Hydropower projects with a total capacity of 4,642 MW were under construction [3]. The construction costs of hydropower projects in Nepal are estimated to vary between $2,000–2,500 per kilowatt [4]. Considering the cost of hydropower generation in Nepal at $2,000–2,500 per kilowatt, the total cost of under-construction hydropower projects (4,642 MW) is estimated to be nearly NRs. 1,021 billion. This signifies that the country's largest share of infrastructure investment is concentrated in hydropower construction projects.

According to Lenin et al. [1], material management in hydropower construction projects (HCPs) constitutes a major component—approximately 50% to 60%—of the total project cost. The estimated cost for under-construction HCPs is around NRs. 500 to 600 billion. Negligence in material management can lead to project delays and subsequent cost overruns, resulting in substantial unproductive expenditure of the nation's capital. Adoption of best practices in material management, particularly through identifying the factors influencing material management, is crucial to avoiding these inefficiencies and saving a significant amount of public funds.

Mat Jusoh et al. [5] identified a total of 50 influential factors for effective material management, categorized into eight components: management, purchasing, expediting, transportation, site storage and condition, supplier, contractual, and governmental interference. Among these, the management category contained the highest number (12) of influential factors. The results of this study contributed to the development of an effective material management model aimed at enhancing project performance and supporting decision-making processes among practitioners.

The reviewed literature consistently suggests that material management in construction projects is influenced by numerous factors. Ineffective material management can lead to delays, cost overruns, reduced quality, and other negative outcomes. These influencing factors vary depending on the type and scope of the project. However, a common classification of factors includes: planning, supplier, finance, staff, transport, storage and handling, management, and environmental/weather conditions. Each of these factors contributes to material management challenges with different levels of severity. A key outcome of previous research is the identification and ranking of the most influential factors, which helps prioritize efforts in improving material tracking and control. The literature recommends that organizations address these factors in the order of their significance to ensure successful project completion in terms of cost, time, and quality.

This research aims to build upon the aforementioned studies by identifying the most influential factors affecting material management in hydropower construction projects in Nepal. Similar to earlier works, this study categorizes the collected data based on feedback from respondents using measurement scales. Furthermore, it explores the tools and techniques currently employed in HCP material management. While previous studies have examined building and highway projects, the specific case of HCPs has not been thoroughly investigated. Therefore, this research helps to fill this gap by focusing on the influential factors in the material management of HCPs in the Nepalese context.

3. Methodology

Professional engineers working with contractors including project manager, project engineers, site engineers, store in-charge, supervisor of various HCP in Nepal are the respondents for this study. Fifteen under construction hydropower projects in Nepal are selected for the study. The developers of the selected projects are still in the business and are pioneer in the field so these projects resemble the majority of projects in the hydropower construction sector in Nepal. The reason behind choosing the under-construction projects is that the present condition of material management in hydropower construction site can be identified. The studied HCP are scattered all over Nepal comprising of nine districts under four provinces namely Koshi, Bagmati, Gandaki and Sudurpaschim. It is believed that overall picture of the material management situation related to HCP for all geographical regions of Nepal are incorporated in this study.

Considering the literatures, the list of influential factors affecting material management in construction project are prepared. Among the list, 34 influential factors in material management, significant and relevant to the HCP is identified and categorized into 10 groups for this study namely; Planning, Supplier, Finance, Staff, Transport, Storage & Handling, Management, Contractual Issue, Governmental Interference and Environment / Weather. The influential factors affecting material management under separate groups

are presented to respondents through questionnaire. It is backed by the research done by [5] in which 50 influential factors for effective material management is presented in questionnaire, categorized into 8 specific components/groups. Similarly, based upon the researches by Ahmad, et al. (2018) [10] responses for twenty factors affecting material management were collected through questionnaire. Also, according to the research by E & Venkatasubramanian (2017) [11] a total 23 factors affecting material management were studied categorizing into 8 separate groups.

3.1. **Data Collection.** Both qualitative and quantitative approaches are used for the collection of most influential factors affecting material management in selected HCP of Nepal. The questionnaire is designed such that respondents can rank to their answers based on the Likert scale. The five point Likert scale is adopted for scaling the responses, having 1 signified strongly disagree and 5 signified strongly agree. Data are collected from the filled questionnaires from respondents including professionals working with contractors/consultant and developers of selected HCP. Due to COVID-19 situation, questionnaires are collected using Google document form rather than face to face meeting. The special sets of structured key questions are included for project managers of selected HCP to identify the current tools and techniques used and possible measures for effective material management. Considering six responses from each studied project, 90 questionnaires are distributed, from which only 55 responses from overall projects are received i.e. 61% of the responses are received from the questionnaire. Table 1 below shows the result of numbers of responses according to their position in the HCP. The selected HCP are all under construction so current tools and techniques of the material management being used are identified and evaluated in real time.

Table 1. Numbers of Responses According to Position in HCP

Position in HCP	**Number of Responses**
Assistant Project Manager	1
Civil Engineer	3
Costing Engineer	2
Electrical Engineer	2
Electrical Site In charge	1
Electro Mechanical Engineer	1
Powerhouse In charge	1
Project Engineer	5
Project Manager	5
Resident Engineer	1
Senior Engineer	1
Site Engineer	20
Site In charge	6
Store In charge	4

3.2. **Data Analysis.** The data collected from both primary and secondary source are summarized, classified, tabulated and categorized. Computer software such as MS Excel, SPSS are used for the tabulation and compilation of the data. SPSS is used for generation of frequency table of various factors affecting material management. Relative Importance Index (RII) technique is used for the data analysis for the research. For validity, all the factors are retrieved from previous researches related to material management so it is

considered valid whereas the Cronbach's Alpha is used to determine the internal reliability. The Cronbach's Alpha for reliability for a total of 55 samples including 34 questions is calculated as 0.89 which is considered reliable.

4. Result and Discussion

4.1. **Existing Practice of Material Management System.** Based upon the responses from the HCP, the existing material management process starts with calculation of the material quantity requirements based upon the bill of quantity of the project. Then synchronizing with construction schedule, forecast of the material requirements prior to the execution is prepared and provided to procurement department. Likewise, procurement department arranges for selection, purchase and delivery of materials. The responses from the studied HCP suggest that every construction company is carrying out material management at their projects. It is done with schedule of the procurement of materials prepared and found to be similar in all of the studied projects.

4.2. **Existing Tools and Techniques Used in Material Management System.** The study found that, only few projects are using third party ERP (enterprise resource planning) software for material management because most of the studied construction sites are located at remote areas where facility of electricity from national grid and internet communication facilities are unavailable. It is also very difficult to connect internet communication facility. The cost of internet connection, according to respondents can vary from NRs. 2.5 million to 3.0 million for the project duration excluding maintenance and operation cost. The implementation of modern ICT (Information and communications technology) technologies such as wireless communications, bar coding, RFID (Radio frequency identification) in these construction sites is very challenging.

4.3. **Factors Affecting Material Management System.** Ranking of the factors affecting material management system is done by responses through questionnaire are calculated according to the highest RII value as is shown in table 2 below. The table 2 shows the results of opinion for each factor from selected HCP. Figure 1 mentioned below is the chart comprising of list of factors affecting material management in studied HCP according to RII rank order. The numerical value at left side of figure 1 indicates the corresponding RII value for each factor, whilst the numerical value at right side of the figure 1 indicates the corresponding rank of each factor affecting material management in studied HCP.

4.3.1. *Planning.* Material requirement planning has highest rank among other 34 factors with RII of 0.916 followed by organizing and scheduling procurement with RII 0.891 and site work schedule with RII 0.855. The result from the research by E & Venkatasubramanian (2017) also supports that the material requirement planning is the most significant factor related to material management. This similarity indicates that material required planning is the highest effecting factors because planning is the first and foremost activity, which is done before starting of any project. Once starting of the project gone wrong then other procedure followed by it is likely to be mistaken. The result is also supported with the study by [12] which suggests that organizational weakness is the most affecting factors in material management. The organizational weakness can be directly linked to poor material required planning because any organization with weak management, staffing ultimately leads to the poor planning. Another reason behind the similarities in result can be the four basic information's of the material requirement planning viz. when to place an order, how much quantity to be ordered, who should be the supplier and when the

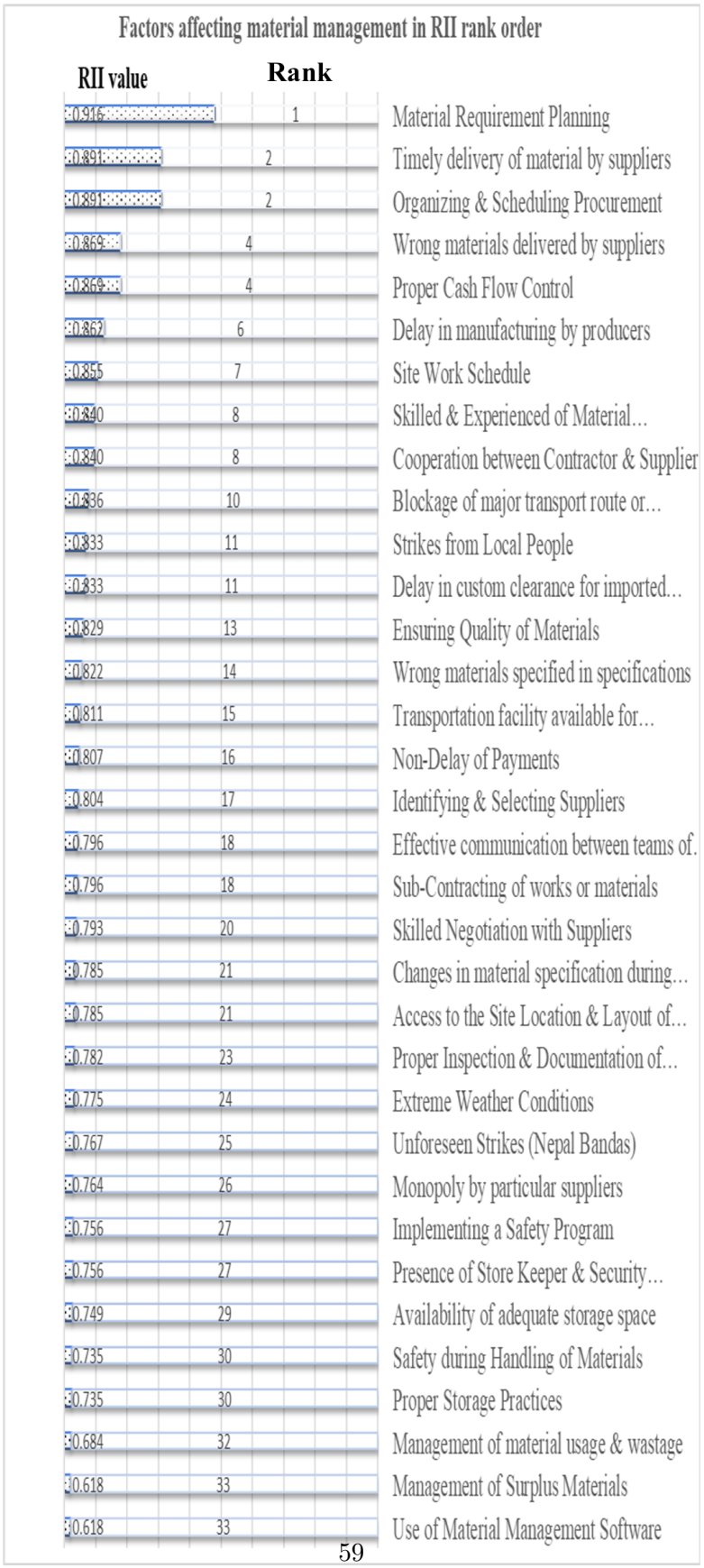

FIGURE 1. Factors Affecting Material Management with RII Rank Order.

TABLE 2. Factors Affecting Material Management with Relative Importance Index (RII) and Ranking

Group	Factors Affecting Material Management	RII= $\Sigma W/N \times A$	Factors Rank	Group RII= $\Sigma W/N \times A$	Group Rank
PLANNING	Material Requirement Planning	0.916	1	0.887	1
	Organizing & Scheduling Procurement	0.891	2		
	Site Work Schedule	0.855	7		
FINANCE	Proper Cash Flow Control	0.869	4	0.838	2
	Non-Delay of Payments	0.807	16		
GOVERNMENTAL INTERFERENCE	Delay in custom clearance for imported materials	0.833	11	0.833	3
SUPPLIER	Identifying & Selecting Suppliers	0.804	17	0.827	4
	Skilled Negotiation with Suppliers	0.793	20		
	Cooperation between Contractor & Supplier	0.840	8		
	Sub-Contracting of works or materials	0.796	18		
	Monopoly by particular suppliers	0.764	26		
	Timely delivery of material by suppliers	0.891	2		
	Delay in manufacturing by producers	0.862	6		
	Wrong materials delivered by suppliers	0.869	4		
TRANSPORT	Transportation facility available for delivery of materials to site	0.811	15	0.811	5
	Access to the Site Location & Layout of project	0.785	21		
	Blockage of major transport route or highways/feeder roads	0.836	10		
CONTRACTUAL ISSUE	Changes in material specification during construction	0.785	21	0.804	6
	Wrong materials specified in specifications	0.822	14		
STAFF	Skilled & Experienced of Material Management Team	0.840	8	0.798	7
	Presence of Store Keeper & Security Personnel	0.756	27		
ENVIRONMENT / WEATHER	Unforeseen Strikes (Nepal Bandas)	0.767	25	0.792	8
	Strikes from Local People	0.833	11		
	Extreme Weather Conditions	0.775	24		
MANAGEMENT	Use of Material Management Software	0.618	33	0.756	9
	Proper Inspection & Documentation of Materials	0.782	23		
	Ensuring Quality of Materials	0.829	13		
	Effective communication between teams of management	0.796	18		
	Implementing a Safety Program	0.756	27		
STORAGE & HANDLING	Proper Storage Practices	0.735	30	0.704	10
	Safety during Handling of Materials	0.735	30		
	Availability of adequate storage space	0.749	29		
	Management of material usage & wastage	0.684	32		
	Management of Surplus Materials	0.618	33		

items to be delivered, which are generally considered as of prime importance in material management regardless of any project type.

4.3.2. *Finance.* According to the research by Ahmad, et al. (2018) [10] and Dhakal (2019) the highest affecting factor in material management is found out to be related to financial status of company and shortage of fund respectively. However, it contradicts with the findings of this research in which financial factors like proper cash flow control and non-delay of payments are ranked at 4th and 16th only. The contrast may be because, generally in HCP the successful execution of financial closure is performed before the starting of construction. So, it is expected that there will be no financial problems during construction of the project expect for some of the unforseen variation works.

4.3.3. *Governmental Interference.* According to the literature reviews from the studies in other countries, it seems delay in custom clearance for imported materials is considered as the least affecting factor. Even in most of the researches this factor is not even considered in questionnaire. However, in this research, its effect on material management is found to be high with overall rank of 11th. The reason behind this dissimilarity can be the capacity of other nations in production i.e. countries like India, Pakistan, Malaysia etc. are capable of producing materials required for construction industry by themselves so there shall be no issues of custom clearance. Whilst in context of Nepal, large portion of materials used in construction are imported from neighboring countries. In addition, the reason for

dissimilarity can be the red tapes by government in construction industry. This means, as compared to red tapes by government in Nepal other countries mentioned in literature review may has less or no governmental interferences related to the construction industry. This is supported based upon the research by [12]in which governmental regulations are the 3rd most affecting factor in material management on highway projects in Nepal.

4.3.4. *Supplier.* With the glance on table 2, timely delivery of material by supplier is the high affecting factor with over rank of second. This result is similar to the study by [12] in which suppliers default is also ranked as 2nd most affecting causes of material and equipment procurement delay on highway projects in Nepal. Similarly, the result indicated that wrong materials delivered by suppliers is ranked as 4th most affecting factors which is supported based upon the research by Kulkarni, et al. (2017) in which rejection due to low quality materials delivered by suppliers is the most affecting factor in material management. In most of the construction projects, generally there is gap in proper communication between supplier and organization which causes delay in order, production and delivery. The reason behind the similarity in results of study can be because of the gap in proper communication. It is also supported according to the study by [13] in which poor communication between supplier and purchase is 3rd most affecting factor.

4.3.5. *Transport.* Findings have showed that blockage of major transport route is high affecting factor with overall rank of eighth. It is backed according to the research by [12] in which transportation delays is one of the major affecting factor ranking 4th in context of highway projects in Nepal. It is also supported with the fact that infrastructure facilities available in Nepal is not reliable due to hilly topography which is prone to calamities like landslides, flood etc. affecting the road networks during heavy rain. In addition, in the literatures based upon other countries like Pakistan, Malasiya and Nigeria the transportation is not considered as high affecting factor in material management. This contrast may be because of geography of these countries. The transportation in plain areas is relatively easier than in hilly terrain. Also, the reason behing the dissimilarity of results may be because of the transportation infrastructure facitlity available in those countries, which is way better than infrastructures in Nepal.

4.3.6. *Contractual Issue.* According to respondents' data, wrong materials specified in specifications has high effect with RII 0.822 in compare to the changes in material specification during construction with RII value of 0.785 with high-medium effect in material management. The reason behind similarities in findings is that, generally in construction projects it is more likely that specified materials are unavailable at market due to various circumstances like market situation, price fluctuation, changes in design, unavalibility of certain products etc. Also there is possibility that client's requirements can change during construction period, engineer cannot fully consider the requirements of client during design. It is also supported based upon the research by [6] in which misunderstanding of owner's requirements by design engineer comes under highest affecting factor in material management. Because of these changes, specification of materials are also changed which affects in material management.

4.3.7. *Staff.* Among the factors inside staff group, the factor viz. skill and experience of material management team is categorized as high affecting factor. The result of this study matches with the findings by [13] and E & Venkatasubramanian (2017) [11] in which skill and experience of material management team of staffs are ranked as most significant and 7th most influenting factors in material management respectively. In most

construction project, there comprises a team performing the material management works, staring from ordering of materials to delivery at site. Without proper communication and well defined system to integrate these activities, efficient material management is impossible. Whereas the proper communication and integration is dependent upon the traits of executing personnel.

4.3.8. *Environment / Weather.* With a glance on table 2 related to environment and weather group, unforeseen strikes like Nepal bandas and extreme weather conditions with RII values of 0.767 and 0.775 respectively are categorized as factors with high-medium effect. Whereas, the strikes from local people with RII value of 0.833 is ranked as high affecting factor in material management. It is backed with the fact that in Nepal, it is more likely to occur unforeseen strikes and strikes from local people in project area due to the unresolved and exaggerated grievances of local people. Whilst, these factors are not even considered as important factor in studied literature reviews. This dissimilarity may be due to policy in construction industry and geographical conditions respectively. The deviations in result suggest that unlikely in Nepal, unforeseen strikes and strikes from local people may not happen in the studied countries. May be these are managed by countries policy in construction industry. Moreover, Nepal is prone to numerous extreme weather condition like landslide, flood, earthquake etc. due to global climatic condition.

4.3.9. *Management.* The result suggests that the factor namely ensuring quality of material has high effect in material management with overall ranking of 13th. It is known to all that quality cost more but lack of quality cost even more. One of the most important functions of material management is insuring right quality of material deliveried at right time. For all construction projects ensuring quality in every steps help in successeful completion of the project. The result shows that implementing a safety program factor is ranked as 27th among 34 factors. The result is similar to the studies based upon the literature reviews. In both of these researches, safety is considered as low affecting factor. This could be because of lack of proper experiences relating material management to implementing a safety program in construction projects. The study indicates that use of material management software is the factor which has rank 33 out of 34, almost last among the listed factors affecting material management. It contradicts with the result based upon the study by [7] in which use of latest technologies helps in improving material management. This dissimilarities in result can be because of the technological gap between construction industries in other countries and Nepal. Also, use of advanced softwares for material management in HCP in Nepal is not yet practised. So, lack of experiences in these type of technologies can also lead to the non priotization of using these.

4.3.10. *Storage and Handling.* Availability of adequate storage space is considered as high-medium affecting factor as a problem related to storage spaces is less likely to occur in HCP. The result indicated that abundant free spaces are available for laydown and storages in HCP.

4.4. **Suggestions for Improving Material Managmenet System.** The responses suggest that coordination and communication is the key factor and common suggestions made by responders of all studied HEP for improving material management system. In order to improve coordination between team of material management, each personnel have to understand his role, responsibility and should be accountable. For effective communication, right information has to be conveyed to right person at right time. In addition, implementation of full functions of ERP software in the HCP can be another way in improving coordination. Because, the integrated information provided by the software is

key for proper material management. This computer-based technology provides information about employee, equipment, vendor, inventory, petty/sub-contractor, bill of quantity, purchase, quotation, accounting, communication, and payments etc. at real time so that tracking of project's progress is possible at any time.

5. Conclusion

The material requirement planning is ranked with highest RII value so it is recommended to be executed with highest priority. The result indicated that, among 34 factors affecting material management, 16 of them have high effects whereas 18 of them have high medium effect. It suggests that all the factors have high importance and none of them can be neglected during material management in HCP. Based on the averaged overall RII values from the study, the factors affecting the material management at the hydropower construction projects in Nepal are by rank planning, finance, government interference, supplier related, transport related, contractual issue, staff related, environment/weather, management related and storage & handling related factors. The review of the literature and the available project specific documents roughly matches the results of the questionnaire survey. The study also suggests that almost all the HCP in Nepal are using ICT in various ways for material management, some project use it more effectively than other does. Despite the importance of ICT in material management, the study has shown that effect of material management software has low ranking than other factors. It has more challenges to implement modern ICT technologies in HCP sites. In addition, the unreliability of internet access and the prohibitive internet collection price have forced many HCP, located in remote parts of Nepal, to use alternative methods of material requisition. The factors affecting material management varies from project to project, the variation on these are identified as varying management system, varying geographical condition, varying site location / accessibility, varying payment terms etc. In addition, proper coordination / communication between different teams of construction is the key for effective material management.

Scope and Limitation of the Study

The study is focused within the selected hydropower construction projects of small to medium size owned by private developers and promoters only. Factors affecting material management are listed form previous literature reviews that can be changed or separate list can be prepared with further study. The prepared list affecting material management were ranked using RII method only.

References

[1] P. Lenin, L. Krishnaraj, D. Narendra Prasad, and V. Prasath Kumar, "Analysis of Improper Material Management Affecting Cost in Construction Project," *International Journal for Research in Applied Science and Engineering Technology*, vol. 2, no. V, pp. 486–492, 2014.

[2] NEA, "A Year in Review, Fiscal Year 2019/2020, Annual Report," *Nepal Electricity Authority, Nepal*, 2009.

[3] H. Gunatilake, P. Wijayatunga, and D. Roland-Holst, "Hydropower Development and Economic Growth in Nepal," *Asian Development Bank South Asia Working Paper Series*, 2020.

[4] M. M. Sherchan, "archieve.nepalitimes.com," 2000. [Online]. Available: `http://archive.nepalitimes.com/news.php?id=9945#.YWveOhpBzIU`. [Accessed: Sep. 15, 2021].

[5] Z. Mat Jusoh, N. Kasim, M. U. Ibrahim, N. Sarpin, M. H. Mohd, and R. Zainal, "Influential Factors for Effective Materials Management in Construction Projects," *International Journal of Sustainable Construction Engineering & Technology*, vol. 9, no. 2, pp. 45–55, 2018.

[6] H. Patel, J. Pitroda, and J. Bhavsar, "Analysis of Factor Affecting Material Management and Inventory Management: Survey of Construction Firms in Gujrat Region of India," *International Journal of Advanced Research in Engineering, Science & Management*, pp. 1–6, 2017.

[7] N. Kasim, A. A. Latiffi, and M. S. Fathi, "RFID Technology for Materials Management in Construction Projects—A Review," *International Journal of Construction Engineering and Management*, vol. 2, no. 4A, pp. 7–12, 2013.

[8] N. Kasim, "ICT Implementation for Materials Management in Construction Projects: Case Studies," *Journal of Construction Engineering and Project Management*, pp. 31–36, 2011.

[9] N. Kasim, R. Kusumaningtias, and N. Sarpin, "Enhancing Material Tracking Practices of Material Management in Construction Project," *International Journal of Sustainable Construction Engineering and Technology*, vol. 10, no. 2, pp. 61–73, 2019.

[10] M. H. Ahmad, Y. I. Badrashi, M. Z. Ahad, Z. Khan, and F. A. Khan, "Factors Affecting Material Management in Construction Industry of Khyber Pakhtunkhwa Pakistan," *International Journal of Advanced Research in Science Engineering and Technology*, vol. 5, no. 11, pp. 7249–7258, 2018.

[11] A. E. and C. Venkatasubramanian, "Factors Affecting Material Management in Construction Industry," *International Journal of Civil Engineering and Technology (IJCIET)*, vol. 8, no. 5, pp. 869–880, 2017.

[12] M. R. Manavazhi and D. K. Adhikari, "Material and Equipment Procurement Delays in Highway Projects in Nepal," *International Journal of Project Management*, vol. 20, pp. 627–632, 2002.

[13] M. M. Sivagami and M. A. Ram, "Assessment of Role of Material Management in Construction Projects," *International Research Journal of Engineering and Technology (IRJET)*, vol. 6, no. 5, pp. 930–934, 2019.

Everest Advances in Science and Technology (EAST), Vol. 1, No. 1, 2025
ISSN: 3102-0410(print), 3102-0429(online)

Nonlinear FVDs for Seismic Resilience of Irregular RC Buildings

BED PRAKASH GUPTA[1*]

Abstract. Passive energy dissipation systems, particularly fluid viscous dampers (FVDs), offer a promising alternative by enhancing damping ratios without significantly altering structural stiffness. Despite their global success, FVDs remain underutilized in Nepal due to limited studies and the absence of specific provisions in the Nepal Building Code (NBC 105:2020). This study addresses this gap by evaluating the efficacy of FVDs in enhancing the seismic performance of a 10-storey representative building with setback, exhibiting vertical irregularities using performance-based design principles in SAP2000 v20. Nonlinear behavior is modeled using a lumped plasticity approach, with user-defined moments M3 hinges for beam and auto hinges PM2M3 for columns as per ASCE 41-13. Pushover analysis determines the capacity curve, which is matched with NBC 105:2020 elastic spectrum to identify performance point and ensure compliance with the Immediate Occupancy (IO) performance level. FVDs are modeled as two-noded nonlinear link elements and strategically placed at stories with maximum inter-storey drift. Nonlinear time history analysis (NLTHA), employing the direct integration and spectrum-compatible ground motion records for Type D soil (DBE, 10% probability of exceedance in 50 years), evaluates maximum storey displacements and hinge states. Comparative results between damped and undamped models are analyzed to quantify performance improvements. The results demonstrate that FVDs significantly reduce displacements and maintain hinge state within the IO performance level, offering practical and effective strategy for enhancing seismic resilience.

Keywords: Fluid viscous damper (FVDs), Plastic hinges, Push over analysis, Roof displacement, Time history analysis.

[1]Department of Civil Engineering, Everest Engineering College, Sanepa, Lalitpur, Nepal
E-mail: bedp.gupta@eemc.edu.np
* Corresponding author
Manuscript received: 29 March, 2025; revised: 12 August 2025; accepted: 3 September, 2025.
Everest Advances in Science and Technology (EAST), Vol. 1, No. 1, 2025

1. Introduction

Nepal, located at the convergence of the Indian and Eurasian tectonic plates, is among the most seismically active regions in the world, ranking 11th globally in terms of earthquake hazard [1]. Historical earthquakes, such as the 1934 Bihar-Nepal earthquake (M8.0) and the 2015 Gorkha earthquake (M7.8), have demonstrated the devastating consequences of seismic events, including significant loss of life, infrastructural damage, and economic disruption. The 2015 Gorkha earthquake alone resulted in over 8,790 fatalities, 22,300 injuries, and an estimated economic loss of $7 billion, underscoring the urgent need for improved seismic resilience in Nepal's built environment [2].

Commonly used energy dissipating technique to reduce dynamic vibration due to earthquake include shear walls, base isolation systems, tuned mass dampers, and viscous dampers Chopra [3]. Seismic retrofitting through supplementary damping had raised as important strategy for enhancing structural resilience against earthquake. Hankouri et al. [4] investigated the effectiveness of nonlinear viscous dampers (NLVDs) in mitigating seismic responses of multi-degree-of-freedom (MDOF) structures through numerical simulations using Newmark's Beta and Wilson' Theta methods. Their key findings reveal that lower nonlinearity exponents (α) and higher damping constants (C) significantly reduce structural displacements, particularly under low peak ground acceleration (PGA) conditions.

Building on this, Kim et al. [5] introduced performance-based design (PBD) procedure for supplemental viscous dampers using the non-iterative capacity spectrum method (CSM) to determine required damping by comparing the demand spectrum with the structure's capacity, achieving displacement error below 10% in both SDOF and MDOF systems. Their study, which distributes dampers proportionally to inter-storey drifts, simplifies the design process such as neglecting higher mode effects. Zhou et al. [6] expanded this work by proposing a practical two-stage design method for retrofitting reinforced concrete (RC) structures with viscous dampers to meet updated seismic codes following the 2008 Wenchuan earthquake. Key findings show that viscous dampers effectively reduce inter-story drifts and story shear forces by approximately 30%; further, they validated through a case study of an RC frame building, demonstrating improved performance under minor, moderate, and major earthquakes. Unlike Kim et al. [5], Zhou's [6] approach does not address higher mode effects explicitly.

Chopra et al. [7] addressed higher mode effects through modal pushover analysis (MPA), combining multiple mode shapes to improve accuracy for mid to high-rise buildings but increased computational complexity, limiting its practicality for rapid assessments. Chopra et al. [8] investigated the seismic response of single-degree-of-freedom (SDF) systems equipped with NLVDs with different damping ratio and non-linearity parameter ($alpha$), concluding supplementary damping effectively reduces deformation by 60% for damping of 30%. Further, they suggested NLVD achieve comparable response reductions to linear dampers but with significantly lower damper forces.

Experimental investigation carried by Hwang et al. [9] from shaking table tests conducted on two scaled down (1/2.5) three-storey RC building models—one with toggle-brace-mounted viscous dampers and one without—found up to 44% reduction in roof displacement under strong ground motions. Effect of bracing stiffness on damper effectiveness was investigated by Dong et al. [10] and suggested that brace stiffness significantly

impacts system performance—brace stiffness ($\geq$5$\times$ storey stiffness) enhances damping effectiveness while flexible braces reduce damping efficiency. Drift-based optimization method by Mousavi et al. [11] for determining the optimal placement of damper shows enhanced seismic performance over uniform distribution in high-rise buildings. Simplified performance-based design method over traditional complex method by Ijmulwar et al. [12] showing column forces and base shear decreased by 20–30% resulting 30% damping cost over uniform distributions.

Traditional seismic design in Nepal relies on ductile detailing and shear walls to dissipate energy through inelastic deformations Chaulagain et al. [13]. However, these methods often lead to localized damage, serviceability issues, and increased construction costs due to oversized structural members Gautam et al. [14]. In high seismic zones, such as Kathmandu Valley, conventional approaches may also amplify base shear due to added mass from stiffer elements Chaulagain et al. [15]. Passive energy dissipation systems, particularly fluid viscous dampers (FVDs), offer a promising alternative by enhancing damping ratios without significantly altering structural stiffness Constantinou et al. [16], Symans et al. [17].

Despite their proven efficacy globally, FVDs remain underutilized in Nepal due to a lack of localized studies and absence of codal provisions (e.g., NBC 105:2020). In context of Nepal, Tiwari et al. [18] studied the use of nonlinear fluid viscous dampers (FVDs) in regular RC framed structures and found significant reduction in maximum storey displacement (up to 80% for DBE, 63% for MCE) in 5-storey RC frame buildings with effectiveness decreasing in taller 10 and 15-storey buildings. Their highlight the need for further research on irregular structures.

Current study addresses this gap by evaluating the impact of fluid viscous dampers for vertically irregular buildings subjected to spectrum-compatible ground motions. The findings aim to inform future code revisions and promote the safe implementation of damping technologies in Nepal's diverse building stock.

2. Methodology

This study evaluates the effectiveness of NLVDs in enhancing the seismic performance of 10-storey reinforced concrete (RC) buildings with setbacks, exhibiting vertical irregularity. Two models—one without dampers (bare frame) and the other with dampers—were modeled in three-dimensional finite element modelling software SAP2000 v20 (see Figure 1, Figure 2, Figure 3 and Figure 4).

Initially, the building was designed using the Equivalent Lateral Force (ELF) method and Response Spectrum Method for the Design Basis Earthquake (DBE) level as per NBC 105:2020, and all the design checks satisfied the required criteria. The design incorporates beams of dimensions 600×400 mm and columns of 650×600 mm using M20 grade concrete and Fe415 grade reinforcement. The overall building plan measures 16 m $\times$ 16 m in the X and Y directions, with a total height of 40 m comprising 10 storeys of 4 m each. Vertical irregularity is introduced in the form of a setback starting from the 5^{th} storey, reducing the floor area by 50% in the upper five storeys.

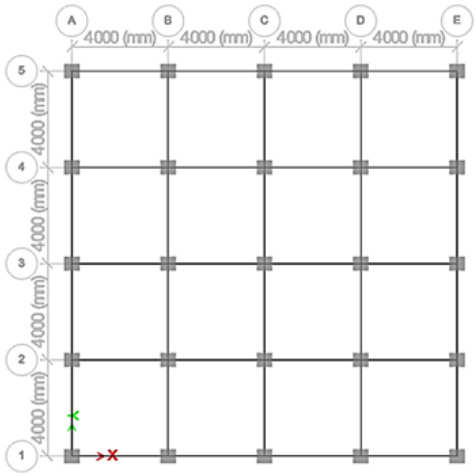

FIGURE 1. Plan of representative building.

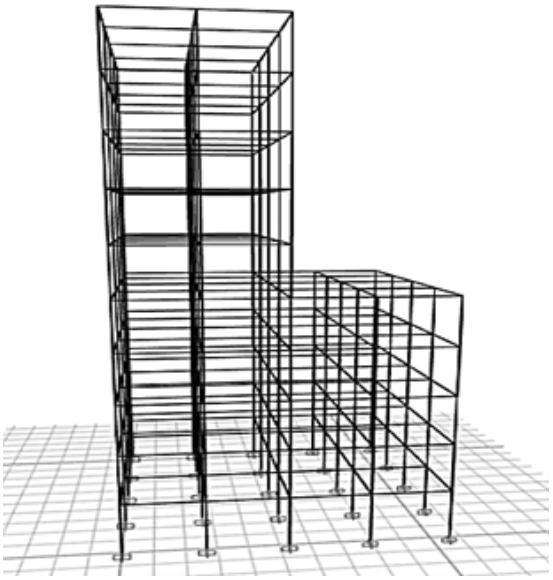

FIGURE 2. 3D Representative building for bare frame.

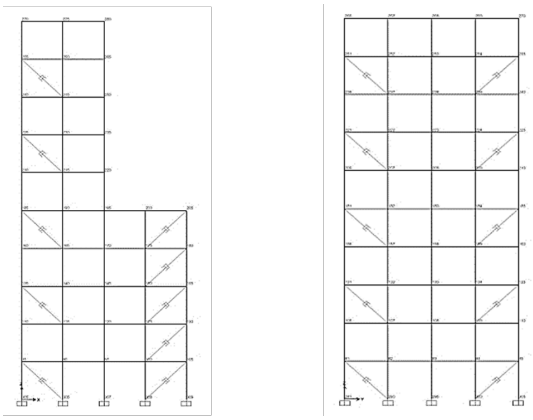

FIGURE 3. Along X-and Y-direction.

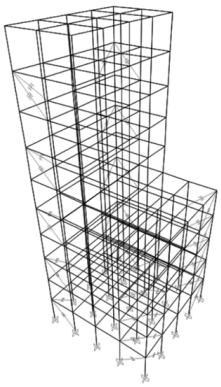

FIGURE 4. 3D representation of building with FVDs.

Nonlinear behavior is incorporated via a lumped plasticity model, where beams are assigned user-defined M3 hinges at offsets of $0.1L$ and $0.9L$ from their ends. Columns are assigned automatic P-M2-M3 hinges at similar offsets, in accordance with ASCE 41-13 guidelines. Pushover analysis was performed to obtain the capacity curve, which was then matched with the elastic spectrum for Type D soil as per NBC 105:2020 [19], in Acceleration-Displacement Response Spectrum (ADRS) format to determine the performance point (see Figure 5 and Figure 6).

After that, hinge states at the performance point were evaluated to ensure compliance with the Immediate Occupancy (IO) performance level. In cases where the IO level was exceeded, fluid viscous dampers (FVDs) were strategically placed at storeys exhibiting maximum inter-storey drift. The target damping ratio was determined by iteratively

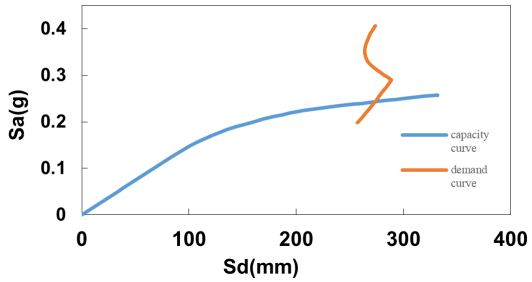

FIGURE 5. Capacity curve and demand curve in X-direction.

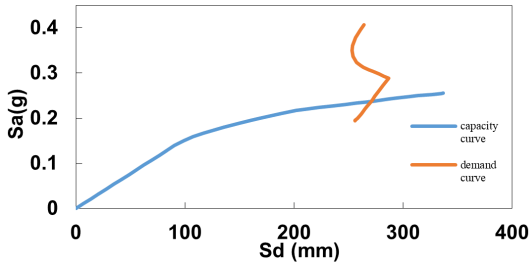

FIGURE 6. Capacity curve and demand curve in Y-direction.

modifying the total damping (inherent + supplementary) in the ADRS procedure, increasing it from the baseline 5% ($\zeta = 0.05$) to higher values (e.g., 0.10, 0.15, 0.20), and observing the shift in the demand spectrum and the resulting performance point. Through this iterative process, it was found that a supplementary damping ratio of approximately 30% was required to achieve the IO performance level. The total supplementary damping coefficient was calculated as per the method proposed by Mousavi et al. [11], using Equation (1):

$$C_A = \frac{(\zeta^* - \zeta)\, T\, K}{\pi} \tag{1}$$

where C_A is the total supplementary damping coefficient (N-sec/mm), ζ^* is the required (supplementary) damping ratio, ζ is the inherent damping ratio, T is the fundamental time period of the structure (sec), and K is the total lateral stiffness of the structure (kN/mm).

The linear properties of FVDs were then converted into nonlinear damper properties following the procedure suggested by Canney et al. [20]. The FVDs were modeled as two-noded nonlinear link elements, characterized by a stiffness of 500 kN/mm, damping coefficients of 1250 N-sec/mm and 1500 N-sec/mm, and a damping exponent $\alpha = 0.3$. The two damping coefficients correspond to dampers with different energy dissipation capacities, strategically placed at different storey levels based on the inter-storey drift ratios identified from the pushover analysis. By introducing velocity-dependent dampers, the structural damping increased, enabling enhanced energy dissipation through forces proportional to relative velocity. This mechanism reduces vibration amplitudes and limits inelastic deformations during seismic events. While the pushover procedure for determining target damping is primarily governed by the fundamental mode, this limitation was mitigated by conducting nonlinear time history analysis (NLTHA) using seven spectrum-compatible ground motions matched to NBC 105:2020.

Seven ground motion records (refer Table 1) were selected and matched to the NBC 105:2020 elastic response spectrum for Type D soil, corresponding to a 10% probability of exceedance in 50 years (DBE) for use in nonlinear time history analysis (NLTHA). Figure 7 represents the mean matched response spectrum for the selected ground motions.

TABLE 1. Selected Ground Motions for Study

S.N.	Earthquake Name	Event Day	PGA (g)	Magnitude (M)	Recording Station
1	Gorkha Earthquake	4/25/2015	0.25	7.8	Kanti Path, Kathmandu
2	Imperial Valley	10/15/1979	0.317	6.6	USGS STATION 5115
3	Chi-Chi	9/20/1999	0.361	7.62	TCU045
4	Kocaeli	8/17/1999	0.349	7.51	Yarimca
5	Landers	6/28/1992	0.78	7.28	Sce Station 24
6	Loma Prieta	10/18/1989	0.367	6.93	CDMG Station 47381
7	Kobe	1/16/1995	0.311	6.9	Kakogawa

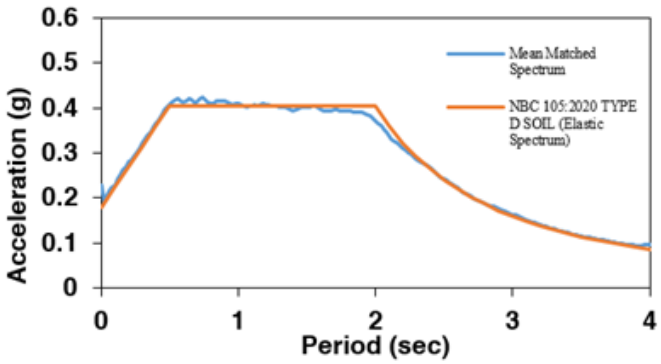

FIGURE 7. Mean matched spectrum matched with NBC105:2020 elastic spectrum at DBE level earthquake.

The analyses were conducted using the Direct Integration method in SAP2000 to capture the full dynamic response of the structure. Maximum storey displacements for each model were evaluated in both X and Y directions, along with hinge states, to confirm compliance with the Immediate Occupancy (IO) performance level as defined by ASCE 41-13 [21]. The IO performance level ensures that the structure sustains minimal damage during a seismic event, allowing for immediate reoccupation post-earthquake.

3. Maximum Storey Displacement

The outcomes from the nonlinear time history analysis (NLTHA) were plotted to compare the maximum displacement at each storey for both models: the bare frame and the frame equipped with fluid viscous dampers (FVDs), under multiple ground motions. Table 2 and Table 3 present the maximum storey displacements for different ground motions in the X and Y directions, respectively, for the bare frame model. Figure 8 and Figure 9 provide a clear visual comparison of displacement profiles for both structural configurations.

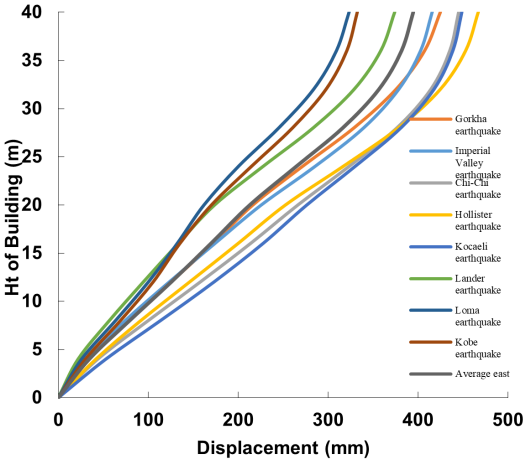

FIGURE 8. Maximum storey displacement of bare frame along X direction.

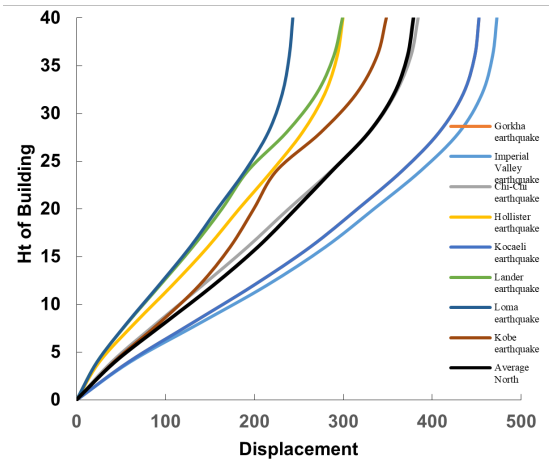

FIGURE 9. Maximum storey displacement of bare frame along Y-direction.

TABLE 2. Maximum storey displacement for bare frame along X direction (mm)

Storey	Gorkha	Imperial - Valley	ChiChi	Kocaeli	Landers	Loma	Kobe
Tenth	425	416	445	449	374	323	332
Ninth	407	403	435	439	358	309	321
Eighth	375	379	414	418	329	284	298
Seventh	329	340	377	381	283	245	261
Sixth	271	286	323	330	228	200	215
Fifth	216	226	267	276	174	162	170
Fourth	172	174	214	228	133	132	135
Third	125	123	158	173	94	100	105
Second	78	74	100	114	57	64	69
First	34	32	44	53	22	26	30
G.F.	0	0	0	0	0	0	0

The integration of fluid viscous dampers (FVDs) into the structural frame significantly enhanced the seismic performance, as evidenced by the maximum storey displacement data presented in the following tables. Analysis of the displacement results revealed that the average maximum displacement for the bare frame, which reached up to 394 mm, was reduced by approximately 60–70% with the incorporation of FVDs. Table 4 and Table 5 present the maximum storey displacements for different ground motions in the X and Y directions, respectively, for the frame equipped with FVDs. Figure 11 and Figure 10 provide clear visual representations of these displacements.

TABLE 3. Maximum Storey Displacement for Bare Frame along Y Direction (mm)

Storey	Gorkha	Imperial-Valley	Chi-Chi	Kocaeli	Landers	Loma	Kobe
Tenth	453	473	384	453	299	243	349
Ninth	448	468	376	448	289	239	338
Eighth	435	456	358	435	270	231	314
Seventh	408	430	329	408	236	216	275
Sixth	366	387	287	366	193	190	225
Fifth	316	334	239	316	163	158	199
Fourth	263	280	192	263	130	128	173
Third	199	214	142	199	94	92	138
Second	129	138	90	129	57	56	92
First	59	60	40	59	23	23	42
G.F.	0	0	0	0	0	0	0

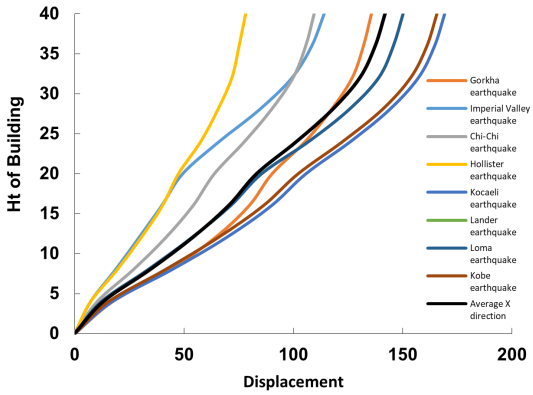

FIGURE 10. Maximum storey displacement of frame with FVDs along X direction.

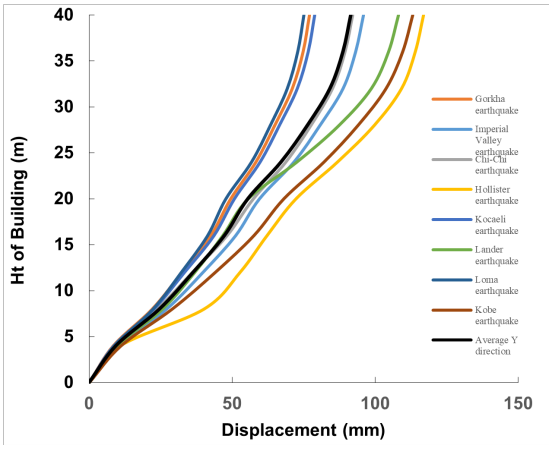

FIGURE 11. Maximum storey displacement of frame with FVDs along Y direction.

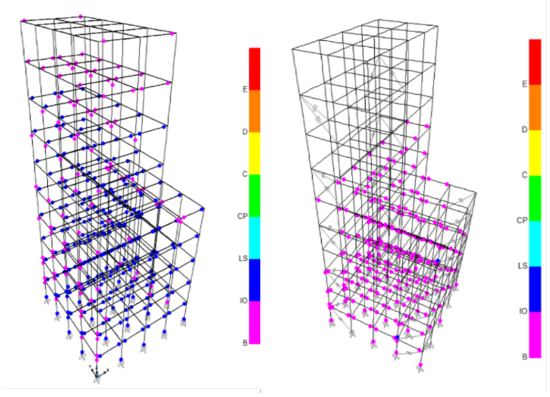

FIGURE 12. Hinge mechanism for Gorkha earthquake.

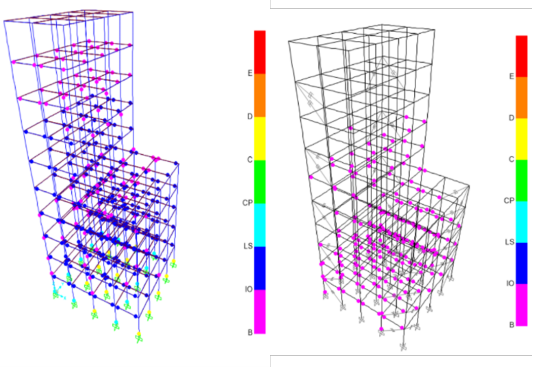

FIGURE 13. Hinge mechanism for Chi-Chi earthquake.

TABLE 4. Maximum Displacement for Frame with FVDs along X Direction (mm)

Storey	Gorkha	Imperial-Valley	Chi-Chi	Kocaeli	Landers	Loma	Kobe
Tenth	136	114	110	169	150	149	166
Ninth	132	108	106	165	146	144	161
Eighth	127	99	100	157	139	137	154
Seventh	117	84	90	144	125	123	140
Sixth	105	66	78	126	107	106	122
Fifth	90	49	64	106	85	86	102
Fourth	80	40	54	90	71	72	86
Third	64	29	42	69	53	54	65
Second	43	19	27	44	33	34	41
First	17	7	10	17	12	13	15
G.F.	0	0	0	0	0	0	0

TABLE 5. Maximum Displacement for Frame with FVDs along Y Direction (mm)

Storey	Gorkha	Imperial-Valley	Chi-Chi	Kocaeli	Landers	Loma	Kobe
Tenth	77	96	92	79	108	75	113
Ninth	75	93	90	77	105	73	110
Eighth	71	89	85	73	99	69	104
Seventh	65	81	78	67	87	63	94
Sixth	58	72	69	60	73	57	82
Fifth	49	60	57	51	56	48	68
Fourth	42	51	48	44	47	41	58
Third	32	40	36	33	37	32	44
Second	22	27	24	23	26	22	29
First	8	10	9	9	10	9	11
G.F.	0	0	0	0	0	0	0

TABLE 6. Hinge State for Bare Frame and Frame with FVDs for Different Ground Motions

	Gorkha Earthquake		Chi-Chi Earthquake			
Storey	Bare Frame B-IO	Frame with FVDs IO-LS	Bare Frame B-IO	Bare Frame IO-LS	Bare Frame LS-CP	Frame with FVDs B-IO
G.F.	3	22	0	17	8	7
First	13	43	25	40	0	46
Second	10	40	10	44	0	42
Third	6	40	10	46	0	40
Fourth	8	40	9	45	0	20
Fifth	22	33	15	41	0	15
Sixth	0	20	6	20	0	18
Seventh	10	20	10	20	0	8
Eighth	14	14	28	0	0	0
Ninth	23	0	19	0	0	0
Tenth	4	0	0	0	0	0

4. Plastic Hinge Mechanism

The results of hinge formation after NLTHA, were evaluated to compare seismic performance of a) bare frame model without FVDs and b) a frame incorporating FVDs against different ground motion. Table 6 represents the hinge state in tabulated form representing different state of performance level for bare frame and frame with FVDs for different

TABLE 7. Hinge State for Bare Frame and Frame with FVDs for Kobe and Loma Earthquakes

	Kobe Earthquake		Loma Earthquake			
Storey	**Bare Frame B-IO**	**Frame with FVDs IO-LS**	**Bare Frame B-IO**	**Bare Frame IO-LS**	**Bare Frame LS-CP**	**Frame with FVDs B-IO**
G.F.	10	15	24	20	5	25
First	7	13	55	38	10	57
Second	9	40	50	13	38	50
Third	46	0	42	35	11	42
Fourth	36	7	40	42	4	40
Fifth	35	19	43	38	20	36
Sixth	0	20	20	0	20	20
Seventh	0	20	11	6	20	20
Eighth	23	0	0	30	0	7
Ninth	20	0	0	20	0	0
Tenth	0	0	0	0	0	0

TABLE 8. Hinge State for Bare Frame and Frame with FVDs for Imperial Valley and Kocaeli Earthquakes

	Imperial Valley			Kocaeli Earthquake					
Storey	**Bare Frame B-IO**	**Frame with FVDs IO-LS**	**Frame with FVDs B-IO**	**Bare Frame B-IO**	**Bare Frame IO-LS**	**Bare Frame LS-CP**	**Bare Frame CP-C**	**Bare Frame C-D**	**Frame with FVDs B-IO**
G.F.		25	7	0	0	12	0	13	21
First	23	34	22	23	40	0	0	0	51
Second	8	40	34	9	47	0	0	0	47
Third	7	41	18	11	46	0	0	0	42
Fourth	5	45	11	12	44	0	0	0	40
Fifth	19	37	25	12	33	0	0	0	33
Sixth	6	20	20	0	20	0	0	0	20
Seventh	10	20	20	6	20	0	0	0	20
Eighth	23	0	14	24	0	0	0	0	4
Ninth	20	0	0	20	0	0	0	0	0
Tenth	0	0	0	0	0	0	0	0	0

Landers Earthquake			
	Bare Frame		**Frame with FVDS**
Storey	**B-IO**	**IO-LS**	**B-IO**
G.F.	20	5	25
First	58	3	55
Second	19	34	44
Third	14	40	40
Fourth	13	38	42
Fifth	33	30	36
Sixth	0	20	20
Seventh	9	20	20
Eighth	16	17	7
Ninth	23	0	0
Tenth	14	0	0

TABLE 9. Color code for Different Performance Level.

Performance Level	B-IO	IO-LS	LS-CP	CP-C	C-D
Color Code					

ground motions. Refer Figure 12 to Figure 18 for clear visual representation of hinge states.

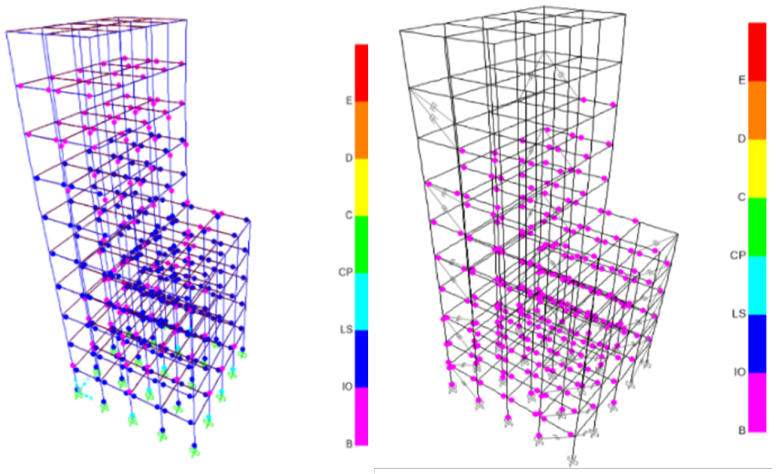

FIGURE 18. Hinge mechanism for Kocaeli earthquake.

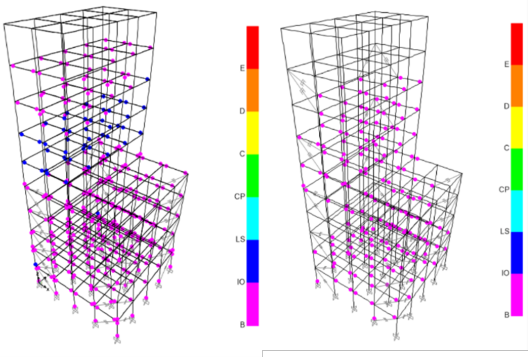

FIGURE 14. Hinge mechanism for Imperial Valley earthquake.

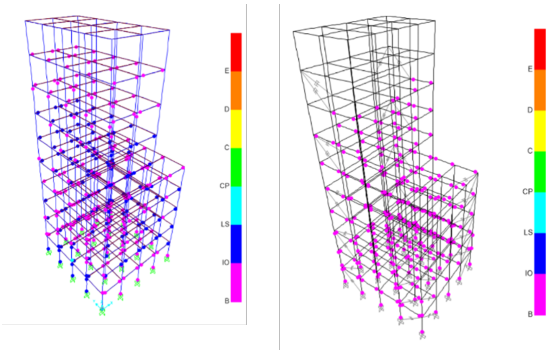

FIGURE 15. Hinge mechanism for Kobe Valley earthquake.

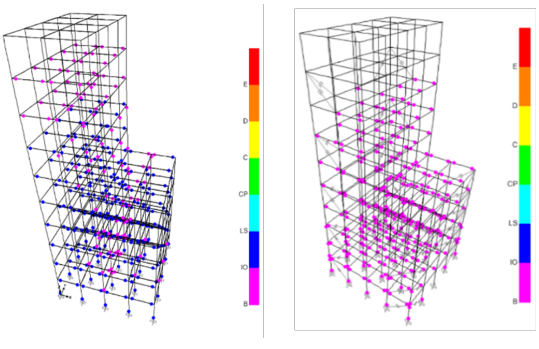

FIGURE 16. Hinge mechanism for Loma Prieta earthquake.

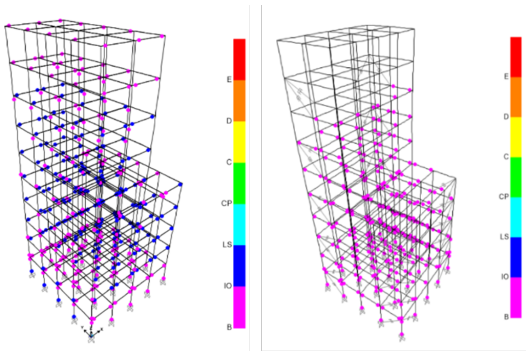

FIGURE 17. Hinge mechanism for Lander earthquake.

5. Conclusion

This study demonstrates the effectiveness of NLVDs in enhancing the seismic performance of a vertically irregular 10-storey RC building with setback. By incorporating performance-based design principles and conducting both pushover and NLTHA, it was observed that the addition of FVDs significantly reduced maximum storey displacements and controlled hinge states within the IO performance level. The strategic placement of FVDs at stories with maximum inter-storey drift proved crucial in improving structural response. These findings highlight the practical applicability of FVDs in Nepalese seismic design, especially for irregular buildings, and support the need for their consideration in future updates to the national building code. However, effectiveness of FVDs with an increase in building height, as well as challenges in addressing complex plan irregularities, which may require further investigation.

References

[1] UNDP, *Reducing disaster risk: a challenge for development, a global report*. New York: United Nations Development Programme, 2004. [Online]. Available: `https://www.undp.org/publications/reducing-disaster-risk-challenge-development`

[2] S. N. Sapkota, L. Bollinger, and F. Perrier, "Fatality rates of the M_w 8.2, 1934, Bihar–Nepal earthquake and comparison with the April 2015 Gorkha earthquake," *Earth Planets Space*, vol. 68, no. 1, Dec. 2016, doi: 10.1186/s40623-016-0416-2.

[3] A. K. Chopra, *Dynamics of Structures: Theory and Applications to Earthquake Engineering*, 4th ed. Pearson, 2012.

[4] Y. El Hankouri and A. El Ghoulbzouri, "A Numerical Investigation of the Impact of Non-linear Viscous Damping on Structural Response to Seismic Excitation," *Iran J Sci Technol Trans Civ Eng*, Feb. 2025, doi: 10.1007/s40996-025-01743-3.

[5] J. Kim, H. Choi, and K.-W. Min, "Performance-based design of added viscous dampers using capacity spectrum method," *J. Earthquake Eng.*, vol. 7, no. 1, pp. 1–24, Jan. 2003, doi: 10.1080/13632460309350439.

[6] Y. Zhou, X. Lu, D. Weng, and R. Zhang, "A practical design method for reinforced concrete structures with viscous dampers," *Eng. Struct.*, vol. 39, pp. 187–198, Jun. 2012, doi: 10.1016/j.engstruct.2012.02.014.

[7] A. K. Chopra and R. K. Goel, "A modal pushover analysis procedure for estimating seismic demands for buildings," *Earthq. Eng. Struct. Dyn.*, vol. 31, no. 3, pp. 561–582, Mar. 2002, doi: 10.1002/eqe.144.

[8] W. Lin and A. K. Chopra, "Earthquake response of elastic SDF systems with non-linear fluid viscous dampers," *Earthq. Eng. Struct. Dyn.*, vol. 31, no. 9, pp. 1623–1642, Sep. 2002, doi: 10.1002/eqe.179.

[9] J.-S. Hwang, C.-H. Tsai, S.-J. Wang, and Y.-N. Huang, "Experimental study of RC building structures with supplemental viscous dampers and lightly reinforced walls," *Eng. Struct.*, vol. 28, no. 13, pp. 1816–1824, Nov. 2006, doi: 10.1016/j.engstruct.2006.03.012.

[10] B. Dong, R. Sause, and J. M. Ricles, "Modeling of nonlinear viscous damper response for analysis and design of earthquake-resistant building structures," *Bull. Earthquake Eng.*, vol. 20, no. 3, pp. 1841–1864, Feb. 2022, doi: 10.1007/s10518-021-01306-7.

[11] S. A. Mousavi and A. K. Ghorbani-Tanha, "Erratum to: Optimum placement and characteristics of velocity-dependent dampers under seismic excitation," *Earthq. Eng. Eng. Vib.*, vol. 11, no. 4, pp. 603–603, Dec. 2012, doi: 10.1007/s11803-012-0145-x.

[12] S. S. Ijmulwar and S. K. Patro, "Seismic design of reinforced concrete buildings equipped with viscous dampers using simplified performance-based approach," *Structures*, vol. 61, p. 106020, Mar. 2024, doi: 10.1016/j.istruc.2024.106020.

[13] D. Gautam and H. Chaulagain, "Structural performance and associated lessons to be learned from world earthquakes in Nepal after 25 April 2015 (MW 7.8) Gorkha earthquake," *Eng. Fail. Anal.*, vol. 68, pp. 222–243, Oct. 2016, doi: 10.1016/j.engfailanal.2016.06.002.

[14] D. Gautam, R. Adhikari, and R. Rupakhety, "Seismic fragility of structural and non-structural elements of Nepali RC buildings," *Eng. Struct.*, vol. 232, p. 111879, Apr. 2021, doi: 10.1016/j.engstruct.2021.111879.

[15] H. Chaulagain, H. Rodrigues, J. Jara, E. Spacone, and H. Varum, "Seismic response of current RC buildings in Nepal: A comparative analysis of different design/construction," *Eng. Struct.*, vol. 49, pp. 284–294, Apr. 2013, doi: 10.1016/j.engstruct.2012.10.036.

[16] M. C. Constantinou, T. T. Soong, and G. F. Dargush, *Passive energy dissipation systems for structural design and retrofit*. Buffalo, NY: Multidisciplinary Center for Earthquake Engineering Research, 1998.

[17] M. D. Symans *et al.*, "Energy Dissipation Systems for Seismic Applications: Current Practice and Recent Developments," *J. Struct. Eng.*, vol. 134, no. 1, pp. 3–21, Jan. 2008, doi: 10.1061/(ASCE)0733-9445(2008)134:1(3).

[18] P. Tiwari, P. Badal, and R. Suwal, "Effectiveness of fluid viscous dampers in the seismic performance enhancement of RC buildings," *Asian J. Civ. Eng.*, vol. 24, no. 1, pp. 309–318, Jan. 2023, doi: 10.1007/s42107-022-00504-1.

[19] Government of Nepal, *NBC 105:2020, Seismic design of buildings in Nepal*.

[20] Taylor Devices Inc., "Non-Ductile Concrete Moment Frame Retrofit Design Guide." [Online]. Available: `https://www.taylordevices.com/wp-content/uploads/Taylor-Devices_Non-Ductile-Concrete-Moment-Frame-Retrofit-Design-Guide.pdf`

[21] American Society of Civil Engineers, *Seismic Evaluation and Retrofit of Existing Buildings*, 41st ed. Reston, VA: ASCE, 2014, doi: 10.1061/9780784412855.

Everest Advances in Science and Technology (EAST), Vol. 1, No. 1, 2025
ISSN: 3102-0410(print), 3102-0429(online)

Modeling and Simulation of Single-Mass PMSG for Embedded Control in Wind Energy Systems

ANIL THAPA[1*]

Abstract. Accurate yet computationally efficient modeling is essential for the real-time control of Permanent Magnet Synchronous Generator (PMSG)-based wind energy conversion systems (WECS), particularly when targeting low-cost embedded platforms. Complex multi-mass drive-train models, while capable of capturing torsional dynamics, introduce significant computational overhead that can limit their applicability in rapid control prototyping and embedded implementations. This paper presents a complete single-mass PMSG model derived from aerodynamic, mechanical, and electrical subsystems, expressed in the d-q reference frame for efficient control integration. The modeling approach consolidates the turbine and generator inertias into a single equivalent inertia, significantly reducing the system order while preserving the key dynamics necessary for steady-state and slow-transient analysis. The model is implemented in MATLAB/Simulink with fixed-step solver configurations to ensure compatibility with embedded hardware such as DSPs, FPGAs, and microcontrollers. Simulation results under variable wind speed conditions demonstrate the model's suitability for maximum power point tracking (MPPT) and DC-link voltage regulation. The proposed lightweight approach provides a balance between model fidelity and execution speed, making it ideal for cost-sensitive, real-time wind energy control applications.

Keywords: Wind energy, single mass, permanent magnet synchronous generator, MPPT.

[1]Department of Computer Engineering, Everest Engineering College, Sanepa, Lalitpur, Nepal
E-mail: bineilthapa@gmail.com
* Corresponding author
Manuscript received: 12 March, 2025; revised: 21 August 2025; accepted: 4 September, 2025.
Everest Advances in Science and Technology (EAST), Vol. 1, No. 1, 2025

1. Introduction

The global warming effect is becoming more conspicuous every day. The lack of snows in the mountains to the wildfire happening around the world clearly substantiate this. Despite the emphasis on renewable energy sources, whole world is still heavily reliant on fossils fuels. Of all the available renewable resources, the wind energy has drawn increased attention [1, 2, 3]. In 2023, a record high 117 GW of new wind power was installed worldwide representing a 50% hike from the previous year [1].

Permanent magnet synchronous generator (PMSG) has been an attractive choice for applications requiring variable speed drives [4]. PMSGs are used in wind turbines for their high frequency and removal of gear box for electricity generation. PMSG transfers the total power generated at the generator side resulting from turbine to grid side with the help Back-To-back (BTB) capacitor which consists of a Machine Side Converter (MSC), dc link capacitor and Grid Side Converter (GSC) [5].

The rapid growth of wind energy has driven the development of efficient and flexible control strategies for variable-speed generators. Among various generator technologies, the Permanent Magnet Synchronous Generator (PMSG) has gained significant attention due to its high efficiency, gearless operation, and direct-drive capability. Accurate modeling of PMSG-based wind energy conversion systems (WECS) is essential for designing, testing, and validating control algorithms prior to deployment in hardware.

Conventional modeling approaches often employ multi-mass drive-train representations to capture torsional oscillations and shaft flexibility. While effective for detailed mechanical stress analysis and transient studies, such models increase system complexity, require additional mechanical parameters, and demand higher computational resources. These characteristics make them less suited for applications where real-time performance and low-latency control execution are critical, such as in embedded controllers with limited processing capacity.

In many scenarios—particularly small to medium-scale wind turbines, educational test benches, and rapid control prototyping environments—a reduced-order mechanical model can provide adequate accuracy with a fraction of the computational burden. This paper develops a mathematically complete single-mass PMSG model that consolidates the turbine and generator inertias into a single equivalent inertia. The model is derived from first principles, combining aerodynamic torque generation, single-mass mechanical dynamics, and electrical equations in the dq reference frame. Implemented in MATLAB/Simulink with fixed-step solver settings, the model is tailored for deployment to digital signal processors (DSPs), microcontrollers, and FPGA platforms.

2. System Model

Figure 1 gives the schematic of a PMSG driven by a wind turbine connected to the single machine infinite bus system (SMIB). Both MSC and GSC emulate the PWM signal generation using tip speed ratio maximum power point algorithm (MPPT). The dc link capacitor in back-to-back converter is responsible for power transfer between generation and grid side. On the generator side, rectifier utilizes tip speed ratio (TSR) MPPT algorithm for the maximum power delivery.

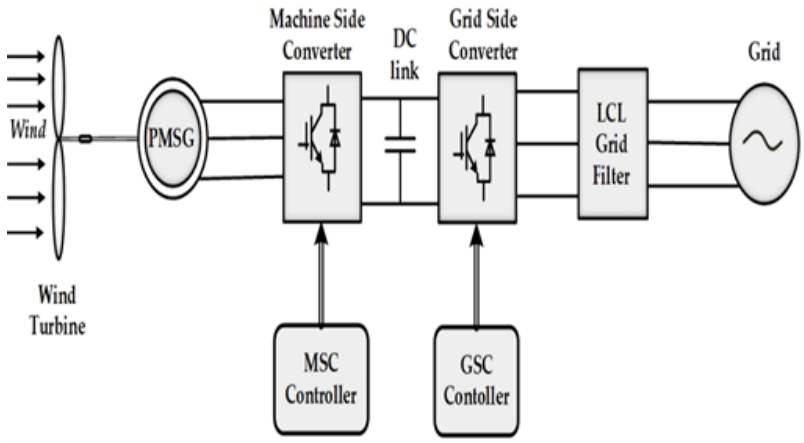

FIGURE 1. Schematic diagram of a. single machine infinite bus (SMIB) system using PMSG wind turbine system.

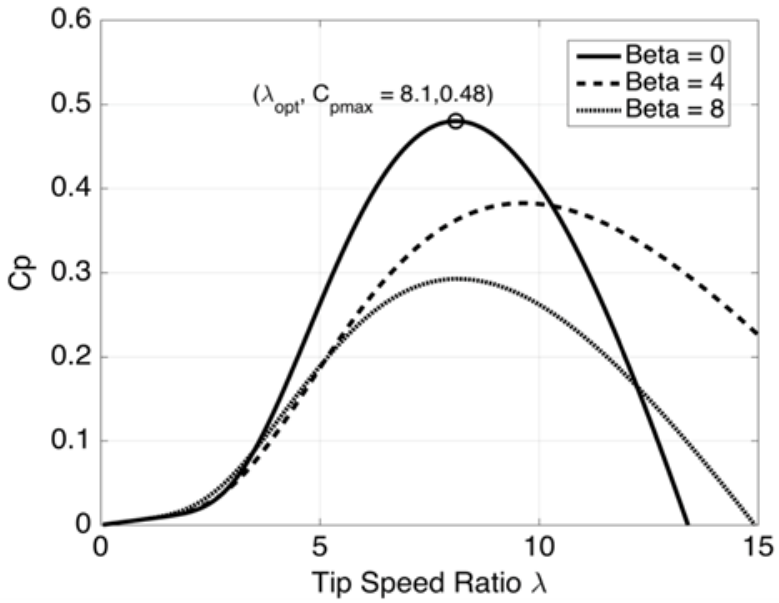

FIGURE 2. Tip speed ratio vs power coefficient curve for different pitch angles.

2.1. **Mechanical Drive Train.** The mechanical power output of a wind turbine is related to the wind speed V_ω by [6, 7, 8]:

$$P_t = 0.5\rho A C_p(\lambda, \beta) V_\omega^3 \tag{1}$$

where, ρ is air density, A is the area swept by the blades, and $C_p(\lambda, \beta)$ is the power coefficient of the blade which is given by

$$C_p(\lambda, \beta) = 0.5176 \left(\frac{116}{\lambda + 0.08\beta} - \frac{4.0}{1 + \beta^3} - 0.4\beta - 5 \right) e^{\left(\frac{-21}{\lambda + 0.08\beta} - \frac{0.735}{1+\beta^3} \right)} + 0.0068 \tag{2}$$

λ is the tip speed ratio and β is the pitch angle.

Figure 2 shows the variation of power coefficient with tip speed ratio for different values of pitch angle. C_p represents the fraction of wind power that can be extracted from the turbine. Pitch angle relates the orientation of the wind turbine blade with respect to its longitudinal axis. The extraction of wind energy is maximum when the blades are facing the wind. The pitch angle is zero degrees at this instance. The turbine power coefficient has a maximum value of 0.48 with the value of tip speed ratio around 8 as shown in Figure 2.
Because of the gearless configuration, the wind turbine system is connected to the generator with a single-mass model of the drive train. The dynamic equation representing the single-mass model of the drive train is expressed as:

$$p(\omega_t) = \frac{1}{2H}(T_m - T_e) \tag{3}$$

Here, ω_t, H, T_m, and T_e are the turbine speed, inertia constant, mechanical torque, and electrical torque, respectively.

2.2. **Permanent Magnet Synchronous Generator Model.** The electrical model of the PMSG in the synchronous reference frame can be expressed as [9]:

$$p(i_{sd}) = \frac{1}{L_d}\left[-R_a i_{sd} + \omega_g X_q i_{sq} - v_{sd}\right] \tag{4}$$

$$p(i_{sq}) = \frac{1}{L_q}\left[-\omega_g X_d i_{sd} - R_a i_{sq} + \omega_g \psi_{pm} - v_{sq}\right] \tag{5}$$

In the above, i_{sd}, i_{sq} and v_{sd}, v_{sq} are the d-q components of the stator current and terminal voltage respectively, and ψ_{pm} is the residual flux of the permanent magnet rotor.
The electrical torque generated is given by:

$$T_e = -L_d i_{sd} i_{sq} + \psi_{pm} i_{sq} + L_q i_{sd} i_{sq} \tag{6}$$

The active power at the PMSG terminal is given by:

$$P_{pmsg} = v_{sd} i_{sd} + v_{sq} i_{sq} \tag{7}$$

2.3. **Machine Side Converter Controller.** The decoupled control strategy is implemented in the MSC controller where the q-axis regulates torque and the d-axis regulates reactive power. The d-q axis is selected in such a way that $v_{sq} = |V|$ and $v_{sd} = 0$, so that the d-axis current reference becomes $i_{sd\_ref} = 0$.
The torque reference is obtained using MPPT and is given by:

$$T_e = k_{opt}\omega_t^2 = \psi_{pm} i_{sq} \tag{8}$$

Hence, the reference value of i_{sq} is:

$$i_{sq\_ref} = \frac{k_{opt}\omega_t^2}{\psi_{pm}} \tag{9}$$

The Simulink model representation of the MSC controller is shown in Figure 3. The blocks MSC_IL1 and MSC_IL2 each include two PI Controllers.

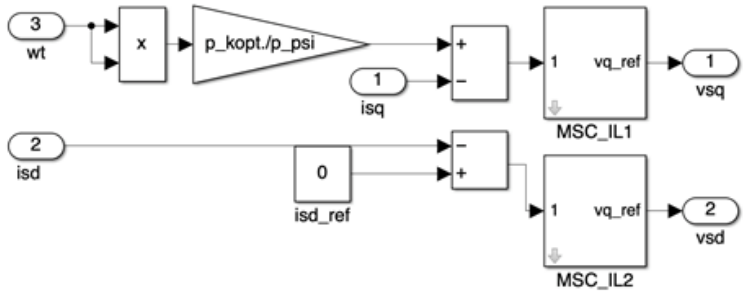

FIGURE 3. Simulink diagram of PMSG Machine Side Converter.

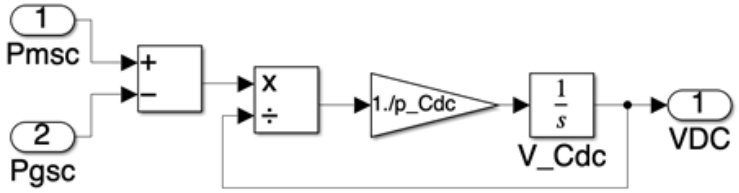

FIGURE 4. Simulink diagram of Back-to-back capacitor Converter.

2.4. **Back-To-Back Capacitor.** The Back-to-back converter consists of an MSC, a DC link capacitor, and a GSC. The losses due to switching of the converter are neglected. It is assumed that the converter dynamics are fast and the converter follows the reference generated by the MSC and GSC in real time.
The converter capacitor voltage is given by the power balance equation, excluding losses. The DC link capacitor voltage is:

$$V_c \left[C \frac{d}{dt}(V_c) \right] = P_{MSC} - P_{GSC} \tag{10}$$

Here, P_{MSC} and P_{GSC} are the power input and power output in the converter, given by:

$$P_{MSC} = V_{sd} i_{sd} + V_{sq} i_{sq} \tag{11}$$

$$P_{GSC} = V_{id} i_{id} + V_{iq} i_{iq} \tag{12}$$

2.5. **LCL Filter.** LCL filter consists of two inductors (L_i, L_g), a capacitor (C_f), and a damping resistor (R_C). The resistances (R_i, R_g) in series with the inductors represent the stray resistance of the inductors [10, 11]. Fig. 5 represents the structure of the LCL filter and Fig. 6 shows its Simulink representation.

The equations pertaining to the LCL filter are as follows:

$$p(i_{iq}) = \frac{w_b}{L_i} \left[v_{iq} - v_{cq} - (R_i + R_c) i_{id} + w L_i i_{id} + R_c i_{gq} \right] \tag{13}$$

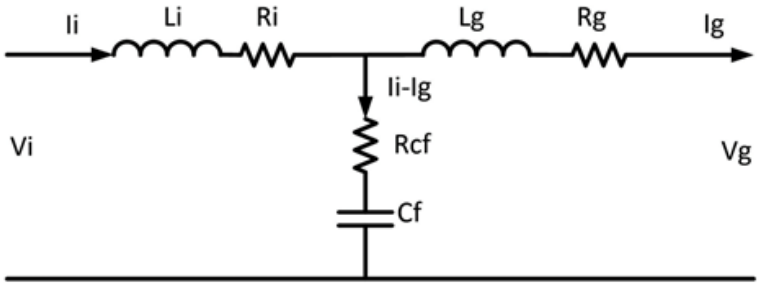

FIGURE 5. LCL filter.

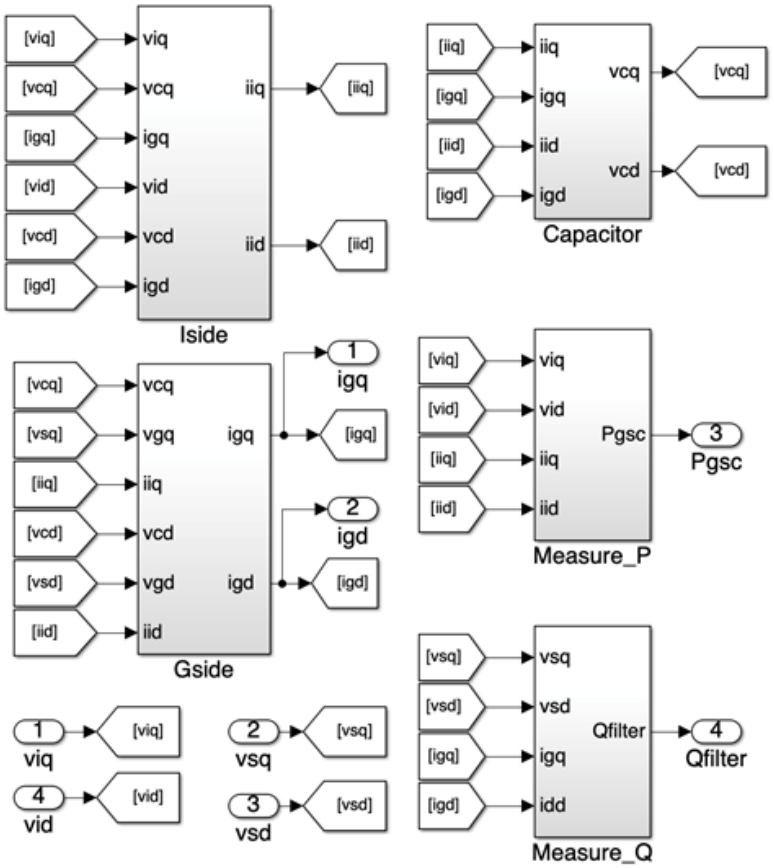

FIGURE 6. . Simulink representation of LCL filter.

$$p(i_{id}) = \frac{w_b}{L_i}\left[v_{id} - v_{cd} - (R_i + R_c)i_{id} - wL_i i_{iq} + R_c i_{gd}\right] \tag{14}$$

$$p(i_{gq}) = \frac{w_b}{L_g}\left[v_{cq} - v_{gq} - (R_g + R_c)i_{gq} + wL_g i_{gd} + R_c i_{iq}\right] \tag{15}$$

$$p(i_{gd}) = \frac{w_b}{L_g}\left[v_{cd} - v_{gd} - (R_g + R_c)i_{gd} + wL_g i_{gq} + R_c i_{id}\right] \tag{16}$$

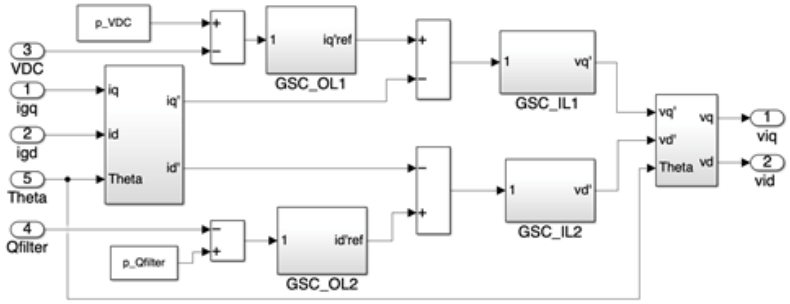

FIGURE 7. Simulink diagram of PMSG Gride Side Converter.

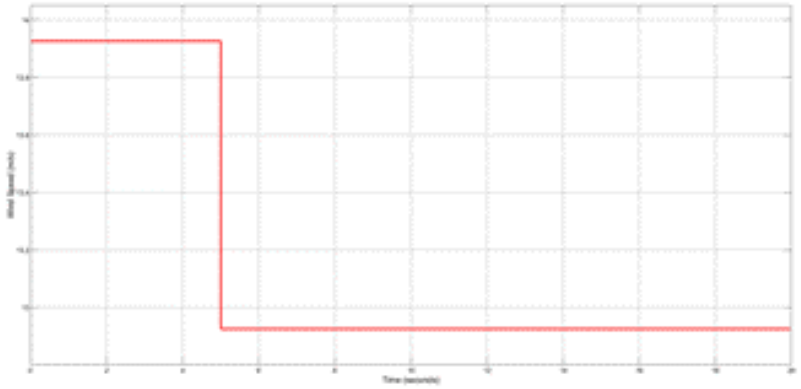

FIGURE 8. Variation in windspeed at time = 1s.

$$p(v_{cq}) = \frac{w_b}{C_f}\left[i_{iq} - i_{gq} - wC_f v_{cd}\right] \tag{17}$$

$$p(v_{cd}) = \frac{w_b}{C_f}\left[i_{id} - i_{gd} - wC_f v_{cq}\right] \tag{18}$$

2.6. **Grid Side Converter Controller.** Figure 7 shows the Simulink representation of the GSC controller, which consists of two inner PI controllers and two outer PI controllers. These controllers, along with the MSC controllers, are responsible for maintaining a constant DC voltage across the DC link capacitor, even when wind speed changes act as disturbances.

3. Simulation Results

The dynamic performance of the PMSG system is simulated using MATLAB SIMULINK. Figure 8 shows the dynamic simulations of the results by applying a step change in wind speed at time = 5s and infinite bus voltage change at time = 15s. It is clear from the figures that the controller performs satisfactorily with less overshoot and immediate stability for both the changes in wind velocity and infinite bus voltage. Moreover, the dc link voltage of the back-to-back capacitor is maintained constant with the overshoot value within the limit of 10% so that the peak overshoot won't damage the capacitor.

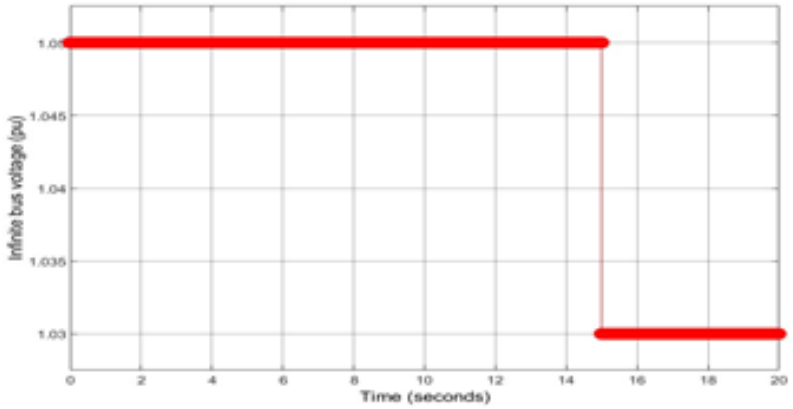

FIGURE 9. Variation in infinite bus voltage at time = 15s.

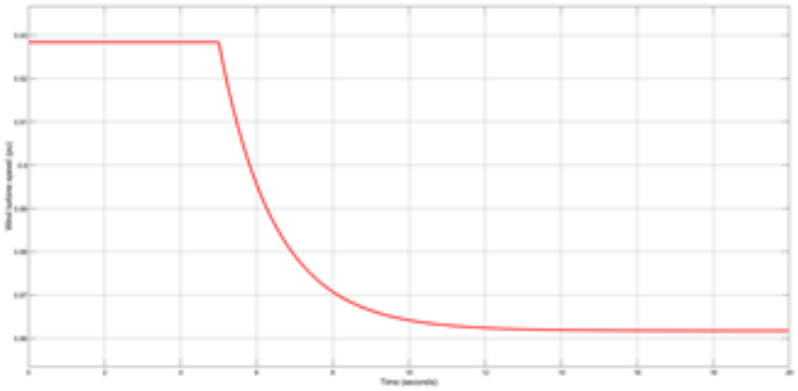

FIGURE 10. Variation in wind turbine speed following change in windspeed at time 5s and infinite bus voltage change at 15s.

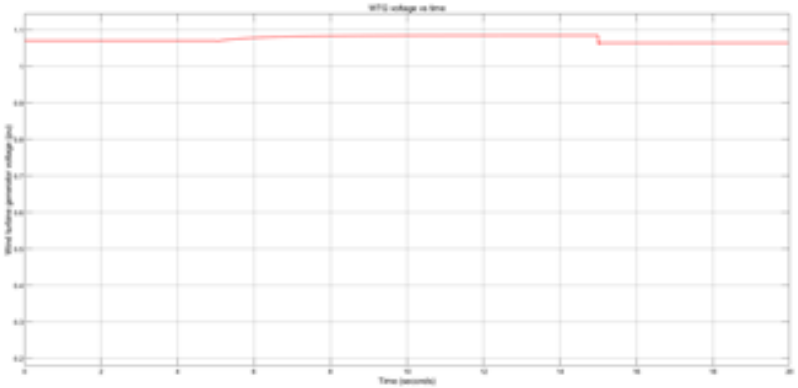

FIGURE 11. Variation in wind turbine generator voltage following change in windspeed at time 5s and infinite bus voltage change at 15s.

4. Conclusion

This paper presents a mathematically complete single-mass model of a Permanent Magnet Synchronous Generator (PMSG) wind energy system, integrating aerodynamic, mechanical, and electrical dynamics within a unified framework. The proposed model consolidates

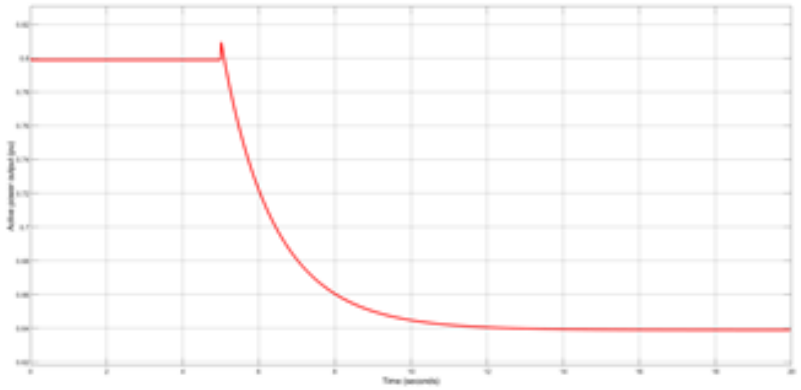

FIGURE 12. Variation in active power output following change in windspeed at time 5s and infinite bus voltage change at 15s.

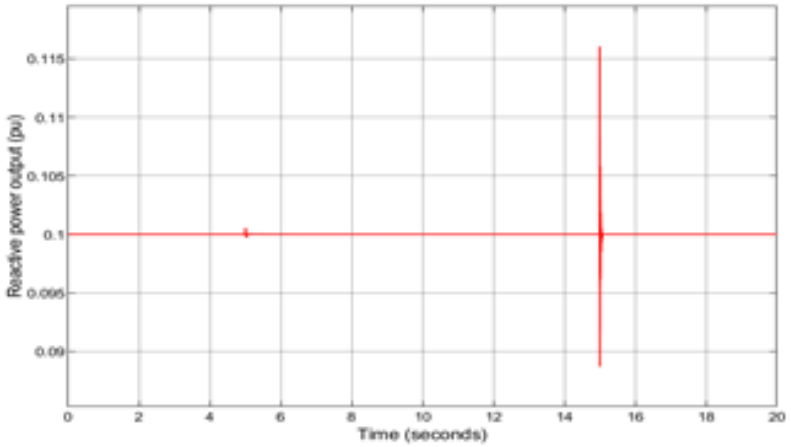

FIGURE 13. Variation in reactive power output following change in windspeed at time 5s and infinite bus voltage change at 15s.

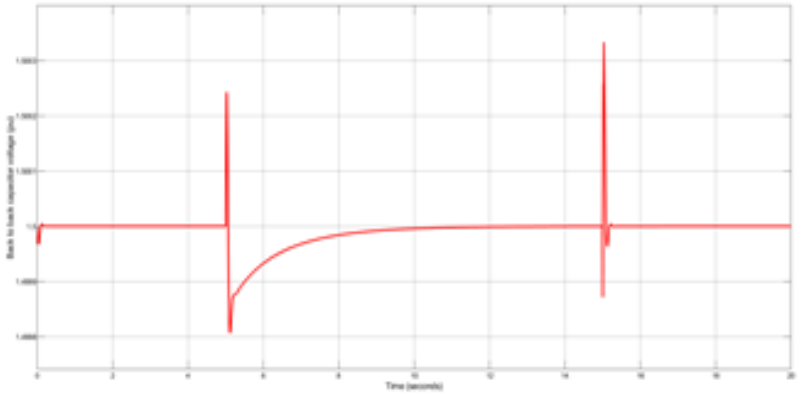

FIGURE 14. Variation in back-to-back capacitor voltage following change in windspeed at time 5s and infinite bus voltage change at 15s.

turbine and generator inertias into a single equivalent mass, significantly reducing computational complexity while preserving the essential dynamic behavior required for steady-state and slow-transient analysis. Implemented in MATLAB/Simulink with fixed-step solver configurations, the model is well-suited for embedded control applications, enabling real-time deployment on digital signal processors, microcontrollers, and FPGA-based platforms. Simulation results under varying wind conditions demonstrate that the single-mass model supports accurate maximum power point tracking (MPPT) and DC-link voltage regulation, while offering a lightweight alternative to more complex multi-mass representations. By balancing model fidelity and computational efficiency, this approach provides a practical framework for rapid prototyping, educational purposes, and cost-sensitive embedded wind energy systems. Future work may extend this model to include real-time hardware-in-the-loop (HIL) validation and integration with advanced control strategies such as fuzzy logic or reinforcement learning-based MPPT.

References

[1] R. Williams and F. Zhao, *Global Wind Report 2024*. Global Wind Energy Council (GWEC), 2024.

[2] E. Brunner and D. Schwegman, "Commercial wind energy installations and local economic development: Evidence from U.S. counties," *Energy Policy*, vol. 165, p. 112993, 2022.

[3] European Wind Energy Association, *Rewarding Ambition in Wind Energy: A Report*. Brussels, Belgium: EWEA, 2015.

[4] L. Barote and C. Marinescu, "PMSG wind turbine system for residential applications," in *Proc. Int. Symposium on Power Electronics, Electrical Drives, Automation and Motion (SPEEDAM)*, Pisa, Italy, Jun. 2010.

[5] B. Pal, S. Kuenzel, and L. Kunjumuhammed, *Simulation of Power System with Renewables*. Cambridge, MA, USA: Academic Press, 2020.

[6] W. Shepherd and L. Zhang, *Electricity Generation Using Wind Power*. Singapore: World Scientific, 2011.

[7] V. Akhmatov, *Analysis of Dynamic Behaviour of Electric Power Systems with Large Amount of Wind Power*. Ørsted-DTU, Technical Univ. of Denmark, 2003.

[8] H. Polinder, S. W. H. de Haan, M. R. Dubois, and J. G. Slootweg, "Basic operation principles and electrical conversion systems of wind turbines," *EPE J.*, vol. 15, pp. 43–50, 2005.

[9] S. Li, T. A. Haskew, and L. Xu, "Conventional and novel control designs for direct driven PMSG wind turbines," *Electr. Power Syst. Res.*, vol. 80, no. 3, pp. 328–338, Mar. 2010, doi: 10.1016/j.epsr.2009.09.016.

[10] M. Rosyadi, S. M. Muyeen, R. Takahashi, and J. Tamura, "New controller design for PMSG-based wind generator with LCL-filter considered," in *Proc. 20th Int. Conf. on Electrical Machines (ICEM)*, Marseille, France, Sep. 2012.

[11] R. L. A. Ribeiro, A. D. Araujo, A. C. Oliveira, and C. B. Jacobina, "A high-performance permanent magnet synchronous motor drive by using a robust adaptive control strategy," in *Proc. IEEE Power Electron. Specialists Conf. (PESC)*, Orlando, FL, USA, 2007.

Everest Advances in Science and Technology (EAST), Vol. 1, No. 1, 2025
ISSN: 3102-0410(print), 3102-0429(online)

A Case Study on Stabilizing Kathmandu Valley Lacustrine Silt with Stone Dust and Sand

UJJWAL NIRAULA[1*], BHIM KUMAR DAHAL [2]

Abstract. High-plasticity soils, like those in the Kathmandu Valley, present significant construction challenges because of their high compressibility, low shear strength, and notable settlement behavior. By evaluating changes in geotechnical properties and shear strength parameters, this study explores the stabilization potential of stone dust and sand in enhancing the geotechnical behavior of lacustrine silt, a common high-plasticity soil type in the Kathmandu Valley. A number of laboratory tests were performed on natural soil samples that were collected from the area close to the Bagmati River. Different proportions of stone dust (10–40%), sand (10–40%), and a combination of the two were used to modify the soil. Assessments were made of parameters like cohesion, internal friction angle, maximum dry density (MDD), and optimal moisture content (OMC). Sand and stone dust increased the internal friction angle and dry density while decreasing cohesion and OMC. It was discovered that the combination of sand and stone dust was especially useful for strength improvement without being overly expensive. According to the study, sand and stone dust are both practical, locally accessible stabilizers that can greatly increase the bearing capacity and lessen the settlement of high-plasticity soils, particularly for shallow foundations used in low-rise buildings.

Keywords: Kathmandu Valley, Lacustrine Soil Stabilization, Silt, Stone dust, Sand.

[1]Everest Engineering College, Sanepa, Lalitpur, Nepal
E-mail: ujjwal.niraula@eemc.edu.np
[2]Tribhuvan University, Institute of Engineering- Pulchowk Campus, Lalitpur, Nepal
E-mail: 076msgte020.ujjwal@pcampus.edu.np
* Corresponding author
Manuscript received: 19 July, 2025; revised: 13 August 2025; accepted: 5 September, 2025.
Everest Advances in Science and Technology (EAST), Vol. 1, No. 1, 2025

1. Introduction

The Kathmandu valley lies above an ancient dried-up lake, and most of the soil in this area is lacustrine and fluvio-deltaic deposits [1]. In some areas within the valley, construction projects face significant challenges due to weak soil conditions[2]. Due to their extremely low strength and stiffness, some of the difficulties encountered when dealing with weak soil in construction projects are instability, bearing capacity failure, or excessive settlement[3][4]. Such soils are not suitable for supporting structural loads without stabilization because of their high compressibility, low shear strength, and significant volumetric changes with moisture fluctuations. Common examples of traditional ground improvement techniques are using stabilizing chemicals or mechanical compaction. Alternative stabilizers, like sand, marble dust, limestone dust, stone dust, and quarry dust, have been investigated recently, though, because of their affordability, accessibility, and environmental advantages. These materials are frequently waste byproducts of the mining and stone crushing industries, which further encourages their sustainable use. The individual and combined effects of sand, and stone dust on the geotechnical behavior of Kathmandu's weak soils have, however, not been thoroughly studied in many studies. To identify the ideal mix proportions, appropriate for real-world applications, it is necessary to assess the compaction properties and shear strength parameters of such stabilized soils.

Broadly, stabilization can be classified into chemical and physical stabilization. Chemical stabilization is a technique that involves the use of chemicals, such as cement, lime, fly ash, or polymer-based binders, to improve the soil properties or aggregate materials for construction[5]. One can either add stabilizing material to an undisturbed soil deposit and allow it to interact by allowing it to permeate through soil voids, or one can mechanically mix and compact the natural soil and stabilizing material together to create a homogeneous mixture[6]. Other common methods used to make weak soil more stable by increasing strength and stiffness are by cementation, grading and compaction, soil replacement, artificial consolidation, by use of chemicals, geosynthetics, grouting, and by use of waste materials: rock dust, rubber dust, eggshell powders, kiln slag, waste geopolymers[3, 7, 8, 9, 10, 11, 12, 13, 14, 15, 16, 17, 18, 19].

Prior studies on using sand and stone dust have shown effective results in the stabilization of weak soil. A study found that adding non-plastic fines increased the Maximum Dry Density (MDD) and California Bearing Ratio (CBR) value of soil types, while decreasing the OMC (Optimum Moisture Content) [20]. As numerous studies have shown, the addition of stone-based additives greatly enhances the geotechnical characteristics of expansive or weak soils. A study found that the addition of stone dust to soil results in a decrease in plasticity index (PI), increased MDD, reduced OMC, and increased Unconfined Compressive Strength (UCS) [14]. Parallelly, laboratory test results from another study showed a significant strength increase when sand was added to soil, with improvements observed at sand percentages up to 60% by soil weight [21]. It has been demonstrated that adding sand or stone dust to weak soils improves the shear strength parameters (cohesion c and internal friction angle ϕ) while lowering compressibility, swelling pressure, and plasticity.

As shown in Table 1 and Table 2, previous studies have explored the use of stone dust and sand, respectively, for improving the geotechnical properties of various soil types. These tables give a comparative overview of the efficacy of stone dust and sand in enhancing the geotechnical qualities of weak soils. Although a number of studies have examined the stabilizing effects of sand or stone dust separately, not many have examined how these

TABLE 1. Effects of Stone Dust Addition on Soil Properties: Summary of Previous Studies

Ref.	Soil Type	Additives	Key Findings
[22]	Laterite	Graphite Nanoparticles (GN)	↓ Swelling pressure beyond 1% GN; ↑ Shear strength; ↑ Impermeability; improved soil strength and reduced volume change
[23]	Expansive Shale	Marble Dust	↓ Plasticity index; ↑ Permeability; reduced dry density; effective in altering plasticity and improving sustainability
[24]	Lateritic Soil	Micro-sized Quarry Dust	↓ Plasticity index; ↑ UCS, MDD, CBR; micro-filler action enhanced strength and compaction
[25]	Fine-Grained Soil	Stone Dust	↓ LL, PL, PI, and OMC; ↑ MDD and UCS up to 50% stone dust; effective in reducing plasticity and improving strength
[26]	Expansive Clayey Soil	Natural Zeolite	↑ UCS (+21% with zeolite); ↓ Swelling slightly; strength significantly improved with optimized CKD and zeolite blend
[27]	Expansive Soil	Quarry Dust	↓ LL, PI; ↑ PL, SL, cohesion, ϕ, OMC; ↑ MDD with quarry dust; reduced plasticity and improved compaction; optimum strength at 5% lime
[28]	Expansive Soil	Limestone Dust	↑ UCS, CBR; ↓ Swelling pressure and shrinkage strain; effective strength gain and swell reduction; suitable for subgrade and landfill liner applications
[29]	Expansive Soil	Stone Dust	↓ Swelling and plasticity; ↑ UCS and compaction; best results with equal proportions of stone dust and fly ash
[14]	Weak Soil	Stone Dust	↑ UCS after 28 days curing; ↑ MDD and ↓ OMC with stone dust; combined use improved the strength of weak Kathmandu soil

two substances work together to affect the strength properties of high-plastic soils that are unique to Kathmandu.

The stabilization of lacustrine high plastic soils from Kathmandu valley using different ratios of sand, stone dust, and their combination is the main focus of this study. In order to determine how these stabilizers affect compaction and strength behavior, the scope of the study includes analyzing the index properties of the natural soil and altering it. Prior to and following modification, cohesion, internal friction angle, maximum dry density (MDD), and optimal moisture content (OMC) are measured. The principal aim is to determine the ideal ratio of sand, stone dust, or both for the successful stabilization of weak soils unique to this area. Particularly for small-to medium-sized infrastructure projects, the results are intended to provide insights on the performance and feasibility of these locally accessible materials for ground improvement. This study builds on earlier research by analyzing the effects of separate stabilizers, such as sand and stone dust, as well as the shear strength properties that arise from applying them together. This approach provides a workable and affordable solution for sustainable soil stabilization in the Kathmandu Valley.

TABLE 2. Effects of Sand Addition on Soil Properties: Summary of Previous Studies

Ref.	Soil Type	Additives	Key Findings
[30]	Swelling soil	Dune Sand	↓ Swelling pressure
[31]	Soil	River sand	Sand is suitable for subgrade stabilization
[21]	Expansive soil	Sand	↓ LL, PL, Shrinkage, OMC; ↑ MDD; UCS ↑ until 60% sand, then ↓
[32]	Expansive soils	Dune Sand	↓ Swelling pressure & potential, ↑ Shear strength, Economic stabilization
[33]	Swelling Clays	Sand	↓ Swelling
[34]	Expansive soils	Dune sand	Stabilization is effective for ¿30% sand
[35]	Clayey soil	Sand & fly ash	30% sand → ↑ MDD, ↓ OMC, ↑ CBR; Beyond 30%, ↓ MDD
[36]	Cohesive Soil	Sand	↓ LL initially, ↓ OMC, ↑ MDD, ↑ CBR significantly
[37]	Clayey Soils	Sand	Bearing Capacity (3.7× untreated soil); 60% sand = optimal for pavements
[38]	Expansive soil	Beach Sand	↓ Consistency parameters, ↓ Swelling; Sand fineness affects plasticity
[39]	Clay	Sand	↓ Swelling, ↓ Consistency limits, ↓ Compressibility, ↑ Dry density
[40]	Laterite	Sand	↓ Atterberg limits, ↓ Shrinkage, ↑ MDD, CBR (irregular trend)
[41]	Swelling Soil	Sand	↓ Swelling pressure; 50% sand = significant ↓ LL & ↓ Free swell
[42]	Clay	Sand	↑ Permeability, ↑ CBR, ↑ UCS up to 40% sand
[43]	Black cotton	Sand & coir	↑ CBR, ↑ Compaction
[44]	Swelling Soil	Geofoam & Sand	↓ Swelling, ↓ LL, ↓ OMC, ↑ Dry density
[45]	Sandy Clay	Dune Sand	↑ Strength at 2-4% sand; ↓ Strength at 6%

2. Methodology

The high-plasticity soil was collected from Kupondole, a location close to the Bagmati River in the central Kathmandu Valley. The site location close to the Bagmati River and the representative sample of lacustrine silt used in this investigation are shown in Figure 1. Samples of bulk soil were taken from shallow depths (0–1.5 m), sealed in plastic bags, air-dried, ground up, and then sieved through a 425-micron sieve to guarantee consistency. The soil was characterized using basic index properties such as Atterberg limits and grain size distribution.

Stabilizers for this study, stone dust (D) and river sand (S), were obtained from a quarry at Dhading, an area close to the Kathmandu Valley. The stone dust was sieved through 425 microns, and was used in varying proportions (10%, 20%, 30% and 40% by dry weight of soil). Similarly, the sand passing through 1 mm was used in varying proportions (10%, 20%, 30% and 40% by dry weight of soil). Both stone dust and sand were also combined at varying proportions (5D-5S%, 10D-10S%, 15D-15S%, and 20D-20S% by dry weight of soil). The framework of the study is depicted in Figure 2. The basic properties of the mix were tested, and following IS 2720 (Part 7), Standard Proctor compaction tests were performed to ascertain each soil mix's MDD and OMC. Furthermore, a set of stabilized samples was subjected to Direct Shear Tests in accordance with IS 2720 (Part 13) in order to ascertain the shear strength parameters, specifically cohesion (c) and angle of internal friction (ϕ). The test results are all based on individual trials for each soil mix.

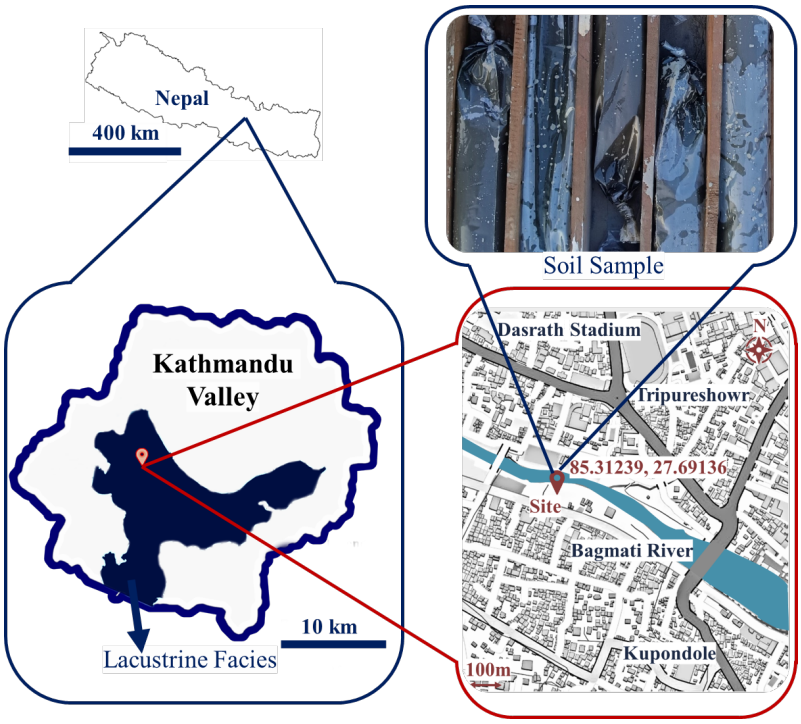

FIGURE 1. Representative sample of lacustrine silt from the study area near the Bagmati River within the Kathmandu Valley, Nepal.

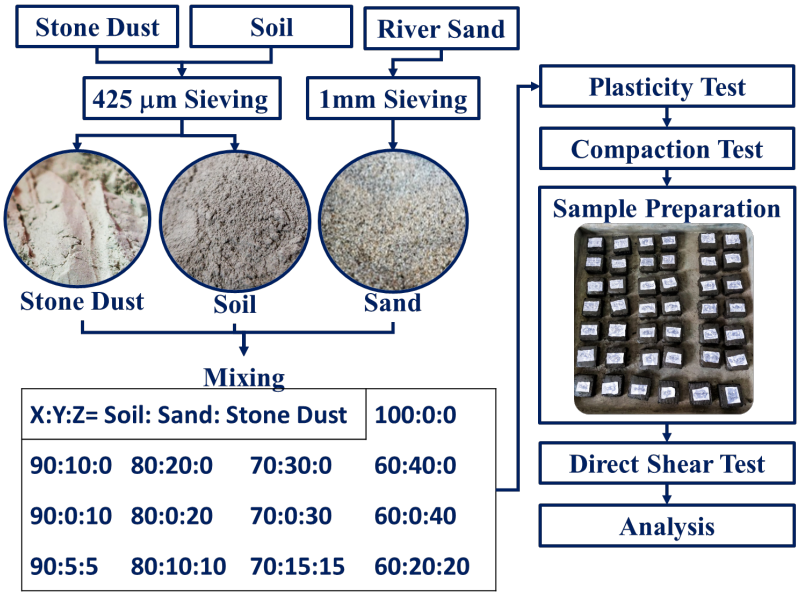

FIGURE 2. Methodological framework of the study.

The number of compositions examined in this study presented practical time and resource constraints, even though multiple repetitions would offer statistical strength and enable uncertainty quantification. The findings are therefore interpreted, emphasizing general

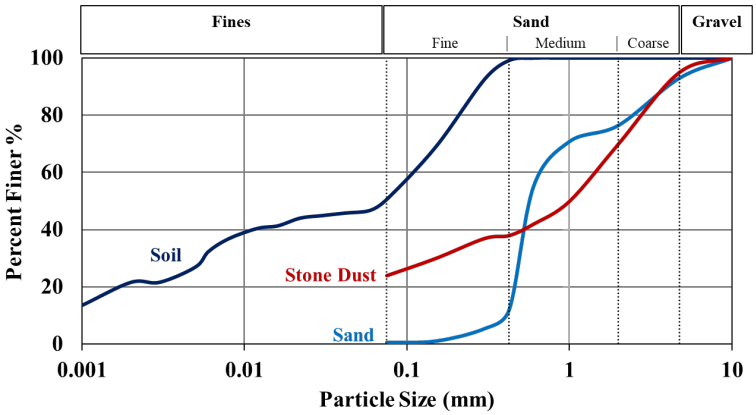

FIGURE 3. Grain size distribution curves for the natural soil, stone dust, and sand used in the stabilization.

behavioral patterns among various stabilizer kinds and contents rather than statistically averaged values.

3. Results and Discussion

3.1. **Index Properties of Natural Soil and Stabilizers.** Prior to stabilization, the classification characteristics of the natural soil from Kupondole, Kathmandu, were determined. The particle size distribution curves for natural soil, sand, and stone dust are shown in Figure 3. The natural soil curves substantially, with a large percentage of particles smaller than 0.075 mm, suggesting that fine-grained particles (clay and silt) predominate. Atterberg limit test demonstrates the soil's high plasticity. The liquid limit is 83.14%, and the plastic limit is 43.44%, resulting in a plasticity index of 39.69%. The liquid limit after oven drying is 69.92%, and the ratio of the liquid limit after oven drying to that before drying is 0.84—above the threshold of 0.75—indicating the soil is inorganic. Therefore, the soil is classified as inorganic MH according to the Unified Soil Classification System. Parallelly, sand is primarily coarse, with the majority of particles lying between 0.075 mm and 4.75 mm, whereas stone dust has a flatter curve with a mixture of fine to medium particles (range from silt to fine sand sizes). The coarser gradation, like sand and stone dust, indicates their ability to improve the structure of the soil by improving interparticle friction, decreasing flexibility, and diluting the fine clay percentage [27, 29].

3.2. **Effect of Stone Dust and Sand on Atterberg Limits.** The Atterberg limits of the stabilized and natural soil mixtures were analyzed to determine the plasticity behavior. The Unified Soil Classification System (USCS)-based plasticity chart is shown in Figure 4, which plots the plasticity index (PI) against the liquid limit (LL) for different soil combinations. With a plasticity index of 39.697 and a liquid limit of 83.137, the natural soil (100:0:0) lies below the A-line and is categorized as a high-plasticity silt (MH). The downward and leftward movement of data points in Figure 4 shows that the addition of sand and stone dust significantly lowers the plasticity index and liquid limit. These patterns are indicated by the arrows, which show how well both stabilizers work to reduce plasticity. For example, the LL and PI are decreased by the mixture containing stone dust. The mixture containing sand also produces a similar reduction, getting closer to the

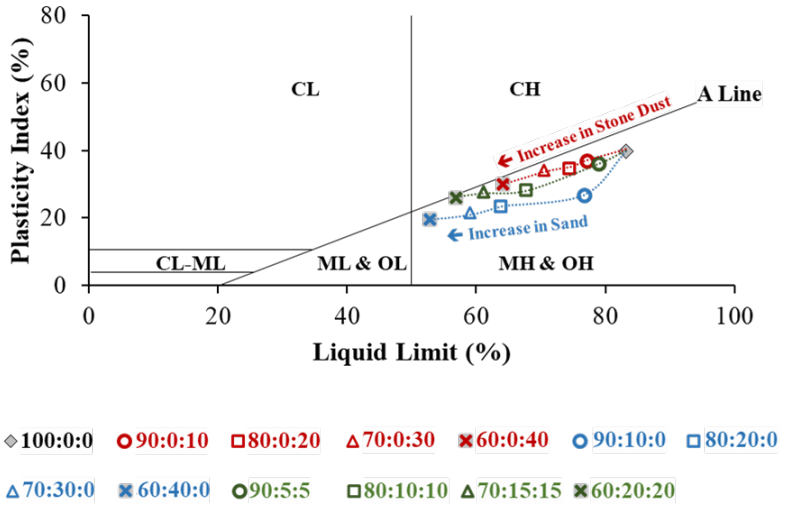

FIGURE 4. Plasticity chart showing the impact of different ratios of sand and stone dust on the Atterberg limits of Kupondole's high-plasticity soil.

ML (low-plasticity silt) zone. The effect of combined mixes is also noticeable, significantly lowering the LL and PI. The non-plastic properties of sand and stone dust dilute the clay content and reduce the soil's capacity to hold water, which lowers the LL and PI. This is the reason for the decrease in plasticity. This is consistent with earlier studies that found that coarse materials lower the plasticity index and swelling potential of expansive soils [27, 29]. The use of sand and stone dust together has a synergistic effect, resulting in appreciable decreases in plasticity. These findings support the materials' suitability for stabilizing Kupondole's high-plasticity soils, especially for small- to medium-sized building projects, by reducing the unfavorable volume change behavior of the native soil.

3.3. **Compaction Test Results.** As shown in Figure 5, when the stone dust content rises from 0% to 40%, the Optimum Moisture Content (OMC) gradually decreases, starting at 38.46% and ending at roughly 34.70%. The OMC, however, decreases down to roughly 34.88% as the amount of sand in the soil mix grows from 0% to 40%, following a similar decreasing trend. However, the Maximum Dry Density (MDD) of soil increases significantly from 11.99 kN/m^3 to 13.803 kN/m^3 with the percentage of stone dust in the soil mixture, from 0% to 40%. The MDD also grows steadily with the addition of sand, reaching 13.398 kN/m^3 when 40% of the soil is replaced with sand. The MDD rises by above 11%, while the OMC falls by nearly 9% when sand content is increased from 0% to 40%. In contrast, increasing stone dust in the same amount results in a nearly 15% rise in MDD and over 9% decrease in OMC.

The presence of both sand and stone dust in soil leads to significant changes in the compaction properties; however, stone dust was found to be more effective than sand. The maximum dry density (MDD) increases due to the angular and varying sizes of these particles, which occupy void spaces between larger soil particles, resulting in improved particle packing. However, the optimum moisture content (OMC) decreases as the percentage of sand and stone dust increases. The reduced porosity of these particles reduces the amount of water that can be held within the soil, reducing the amount of water needed for optimal

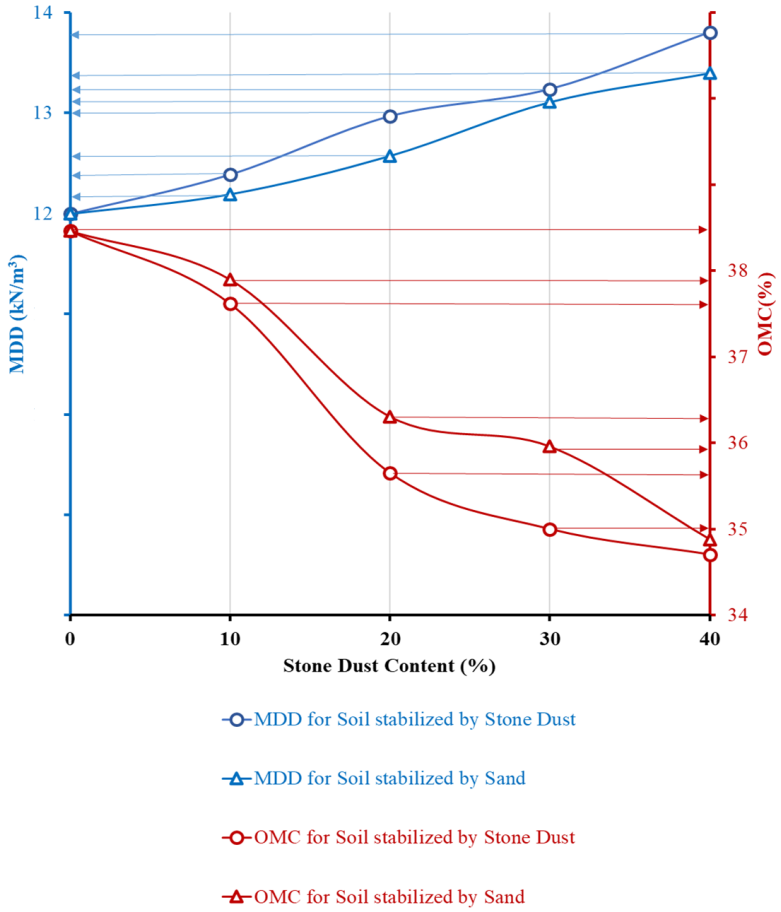

FIGURE 5. Comparison of Compaction Properties (OMC and MDD) for sand and stone dust.

compaction. This can be beneficial in construction projects, as it allows earth to be compacted with less water, potentially saving costs and reducing post-construction settlement risk. This also reduces the likelihood of soil shrinkage or expansion.

4. Direct Shear Test Results

As shown in Figure 6, as percentages of sand, stone dust, or a combination of both were added to the soil mixture, the data showed a steady rise in the friction angle. With no addition of admixtures in the soil, the friction angle was around 20.44 degrees. However, the friction angle reached 34.90 degrees when the sand content rose to 40% and it reached 36.8 degrees when the stone dust content rose to 40%. The friction angle increased to roughly 40.02 degrees when both sand and stone dust were mixed together at a percentage of 40%.

Unlike the friction angle, the cohesiveness of the soil mixtures showed a divergent pattern of improvement with the addition of sand and stone dust. As the percentages of sand, stone dust, or both were raised in the soil mixture, cohesion, which is a measure of the soil's intrinsic strength, rapidly reduced. For instance, cohesiveness reduced from 23.39

kN/m^2 to roughly 7.18 kN/m^2 when 40% sand was added to the soil and to approximately 7.12 kN/m^2 when 40% stone dust was added. Cohesion decreased to 5.42 kN/m^2 when both sand and stone dust were mixed together at a percentage of 40%.

The friction angle rises by above 70%, while the cohesion falls by nearly 69% when sand content is increased from 0% to 40%. In contrast, increasing stone dust in the same amount results in a nearly 80% rise in friction angle and over 69% decrease in cohesion. However, the friction angle rises by above 95%, while the cohesion falls by nearly 77% when both sand and stone dust are combined and the percentage by weight is increased from 0% to 40%.

Cohesion was found to decrease noticeably as stabilizer content increased, while the internal friction angle increased as well. The substitution of non-cohesive granular stabilizers for fines explains this behavior. The addition of coarser particles also improves interparticle interlocking, which raises frictional resistance. The soil structure changes from a clustered and plastic matrix to a more granular and friction-dependent framework as the stabilizer content rises [46]. This change causes the components of shear strength to be redistributed, increasing the frictional strength while decreasing the cohesive contribution.

So, sand and stone dust significantly impact soil behavior in geotechnical engineering applications. Sand is a stabilizer, increasing soil stability by improving resistance to shear deformation. Stone dust enhances soil stability by increasing its capacity to withstand shear stresses. As more stone dust is added, the friction angle rises, indicating improved shear resistance. However, the trade-off between cohesiveness and shear strength is important. With the addition of sand or stone dust, the friction angle increases, but the soil's cohesiveness decreases, indicating increased shear resistance. This allows for modification of soil compositions to meet specific project needs, improving soil performance in situations where shear deformation is crucial.

5. Conclusion

The study assessed weak soil's geotechnical properties, examined how sand, stone dust, or a combination altered compaction characteristics, and identified stabilized soil's shear strength parameters, providing valuable insights into poor soil behavior. The lacustrine soil from Kupondole was inorganic, high plastic silt. The laboratory testing of the soil resulted in MDD of 12.0 kN/m^3, OMC of 38.46%, friction angle of 20.44 degrees, cohesion of 23.39 kN/m^2, and specific gravity of 2.36. Meanwhile, sand and stone dust added coarser particles to improve the soil's gradation.

The results demonstrate the effectiveness of sand and stone dust to improve the plasticity characteristics of the lacustrine MH, with combined mixes showing noticeable reductions in LL and PI. Similarly, when mixing sand and stone dust in the soil, the compaction tests showed a significant increase in MDD and a decrease in OMC, enhancing compaction properties in weak soil, with 40% content showing the best results. Likewise, both stabilizers significantly improved the lacustrine soil's shear strength. Particularly, the friction angle of stabilized soil increased with the addition of sand and stone dust. For both sand and stone dust, the greatest improvements in the friction angle were consistently observed at the 40% content level. However, the addition of the stabilizers led to a decline in cohesion, emphasizing the importance of balance between increased friction angle with decreased

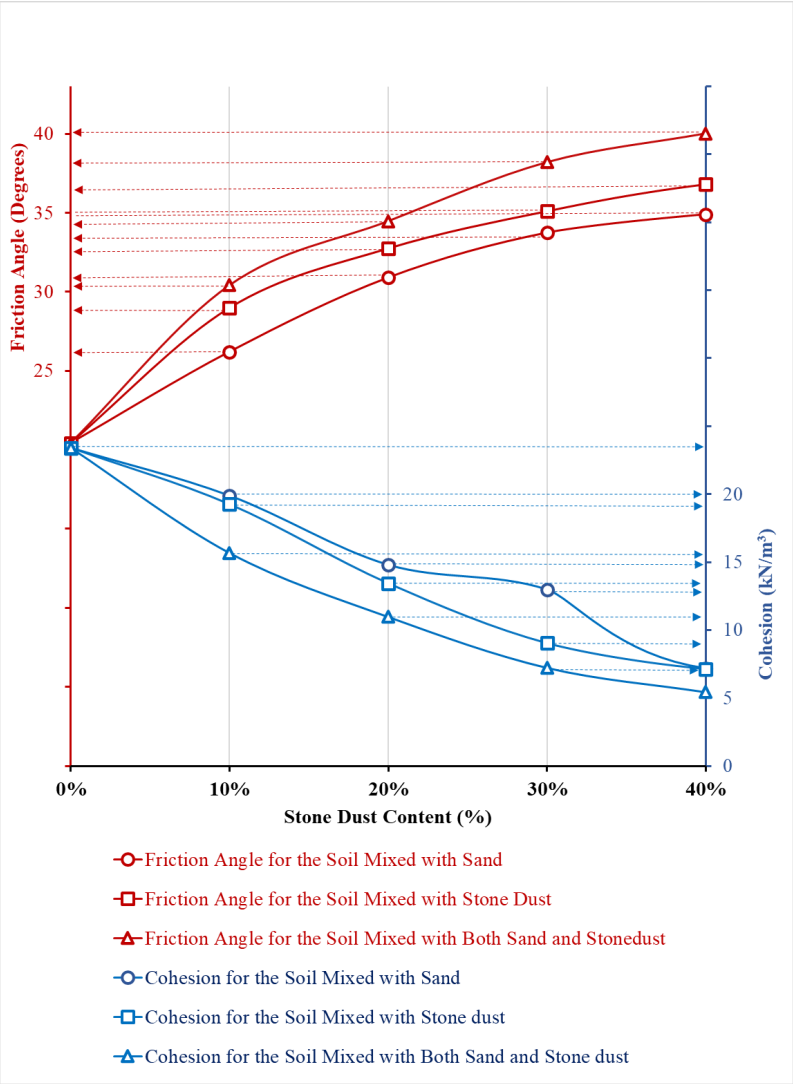

FIGURE 6. Comparison of cohesion and friction angle for soil stabilized with sand, stone dust, and the combination of both.

cohesiveness in the shear strength of soil.

On comparison, the 40% addition of the stone dust in the weak soil resulted in around a 15% rise in MDD and an 80% rise in friction angle, which was more effective than sand. When comparing the compaction and shear strength parameters between the sand and stone dust individually in stabilization of weak soil, it is clear that stone dust is a more effective stabilizer than sand. However, the impacts of the combined mix (both sand and stone dust) from 0% to 40% result in nearly a 1.96 times increase in friction angle when compared to untreated (natural) soil condition, indicating that the combination acts as an efficient stabilizing agent. So, sand and stone dust are cost-effective, long-lasting materials to reinforce weak soils and address engineering and environmental concerns [1, 14, 21, 27, 29, 46].

From a practical standpoint, incorporating 30–40% stone dust emerged as the most effective and economical strategy for enhancing weak soils in Kathmandu Valley. This method is particularly suitable for use in shallow foundations, road subgrade layers, and fill materials in small- to medium-scale infrastructure projects. Moreover, the approach promotes the reuse of local quarry by-products, aligning with sustainable construction practices and cost efficiency [20, 27, 29].

References

[1] H. G. Dill, B. D. Kharel, V. K. Singh, B. Piya, K. Busch, and M. Geyh, "Sedimentology and paleogeographic evolution of the intermontane Kathmandu basin, Nepal, during the Pliocene and Quaternary. Implications for formation of deposits of economic interest," *J. Asian Earth Sci.*, vol. 19, no. 6, pp. 777–804, 2001.

[2] B. K. Dahal and J. J. Zheng, "Compression behavior of reconstituted clay: A study on black clay," *J. Nepal Geol. Soc.*, vol. 55, no. 1, pp. 55–60, 2018.

[3] B. K. Dahal, J. J. Zheng, and R. J. Zhang, "Evaluation and Modelling of the Reconstituted Clays Considering Pre-peak Stiffness Degradation," *Int. J. Geosynth. Gr. Eng.*, vol. 5, no. 2, Jun. 2019.

[4] A. Joseph, S. Chandrakaran, and N. Sankar, "Performance of Compacted Lime Column and Lime-Fly Ash Column Techniques for Cochin Marine Clays," *Int. J. Geosynth. Gr. Eng.*, vol. 4, no. 4, 2018. [Online]. Available: http://dx.doi.org/10.1007/s40891-018-0147-5

[5] D. Barman and S. K. Dash, "Stabilization of expansive soils using chemical additives: A review," *J. Rock Mech. Geotech. Eng.*, vol. 14, no. 4, pp. 1319–1342, 2022. [Online]. Available: https://doi.org/10.1016/j.jrmge.2022.02.011

[6] H. Afrin, "A Review on Different Types Soil Stabilization Techniques," *Int. J. Transp. Eng. Technol.*, vol. 3, no. 2, pp. 19, 2017.

[7] S. Ahmad, M. Shah Alam Ghazi, M. Syed, and M. A. Al-Osta, "Utilization of fly ash with and without secondary additives for stabilizing expansive soils: A review," *Results Eng.*, vol. 22, p. 102079, 2024. [Online]. Available: https://doi.org/10.1016/j.rineng.2024.102079

[8] M. J. Cui, J. J. Zheng, B. K. Dahal, H. J. Lai, Z. F. Huang, and C. C. Wu, "Effect of waste rubber particles on the shear behaviour of bio-cemented calcareous sand," *Acta Geotech.*, vol. 16, no. 5, pp. 1429–1439, 2021.

[9] B. K. Dahal, J. J. Zheng, and R. J. Zhang, "Experimental Investigation on Physical and Mechanical Behavior of Kathmandu Clay," *Adv. Mater. Res.*, vol. 1145, pp. 112–116, Mar. 2018.

[10] D. L. K. Heng, M. S. Takahashi, and M. T. Ohashi, "Super well point technology with advancements in soil improvements for land reclamations," *Energy Procedia*, vol. 143, pp. 442–447, 2017.

[11] N. W. Jassim, H. A. Hassan, H. A. Mohammed, and M. Y. Fattah, "Utilization of waste marble powder as sustainable stabilization materials for subgrade layer," *Results Eng.*, vol. 14, p. 100436, 2022. [Online]. Available: https://doi.org/10.1016/j.rineng.2022.100436

[12] C. F. Leung, Y. W. Yee, and K. W. Leong, "Principles and case histories of deep vibro techniques," in *Ground Improvement Case Histories: Compaction, Grouting and Geosynthetics*, Elsevier Ltd., 2015, pp. 337–364.

[13] Z. C. Moh and P. Lin, "Case Study of Ground Improvement Work at the Suvarnabhumi Airport of Thailand," in *Ground Improvement Case Histories*, Elsevier Ltd., 2015, pp. 165–208.

[14] U. Niraula and B. K. Dahal, "Compaction and Strength Properties (after 28 days of curing) of Soil Stabilized by Stone Dust and Cement," in *Proc. 11th IOE Graduate Conf.*, 2023.

[15] B. Pokharel and S. Siddiqua, "Effect of calcium bentonite clay and fly ash on the stabilization of organic soil from Alberta, Canada," *Eng. Geol.*, vol. 293, p. 106291, 2021. [Online]. Available: https://doi.org/10.1016/j.enggeo.2021.106291

[16] P. Ghadir and N. Ranjbar, "Clayey soil stabilization using geopolymer and Portland cement," *Constr. Build. Mater.*, vol. 188, pp. 361–371, 2018. [Online]. Available: https://doi.org/10.1016/j.conbuildmat.2018.07.207

[17] L. Li *et al.*, "Performance of the one-part geopolymer stabilized soft clay under acids attack," *J. Clean. Prod.*, vol. 452, p. 142183, 2024. [Online]. Available: https://doi.org/10.1016/j.jclepro.2024.142183

[18] Y. Min, J. Wu, B. Li, and J. Zhang, "Effects of Fly Ash Content on the Strength Development of Soft Clay Stabilized by One-Part Geopolymer under Curing Stress," *J. Mater. Civ. Eng.*, vol. 33, no. 10, 2021.

[19] J. Wu, Y. Min, B. Li, and X. Zheng, "Stiffness and strength development of the soft clay stabilized by the one-part geopolymer under one-dimensional compressive loading," *Soils Found.*, vol. 61, no. 4, pp. 974–988, 2021.

[20] S. Mishra, S. N. Sachdeva, and R. Manocha, "Subgrade Soil Stabilization Using Stone Dust and Coarse Aggregate: A Cost Effective Approach," *Int. J. Geosynth. Gr. Eng.*, vol. 5, no. 3, 2019. [Online]. Available: https://doi.org/10.1007/s40891-019-0171-0

[21] G. Kollaros and A. Athanasopoulou, "Sand as a soil stabilizer," *Bull. Geol. Soc. Greece*, vol. 50, no. 2 SE-Engineering Geology, Hydrogeology, Urban Geology, pp. 770–777, Jul. 2016. [Online]. Available: https://ejournals.epublishing.ekt.gr/index.php/geosociety/article/view/11783

[22] Y. Gao, J. Li, Y. Zhang, X. Sun, and L. Yang, "Mechanical and Microscopic Properties of Graphite/Laterite Nanocomposites," *Adv. Mater. Sci. Eng.*, vol. 2021, 2021.

[23] M. R. Hakro *et al.*, "Compaction Characteristics and Permeability of Expansive Shale Stabilized with Locally Produced Waste Materials," *Materials (Basel)*, vol. 15, no. 6, pp. 1–21, 2022.

[24] R. K. Etim, D. U. Ekpo, I. C. Attah, and K. C. Onyelowe, "Effect of micro sized quarry dust particle on the compaction and strength properties of cement stabilized lateritic soil," *Clean Mater.*, vol. 2, Nov. 2021, p. 100023. [Online]. Available: https://doi.org/10.1016/j.clema.2021.100023

[25] P. Phuyal and B. K. Dahal, "Effect of Stone Dust on Geotechnical Parameter of Fine Grained Soil," in *Proc. 10th IOE Graduate Conf.*, 2021, pp. 1435–1440.

[26] A. A. Sharo, F. M. Shaqour, and J. M. Ayyad, "Maximizing Strength of CKD — Stabilized Expansive Clayey Soil Using Natural Zeolite," *KSCE J. Civ. Eng.*, vol. 25, no. 4, pp. 1204–1213, 2021.

[27] A. Sabat, "A study on some geotechnical properties of lime stabilised expansive soil-quarry dust mixes," *Int. J. Emerg. Trends Eng. Dev.*, vol. 1, no. 2, pp. 42–49, 2012. [Online]. Available: http://rspublication.com/ijeted/jan

[28] A. K. Sabat and S. Mohanta, "Performance of limestone dust stabilized expansive soil-fly ash mixes as construction material," *Int. J. Civ. Eng. Technol.*, vol. 7, no. 6, pp. 482–488, 2016.

[29] M. S. Ali and S. S. Koranne, "Performance analysis of expansive soil treated with stone dust and fly ash," *Electron. J. Geotech. Eng.*, vol. 16 I, pp. 913–982, 2011.

[30] N. K. Ameta, D. G. M. Purohit, and A. S. Wayal, "Characteristics, problems and remedies of expansive soils of Rajasthan, India," *Electron. J. Geotech. Eng.*, vol. 13 A, 2008.

[31] C. C. Ikeagwuani and D. C. Nwonu, "Emerging trends in expansive soil stabilisation: A review," *J. Rock Mech. Geotech. Eng.*, vol. 11, no. 2, pp. 423–440, 2019. [Online]. Available: https://doi.org/10.1016/j.jrmge.2018.08.013

[32] M. K. Gueddouda, I. Goual, M. Lamara, and M. S. Goual, "Comportement mecanique d'un sol expansif stabilise par ajout de sable de dune," *Rev. Sci. et Sci. de l'Ingénieur*, 2.

[33] B. Abouar, P. M. Mpélé, K. K. Dieudonné, and M. Amadou, "Prediction of Swelling and Effects of Sand on Swelling Clays from the Far North Region of Cameroon," 2023, pp. 42–53.

[34] M. Lamara, M. K. Gueddouda, and B. Benabed, "Stabilisation physico-chimique des sols gonflants (sable de dune + sel)," *Rev. Française Géotechnique*, no. 115, pp. 25–35, 2006.

[35] C. R. V. Prasad and R. K. Sharma, "Influence of sand and fly ash on clayey soil stabilization," *Iosr-Jmce*, vol. 2014, pp. 36–40, 2014.

[36] T. K. Roy, "Influence of Sand on Strength Characteristics of Cohesive Soil for Using as Subgrade of Road," *Procedia - Soc. Behav. Sci.*, vol. 104, pp. 218–224, 2013. [Online]. Available: http://dx.doi.org/10.1016/j.sbspro.2013.11.114

[37] S. Jjuuko, D. Kalumba, and U. Bagampadde, "The use of locally available sand in stabilization of Ugandan clayey soils: Case study of clayey soil from Busega area," in *Uganda Institution of Professional Engineers 16th National Technology Conference (NTC 2011)*, 2011.

[38] B. Louafi and R. Bahar, "Sand: An Additive for Stabilization of Swelling Clay Soils," *Int. J. Geosci.*, vol. 3, no. 4, pp. 719–725, 2012.

[39] B. Ghania, S. R. Souhila, and M. Djenette, "The Influence of Varying Percentage of Sand on The Properties of Coherent Soil," 2021, pp. 2–6.

[40] R. Madu, "Sand-laterite mixtures for road construction (a laboratory investigation)," *Niger J. Technol.*, vol. 1, no. 1, 1975.

[41] M. A. Sakr, M. A. El Swaf, A. K. Nazir, and M. Ali, "Swelling Soil Stabilized with Sand," vol. 8, no. 3, 2024.

[42] A. U. R. Shankar, A. Chandrashekhar, and H. P. Bhat, "Experimental Investigation on Lithomargic Clay Stabilized with Sand and Coir," *Indian Highw.*, vol. 40, no. 2, pp. 21–31, 2012.

[43] V. Tare, D. Singh, and K. Meshram, "Stabilization of Black Cotton Soil with Sand and Non Woven Coir," *Indian Highw.*, Feb. 2018, pp. 39–44.

[44] M. Sakr and A. Nazir, "Swelling Soil Improved with Geofoam and Sand," Dec. 2022.
[45] A. Bouazza, B. Labbaci, and T. Rikioui, "Effect of dune sand on the compressive strength of a matrix soil of sandy-clay-gypsum," *Int. J. Civ. Eng. Technol.*, vol. 9, no. 1, pp. 830–836, 2018.
[46] U. Niraula, B. K. Dahal, S. Acharya, and P. Phuyal, "High-plasticity silt stabilization: Role of waste stone dust, cement, and curing time," *Results Eng.*, vol. 26, p. 104877, Apr. 2025. [Online]. Available: https://doi.org/10.1016/j.rineng.2025.104877

Everest Advances in Science and Technology (EAST), Vol. 1, No. 1, 2025
ISSN: 3102-0410(print), 3102-0429(online)

Numerical Solutions of Non-Linear Systems of ODES: Lotka–Volterra Predator–Prey Model

NARAYAN SAPKOTA[1,2*], KHIM B. KHATTRI [2]

Abstract. This study investigates the dynamic behavior of predator–prey interactions using the classical Lotka–Volterra system of nonlinear ordinary differential equations. We employ both analytical and numerical techniques to analyze population fluctuations of hares and lynx, based on historical Hudson Bay Company records. An approximate analytical solution is derived using the Ritz method, while a numerical solution is obtained via the fourth-order Runge–Kutta (RK4) method. To enhance model realism, we estimate system parameters $(\alpha, \beta, \gamma, \delta)$ using Simulated Annealing (SA), a global optimization technique well-suited for non-convex landscapes. The model is calibrated against empirical data, and SA-based optimization achieved mean RMSE values of 4.12 for hares and 4.01 for lynx across five independent runs. Comparative plots between observed and predicted populations confirm the model's ability to capture oscillatory behavior and phase shifts. This work compares analytical and numerical solution methods for the Lotka–Volterra system using parameters estimated via Simulated Annealing, demonstrating the relative strengths of the Ritz and Runge–Kutta approaches in modeling real-world population dynamics.

Keywords: Lotka–Volterra Model, Nonlinear Ordinary Differential Equations, Ritz method, Runge-Kutta method, Simulated Annealing.

[1]Department of Computer Engineering, Everest Engineering College, Nepal
E-mail: narayan_sapkota@outlook.com
[2]Department of Mathematics, School of Science, Kathmandu University, Nepal
E-mail: khimkhattri@ku.edu.np
* Corresponding author
Manuscript received: 19 July, 2025; revised: 13 August 2025; accepted: 5 September, 2025.
Everest Advances in Science and Technology (EAST), Vol. 1, No. 1, 2025

1. Introduction

The Lotka–Volterra predator–prey model stands as a foundational framework in the study of nonlinear dynamical systems, originally developed to describe ecological interactions between predator and prey populations [18, 27]. This model captures the cyclical nature of population dynamics through a system of first-order nonlinear differential equations, assuming that prey populations grow exponentially in the absence of predators, while predator populations decline without prey. Their interaction introduces a regulatory feedback mechanism that leads to oscillatory behavior in both species [12]. Due to its simplicity and interpretability, the Lotka–Volterra model has been extensively studied and applied across a wide range of disciplines. In theoretical ecology, it offers insights into species interactions such as wolves and rabbits in terrestrial ecosystems or bass and redear fish in aquatic environments [7]. It has also been used in conservation biology to simulate intervention scenarios, including predator control and endangered species management.

Beyond ecology, the model has found applications in fields such as epidemiology, where it helps simulate interactions between hosts and vectors in diseases like malaria and dengue fever [2, 11]. In economics, it has been adapted to describe competitive market dynamics where firms compete for market dominance, mimicking predator–prey relationships in terms of resource or customer share [19, 28]. The model also extends to engineering systems such as power grids and communication networks, where it describes the balance between supply and demand or the flow of competing data packets [25, 3, 26]. In cell biology and immunology, predator–prey analogues represent virus-infected cells and immune responses, contributing to the understanding of infection dynamics and therapeutic design [10, 21]. Social sciences and artificial intelligence have further leveraged Lotka–Volterra frameworks to simulate cultural interactions, ideological shifts, and the dynamics of neural networks [17, 22]. Despite its versatility, the classical Lotka–Volterra model presents analytical challenges due to its inherent nonlinearity. While qualitative analysis using phase plane methods and stability theory provides insight into equilibrium behavior [1], closed-form solutions are rarely available, especially under realistic ecological conditions involving stochasticity, migration, or environmental constraints [11]. Consequently, numerical approximation methods such as Euler's method and Runge–Kutta schemes have become essential tools for exploring these systems [13].

This study focuses on evaluating the Lotka–Volterra system using both analytical and numerical strategies. We begin with an approximate analytical solution via the Ritz method, highlighting its utility and limitations in capturing the system's inherent oscillations [29]. We then implement a fourth-order Runge–Kutta (RK4) method to numerically simulate population dynamics over time. To align the model with real-world observations, we perform parameter estimation using Simulated Annealing—a global optimization algorithm well-suited for nonlinear systems with complex error surfaces. The model is calibrated against historical lynx–hare data from the Hudson Bay Company, and predictive accuracy is evaluated using root mean square error (RMSE). Finally, we analyze the system's long-term behavior through phase portraits and discuss the broader applicability of the approach in ecological modeling and interdisciplinary research.

2. Lotka–Volterra Model

2.1. **Mathematical Formulation.** The Lotka–Volterra predator-prey model [7, 1, 29] is governed by the following system of two nonlinear ODEs:

$$\begin{cases} \frac{dx}{dt} = \alpha x(t) - \beta x(t)y(t) \\ \frac{dy}{dt} = \delta x(t)y(t) - \gamma y(t) \end{cases} \tag{1}$$

where:

- $x(t)$ represents the prey population at time t,
- $y(t)$ represents the predator population at time t,
- α is the growth rate of the prey in the absence of predators,
- β is the predation rate, describing how often predators catch prey,
- δ is the rate at which predators reproduce based on the availability of prey,
- γ is the death rate of the predators in the absence of food (prey).

The constants α, β, δ and γ are all positive. When the predator is absent, the prey population grows at a rate proportional to its current population. This is described by the equation $\frac{dx}{dt} = \alpha x(t)$ and $y(t) = 0$. Similarly, in the absence of the prey, the predator population declines, with the rate of change given by $\frac{dy}{dt} = -\gamma y(t)$ and $x(t) = 0$.

Experimental studies have documented numerous prey-predator interactions that closely resemble the dynamics predicted by the Lotka–Volterra model. These investigations have examined different species pairs, including the Canada lynx and snowshoe hare [14], as well as moose and wolf populations in Isle Royale National Park [16] and more examples can be found on [29].

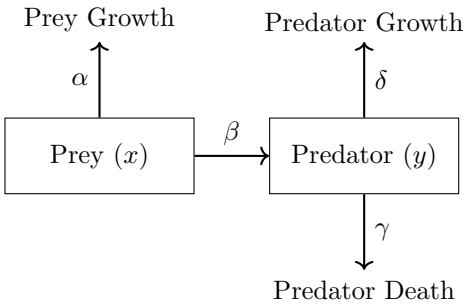

FIGURE 1. Schematic representation of the Lotka–Volterra predator–prey model showing growth, interaction, and death rates.

2.1.1. *Biological Interpretation and Model Assumptions.* The prey are assumed to have an unlimited food supply and reproduce exponentially, except when preyed upon. This exponential growth is represented in Equation (1) by the term αx. The rate of predation on the prey is assumed to be proportional to the rate at which predators and prey encounter one another, represented by βxy. If either x or y is zero, no predation occurs. Hence, the prey equation in Equation (1) describes the rate of change of the prey population as its growth rate minus the predation rate. The term δxy represents the growth of the predator population, which is proportional to the number of prey consumed. The predator growth rate differs from the predation rate, which is why a different constant is used. The term γy represents the predator mortality rate, encompassing natural death or emigration. In the absence of prey, this leads to exponential decay. Therefore, the predator equation in Equation (1) expresses the rate of change of the predator population as the predation rate minus its intrinsic death rate.

The Lotka–Volterra predator-prey model makes several assumptions about the environment and the biology of the populations [7], [29], [6]:

- The prey population has an unlimited food supply at all times.
- The predator population's food supply depends entirely on the prey population.
- The rate of population change is proportional to the population size.
- Environmental factors do not favor one species over the other, and genetic adaptation does not play a significant role during the modeling period.
- Predators have an unlimited appetite.
- Both populations are modeled as a single variable, implying that spatial or age distribution does not influence population dynamics.

2.1.2. *Significance of the Model in Real-World Applications.* The Lotka–Volterra model serves as a foundational framework in ecology, particularly for understanding the dynamics between interacting species in an ecosystem. It illustrates how changes in the population of one species affect the other, showing the cyclical nature of predator-prey dynamics: increases in prey populations lead to higher predator populations, which then reduce the prey population, causing a subsequent decline in predators. In ecology, the model is commonly applied to species such as predators (e.g., wolves) and prey (e.g., rabbits). It can also be used to simulate various scenarios, such as conservation efforts or managing endangered species. The model can be extended to include factors like environmental carrying capacity, external predation pressures, migration, or disease, all of which are nonlinear and complicate the model's analytical solutions.

Beyond ecology, the Lotka-Volterra model has been extensively adapted to describe a wide range of systems across various disciplines. In epidemiology, the model is used to simulate interactions between disease-carrying organisms, such as mosquitoes, and the spread of infections. A prominent application is in the study of vector-borne diseases, where interactions between mosquito populations (the vectors) and human populations (the hosts) are crucial for understanding disease dynamics, such as malaria and dengue fever [2]. This application is key for predicting disease outbreaks and devising control strategies [11]. In economics, the model has been adapted to represent competitive market dynamics [28]. Specifically, it has been applied to model competition between firms, where one firm acts as the "predator" and the other as the "prey" in terms of market share [19]. Additionally, the model has been used to study resource allocation in various economic sectors, providing insights into market stability and the long-term behavior of competing entities [23].

In cell biology, the Lotka-Volterra model helps represent interactions between different cell types, such as infected and uninfected cells, to understand infection dynamics within populations [10]. It has been used to simulate viral infections, examining interactions between virus-infected cells and immune cells [21] [20]. These insights are crucial for developing effective treatments, vaccines, and for understanding how infections spread and persist within populations. In engineering, the Lotka-Volterra model is employed to simulate systems with two interacting components, such as the balance between supply and demand or resource allocation in networks. For example, in power grid management, the model describes the interactions between energy supply and consumption [25] [26]. Similarly, in communication networks, it has been used to represent traffic flow, where competing entities (such as data packets) interact and influence overall network performance [3] [4] [5]. These applications illustrate how predator-prey dynamics govern systems in which

competition or cooperation between components drives the overall behavior of the system.

Finally, the Lotka-Volterra model can also be applied to understand social behavior dynamics, such as interactions between competing social groups, ideologies, or cultures [17]. It has been adapted for use in neural networks to study the dynamics of interacting components in complex systems [22]. This broad applicability across various fields highlights the model's versatility in describing complex interactions beyond its original ecological context.

3. Analytical Methods

Despite the increasing applications of the Lotka-Volterra model, no closed-form analytical solution for this predator-prey system has been established in the literature [24]. The Equation (1) is recognized as conservative, meaning that its solutions must exhibit periodic behavior and do not have a simple expression in terms of the usual trigonometric functions; however, the exact analytical expressions for these solutions remain unknown [24]. In this section, we will first discuss the theoretical background of the Ritz method also known as principle of harmonic balance, followed by its application to the LV system, as demonstrated in [8].

3.1. **Theoretical Background of Ritz Method.** The Ritz method provides an approximate solution, $x(t)$, to the equation

$$\ddot{x} + f(x) = 0$$

by ensuring that the functional

$$J = \int_{t_a}^{t_b} F(x, \dot{x}, t)\, dt$$

is minimized. Here, $F(x, \dot{x}, t)$ is selected such that the solution to the minimum of J, governed by the Euler-Lagrange equation, corresponds to the differential equation we aim to solve:

$$\frac{\partial F}{\partial x} - \frac{d}{dt}\left(\frac{\partial F}{\partial \dot{x}}\right) = \ddot{x} + f(x) = E(x) = 0.$$

The approximate solution $x(t)$ is expressed as

$$x(t) = \sum a_i \varphi_i(t)$$

where the $\varphi_i(t)$ are a linearly independent set chosen based on prior knowledge of the differential equation's behavior.

To determine $\tilde{x}(t)$, the functional J must be minimized with respect to the n coefficients a_i. If we impose the condition that $\varphi_i(t_a) = \varphi_i(t_b) = 0$, or that φ_i is periodic over the interval $t_a - t_b$, we obtain the following conditions:

$$\int_{t_a}^{t_b} \varphi_i(t) E(\tilde{x}(t))\, dt = 0, \quad i = 1, \ldots, n$$

For oscillatory systems, the Ritz method simplifies the process by eliminating the need to perform the n integrations mentioned earlier. When we take $\tilde{x}(t) = A\cos(\omega t)$ as an approximate solution to $\ddot{x} + f(x) = 0$, we find, through evaluating the integral, that the Ritz method is equivalent to selecting ω and A such that $\tilde{x}(t)$ satisfies the differential equation, while disregarding the higher harmonics produced by $f(\tilde{x})$. In other words,

the sum of the coefficients of $\cos(\omega t)$ in $E(\tilde{x}(t))$ must be zero. Similarly, when we take $\tilde{x}(t) = \sum_{n=0}^{N} a_n \cos(n\omega t)$, we find that the coefficients of $\cos(n\omega t)$, for $n = 0, \ldots, N$ in $E(\tilde{x}(t))$ must balance to zero, which is the essence of the principle of harmonic balance.

3.2. **Ritz Method for Solving the LV System.** Equilibrium points, also known as fixed points, are locations where both populations remain constant over time, meaning $\frac{dx}{dt} = 0$ and $\frac{dy}{dt} = 0$. To determine the equilibrium points, set the right-hand sides of the equation (1) equal to zero:

$$\alpha x - \beta xy = 0 \tag{2}$$

$$\delta xy - \gamma y = 0 \tag{3}$$

The Equation (2), has two possibilities:

(1) $x = 0$ (which is a trivial equilibrium corresponding to the extinction of the prey population),
(2) $\alpha - \beta y = 0 \Rightarrow y = \frac{\alpha}{\beta}$ (for a non-zero prey population).

Similarly, Equation (3) has two possibilities

(1) $y = 0$ (which corresponds to the extinction of the predator population),
(2) $\delta x - \gamma = 0 \Rightarrow x = \frac{\gamma}{\delta}$ (for a non-zero predator population).

Thus, the only non-trivial equilibrium point is:

$$x^* = \frac{\gamma}{\delta}, \quad y^* = \frac{\alpha}{\beta}$$

As a result, the system (2) has two singularities at the points $(x, y) = (0, 0)$ and $\left(\frac{y}{\delta}, \frac{\alpha}{\beta}\right)$. These are referred to as the *prey and predator equilibrium populations*. By linearizing around these singularities, we find that the first is a saddle point, while the second is a center. We will apply the equivalent Ritz method to derive approximate solutions in the vicinity of the center. We postulate an approximate solution of the form:

$$\begin{aligned} x(t) &= A + B\cos(\omega t) + C\sin(\omega t) \\ y(t) &= D + E\cos(\omega t) + F\sin(\omega t) \end{aligned} \tag{4}$$

Differentiating with respect to t :

$$\begin{aligned} \frac{dx}{dt} &= -B\omega\sin(\omega t) + C\omega\cos(\omega t) \\ \frac{dy}{dt} &= -E\omega\sin(\omega t) + F\omega\cos(\omega t) \end{aligned} \tag{5}$$

Substituting these solutions into the differential equations (1), we get

$$\begin{aligned} \frac{dx}{dt} &= \alpha\left(A + B\cos(\omega t) + C\sin(\omega t)\right) \\ &-\beta\left(A + B\cos(\omega t) + C\sin(\omega t)\right)\left(D + E\cos(\omega t) + F\sin(\omega t)\right) \end{aligned}$$

$$\begin{aligned} -B\omega\sin(\omega t) + C\omega\cos(\omega t) &= \alpha\left(A + B\cos(\omega t) + C\sin(\omega t)\right) \\ &-\beta\left(A + B\cos(\omega t) + C\sin(\omega t)\right)\left(D + E\cos(\omega t) + F\sin(\omega t)\right) \end{aligned}$$

Similarly,

$$\begin{aligned} \frac{dy}{dt} &= \delta\left(A + B\cos(\omega t) + C\sin(\omega t)\right) \\ &\left(D + E\cos(\omega t) + F\sin(\omega t)\right) - \gamma\left(D + E\cos(\omega t) + F\sin(\omega t)\right) \end{aligned}$$

$$-E\omega\sin(\omega t) + F\omega\cos(\omega t) = \delta\left(A + B\cos(\omega t) + C\sin(\omega t)\right)$$
$$\left(D + E\cos(\omega t) + F\sin(\omega t)\right) - \gamma\left(D + E\cos(\omega t) + F\sin(\omega t)\right)$$

By simplifying above equations and setting the coefficients of $\cos(\omega t)$, $\sin(\omega t)$, and the constant terms to zero, we derive a system of algebraic equations for the variables A, B, C, D, E, F, and ω as:

$$\begin{aligned}
\alpha C - \beta AF - \beta CD + \omega B &= 0\\
\omega C - \alpha B + \beta AE + \beta BD &= 0\\
\alpha A - \beta AD - \left(\frac{\beta BE}{2}\right) - \left(\frac{\beta CF}{2}\right) &= 0\\
\omega E - \gamma F + \delta AF + \delta CD &= 0\\
\omega F + \gamma E - \delta AE - \delta BD &= 0\\
\delta AD - \gamma D + \left(\frac{\delta BE}{2}\right) + \left(\frac{\delta CF}{2}\right) &= 0
\end{aligned}$$

From the initial condition($t = 0$), we have:

$$\begin{aligned}
x(0) &= A + B\\
y(0) &= D + E
\end{aligned}$$

It is clear that for the desired equilibrium point to be achieved, we must set $A = \frac{\gamma}{\delta}$ and $D = \frac{\alpha}{\beta}$. By solving the system of equations above, we derive the following results:

$$\begin{aligned}
B &= x(0) - \frac{\gamma}{\delta}\\
C &= \pm\left(y(0) - \frac{\alpha}{\beta}\right)\left(\frac{\beta}{\delta}\right)\sqrt{\frac{\gamma}{\alpha}}\\
E &= y(0) - \frac{\alpha}{\beta}\\
F &= \pm(x(0) - \frac{\gamma}{\delta})\left(\frac{\delta}{\beta}\right)\sqrt{\frac{\alpha}{\gamma}}\\
\omega &= \pm\sqrt{\gamma\alpha}
\end{aligned} \tag{6}$$

Thus, the approximate solutions are given by

$$\begin{aligned}
x(t) &= \frac{\gamma}{\delta} + (x(0) - \frac{\gamma}{\delta})\cos(\sqrt{\gamma\alpha}t) - (y(0) - \frac{\alpha}{\beta})\left(\frac{\beta}{\delta}\right)\sqrt{\frac{\gamma}{\alpha}}\sin(\sqrt{\gamma\alpha}t)\\
y(t) &= \frac{\alpha}{\beta} + (y(0) - \frac{\alpha}{\beta})\cos(\sqrt{\gamma\alpha}t) + (x(0) - \frac{\gamma}{\delta})\left(\frac{\delta}{\beta}\right)\sqrt{\frac{\alpha}{\gamma}}\sin(\sqrt{\gamma\alpha}t)
\end{aligned} \tag{7}$$

These equations describe an elliptical trajectory in the x-y plane with closed orbits around the equilibrium point.This indicates that the populations of both species oscillate in a cyclical manner, as predators and prey undergo regular cycles of growth and decline.

3.3. **Limitations of the Ritz Method.** While the Ritz method provides an efficient way to approximate periodic or quasi-periodic behavior in nonlinear systems, it is subject to several important limitations:

- The method assumes that the solution remains smooth and approximately harmonic. It performs well near equilibrium but fails under strongly nonlinear or chaotic conditions.
- Discontinuities, sharp transitions, or external forcing (e.g., environmental perturbations) are not handled well due to the fixed functional form.

- The quality of the solution heavily depends on the choice of trial functions. Inadequate basis functions can lead to poor approximations even if residuals are minimized.

Despite these limitations, the Ritz method remains valuable for gaining qualitative insight into the dynamics of ecological models and for validating trends observed in numerical simulations.

3.4. **Stability Analysis.** To determine the stability of the equilibrium point, we linearize the system near the equilibrium using the Jacobian matrix. The Jacobian matrix is given by:

$$J = \begin{pmatrix} \frac{\partial}{\partial x}(\alpha x - \beta xy) & \frac{\partial}{\partial y}(\alpha x - \beta xy) \\ \frac{\partial}{\partial x}(\delta xy - \gamma y) & \frac{\partial}{\partial y}(\delta xy - \gamma y) \end{pmatrix} = \begin{pmatrix} \alpha - \beta y & -\beta x \\ \delta y & \delta x - \gamma \end{pmatrix}$$

Jacobian at the equilibrium point $\left(\frac{\gamma}{\delta}, \frac{\alpha}{\beta}\right)$:

$$J = \begin{pmatrix} \alpha - \beta\frac{\alpha}{\beta} & -\beta\frac{\gamma}{\delta} \\ \delta\frac{\alpha}{\beta} & \delta\frac{\gamma}{\delta} - \gamma \end{pmatrix} = \begin{pmatrix} 0 & -\beta\frac{\gamma}{\delta} \\ \delta\frac{\alpha}{\beta} & 0 \end{pmatrix}$$

The eigenvalues λ of the Jacobian matrix can be found by solving the characteristic equation:

$$\det(J - \lambda I) = 0$$

This simplifies to:

$$\lambda^2 = \beta\gamma\frac{\alpha}{\delta}$$

Thus, the eigenvalues are:

$$\lambda = \pm\sqrt{\beta\gamma\frac{\alpha}{\delta}}$$

Based on these eigenvalues, we can conclude the stability of the equilibrium points. If the real parts of the eigenvalues are positive, the equilibrium point is unstable, while if the real parts are negative, the equilibrium point is stable. The sign of the eigenvalues determines whether the system experiences growth or decay around the equilibrium point, providing insight into the system's behavior over time.

4. Numerical Methods

4.1. **Runge-Kutta Methods.** The Runge-Kutta family of methods is one of the most commonly used numerical techniques for solving ODEs. The most widely known is the fourth-order Runge-Kutta method (RK4), which provides a good balance between computational efficiency and accuracy. The RK4 method is applied as follows to solve Equation (1):

$$\mathbf{x}_{n+1} = \mathbf{x}_n + \frac{h}{6}(L_1 + 2L_2 + 2L_3 + L_4) \tag{8}$$

where h is the step size and the terms L_1, L_2, L_3, L_4 are defined as:

$$\begin{aligned} L_1 &= f(t_n, \mathbf{x}_n) \\ L_2 &= f\left(t_n + \frac{h}{2}, \mathbf{x}_n + \frac{h}{2}L_1\right) \\ L_3 &= f\left(t_n + \frac{h}{2}, \mathbf{x}_n + \frac{h}{2}L_2\right) \\ L_4 &= f(t_n + h, \mathbf{x}_n + hL_3) \end{aligned}$$

$$\mathbf{y}_{n+1} = \mathbf{y}_n + \frac{h}{6}\left(k_1 + 2k_2 + 2k_3 + k_4\right) \tag{9}$$

where h is the step size and the terms k_1, k_2, k_3, k_4 are defined as:

$$\begin{aligned} k_1 &= f(t_n, \mathbf{y}_n) \\ k_2 &= f\left(t_n + \frac{h}{2}, \mathbf{y}_n + \frac{h}{2}k_1\right) \\ k_3 &= f\left(t_n + \frac{h}{2}, \mathbf{y}_n + \frac{h}{2}k_2\right) \\ k_4 &= f(t_n + h, \mathbf{y}_n + hk_3) \end{aligned}$$

In this method, the values k_1, k_2, k_3, k_4 and L_1, L_2, L_3, L_4 represent different approximations of the slope at various points within the interval, and their weighted average provides the next value in the solution.

5. Results and Discussion

5.1. **Experimental Setup.** The table below, Table 1, illustrates a sample dataset of lynx (predator) and hare (prey) populations, measured in thousands of individuals, recorded by the Hudson Bay Company from 1900 to 1935 in a forest in northern Canada [14], [9], [15]. The initial populations of the predator and prey, taken from the year 1900, were $x(0) = 12.82$ and $y(0) = 7.13$. The cyclical pattern (see Figure 2)in the data suggests periodic fluctuations in both species, which align with the theoretical predictions of the Lotka–Volterra equations. The observed trend indicates that as hare populations increase, lynx populations follow with a time lag, leading to periodic oscillations.

TABLE 1. Samples of Lynx and Hares in thousands of individuals from year 1900 to 1935 [15]

Year	Hares	Lynxes	Year	Hares	Lynxes
1900	12.82	7.13	1918	4.50	6.82
1901	4.72	9.47	1919	11.21	3.19
1902	4.73	14.86	1920	56.60	3.52
1903	37.22	31.47	1921	69.63	9.94
1904	69.72	60.57	1922	77.74	20.30
1905	57.78	63.51	1923	80.53	31.99
1906	28.68	54.70	1924	73.38	42.36
1907	23.37	6.30	1925	36.93	49.08
1908	21.54	3.41	1926	4.64	53.99
1909	26.34	5.44	1927	2.54	52.25
1910	53.10	11.65	1928	1.80	37.70
1911	68.48	20.35	1929	2.39	19.14
1912	75.58	32.88	1930	4.23	6.98
1913	57.92	39.55	1931	19.52	8.31
1914	40.97	43.36	1932	82.11	16.01
1915	24.95	40.83	1933	89.76	24.82
1916	12.59	30.36	1934	81.66	29.70
1917	4.97	17.18	1935	15.76	35.40

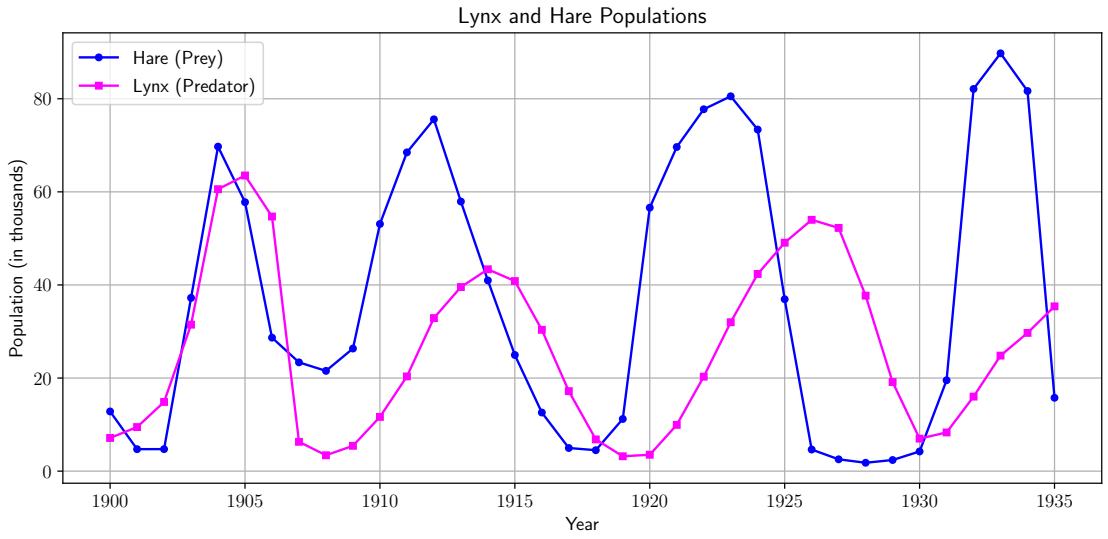

FIGURE 2. Original Data

Figure 2 illustrates the fluctuations in hare and lynx populations over time. The hare population (prey) exhibits a peak approximately every 10 years, followed by an increase in lynx population (predators). This phase shift is characteristic of predator-prey dynamics, where predator populations lag behind prey populations.

5.2. **Parameter Estimation via Simulated Annealing.** To calibrate the parameters of the Lotka–Volterra predator–prey model using empirical data, we employed the Simulated Annealing (SA) optimization algorithm. SA is a stochastic global search technique inspired by the annealing process in metallurgy. It is particularly effective for non-convex optimization landscapes, making it suitable for nonlinear systems such as the Lotka–Volterra equations.

5.2.1. *Objective Function.* Let x_i^{obs} and y_i^{obs} denote the observed hare and lynx populations at discrete time points t_i, and x_i^{sim}, y_i^{sim} the simulated populations from the model. The cost function is defined as the sum of squared residuals:

$$J(\alpha, \beta, \gamma, \delta) = \sum_{i=1}^{N} \left[(x_i^{\text{sim}} - x_i^{\text{obs}})^2 + (y_i^{\text{sim}} - y_i^{\text{obs}})^2 \right], \tag{10}$$

which is minimized using SA to obtain the best-fitting parameters.
We used the `dual_annealing` optimizer from the SciPy library to minimize the objective function. The optimization was constrained within biologically plausible bounds:

$$\alpha \in [0.1, 1.0], \quad \beta \in [0.001, 0.05], \quad \gamma \in [0.1, 2.0], \quad \delta \in [0.001, 0.05].$$

To assess robustness and repeatability, we repeated the SA optimization over five independent runs with different random seeds. For each run, the estimated parameters and RMSEs were recorded. RMSE was computed for each species as:

$$\text{RMSE}_x = \sqrt{\frac{1}{N} \sum_{i=1}^{N} (x_i^{\text{sim}} - x_i^{\text{obs}})^2}, \qquad \text{RMSE}_y = \sqrt{\frac{1}{N} \sum_{i=1}^{N} (y_i^{\text{sim}} - y_i^{\text{obs}})^2}. \tag{11}$$

The average parameter values and RMSEs over five runs were:

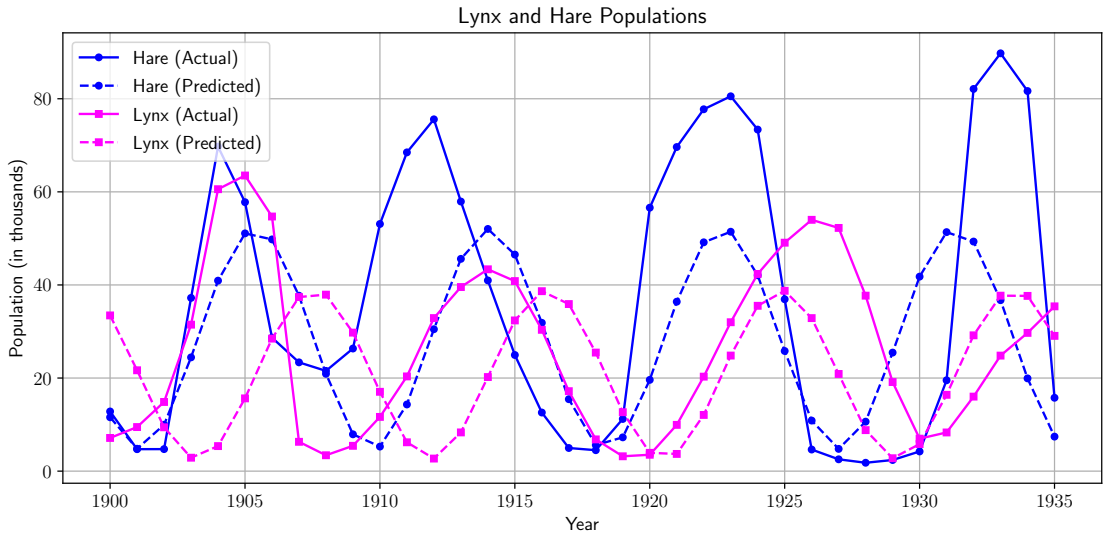

FIGURE 3. Numerical solution of a trajectory using the Ritz Method

Parameter	Mean	Std. Dev.
α	0.6923	0.0684
β	0.0334	0.0031
γ	0.7627	0.0861
δ	0.0268	0.0034

TABLE 2. Simulated Annealing estimated parameter statistics (5 runs)

By using the parameters found for α, β, γ, and δ, we have:

$$\begin{cases} \frac{dx}{dt} = 0.6923x(t) - 0.0333x(t)y(t) \\ \frac{dy}{dt} = 0.02684x(t)y(t) - 0.7627y(t) \end{cases} \tag{12}$$

The relatively small standard deviations across all parameters indicate that the SA algorithm produces stable and consistent parameter estimates.

5.3. **Ritz Method.** Figure 3 illustrates the numerical solution of the Lotka–Volterra system obtained using the Ritz method, a physics-based numerical approach. The numerical predictions closely follow the observed data, capturing the cyclic nature of the population dynamics. The model effectively reproduces the observed trends, demonstrating the validity of the chosen numerical approach for solving non-linear ODEs. Despite the general agreement, discrepancies exist between the predicted and actual values, particularly in the amplitude of population peaks. These differences may stem from simplifying assumptions in the classical Lotka–Volterra equations, such as constant interaction coefficients and absence of external environmental influences. In reality, stochastic factors like climate variations, food availability, and disease outbreaks could contribute to deviations from the idealized model.

5.4. **RK 4th Order.** The results of the LV systems simulation using the Runge-Kutta 4th-order (RK4) method demonstrate (see Figure 4) the cyclical nature of predator-prey

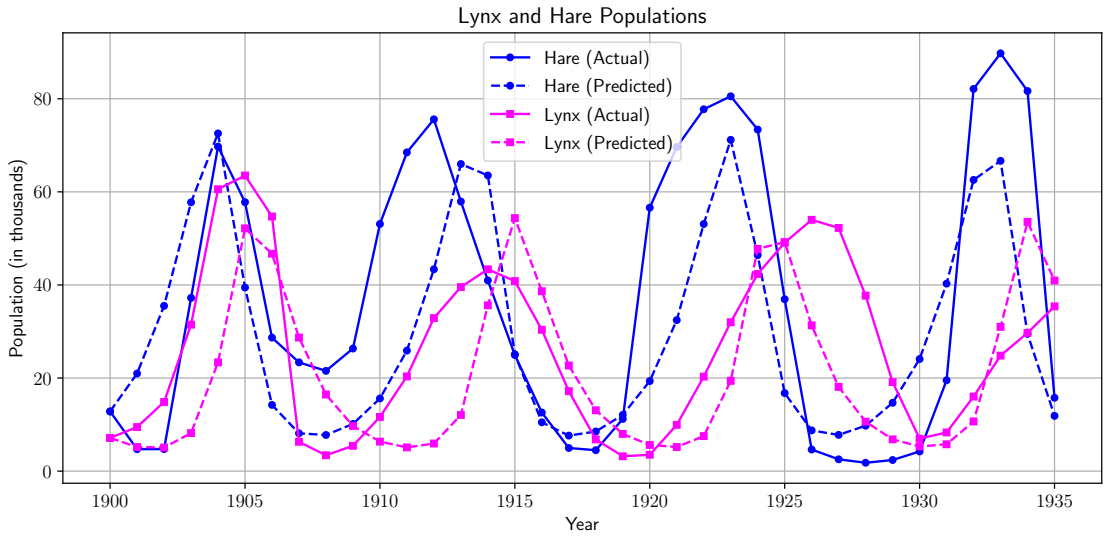

FIGURE 4. Numerical solution of a trajectory using the RK4 Method

interactions. The figure compares the actual population data of lynx and hares with the numerically predicted values over a series of years. The RK4 method effectively captures the oscillatory behavior of both species, where the prey population (hares) increases first, followed by a delayed rise in the predator population (lynx), after which both decline in a continuous cycle. The predicted results align well with the actual data, indicating that the RK4 method provides an accurate numerical approximation of the nonlinear LV equations.

While the general trends are well-represented, minor deviations exist, likely due to environmental factors not accounted for in the classical model, parameter estimation uncertainties, or natural fluctuations in the real-world data. Despite these discrepancies, the RK4 method produces smooth and stable numerical solutions, demonstrating its reliability in modeling complex ecological interactions. These results reinforce the importance of numerical methods for solving nonlinear ODEs, especially when analytical solutions are impractical. The presence of multiple trajectories corresponding to different initial predator population values suggests that the system's behavior depends on initial conditions but follows a stable, repeating pattern. The variation in initial predator populations (e.g., y = 4.0, y = 41.7, y = 7.4, etc.) affects the trajectory, but all orbits remain closed, reinforcing the theoretical prediction that predator-prey interactions remain bounded in a limit cycle rather than leading to extinction. To conclude, the phase-space plot confirms the characteristic oscillatory behavior of the LV model, demonstrating that populations follow periodic cycles rather than reaching a steady equilibrium. The RK4 method effectively captures this dynamic, providing accurate numerical approximations of the nonlinear system.

5.5. **RMSE Comparison Between RK4 and Ritz Methods.** To evaluate the accuracy of the numerical methods used to model the Hare and Lynx population dynamics, we computed the Root Mean Square Error (RMSE) for both species using the RK4 (Runge-Kutta 4th order) and Ritz methods. The RMSE quantifies the difference between the

observed data and the numerical simulation results. Table 3 summarizes the RMSE values for both populations:

Method	**RMSE (Hare)**	**RMSE (Lynx)**
RK4 Method	21.77	15.54
Ritz Method	27.20	21.98

TABLE 3. Comparison of RMSE for Hare and Lynx Populations Using RK4 and Ritz Methods

As shown in the table, the RK4 method yields lower RMSE values for both the hare and lynx populations compared to the Ritz method. Specifically, the RMSE for the hare population is 21.77 using RK4 and 27.20 using Ritz, while for the lynx population, the RMSE is 15.54 for RK4 and 21.98 for Ritz.
This indicates that the RK4 method provides a more accurate numerical approximation of the observed population data. The higher errors in the Ritz method may be attributed to its weaker handling of rapid nonlinear dynamics present in predator-prey systems. Therefore, for problems involving sharp oscillations or highly dynamic systems like the Lotka-Volterra model, the RK4 method appears to be more suitable.

6. Conclusion and Future Research

The numerical analysis of the LV predator-prey model using the RK4 and Ritz methods demonstrates the effectiveness of numerical techniques in solving nonlinear differential equations. The results show that both methods successfully capture the oscillatory behavior of predator and prey populations, as confirmed by the time-series and phase-space plots. The RK4 method provides a stable and accurate numerical solution, while the Ritz method offers an alternative approach with comparable results. The phase plots reveal the characteristic limit cycles of predator-prey interactions, reinforcing the theoretical predictions of the LV model. However, due to inaccurate parameter estimations of α, β, δ and γ using the maximum likelihood method, the model can sometimes deviate from real-world data. While the general predator-prey cycles remain intact, small errors in parameter estimation can lead to discrepancies in amplitude and phase shifts between predicted and actual population trends.

Future research can focus on improving parameter estimation techniques to enhance the model's predictive accuracy. AI-based approaches, such as machine learning and deep learning, could be integrated to optimize the estimation of system parameters (α, β, δ and γ) reducing uncertainties in model predictions. Additionally, extending the classical LV system to include ecological complexities like seasonal effects, environmental changes, and stochastic influences could provide a more realistic representation of predator-prey dynamics. Further comparisons between numerical methods, including higher-order solvers and hybrid AI-numerical techniques, could enhance computational efficiency and stability. Investigating these advanced modeling strategies would offer deeper insights into ecosystem interactions and contribute to better wildlife conservation and resource management.

References

[1] H. A. Adamu, "Mathematical analysis of predator-prey model with two preys and one predator," *International Journal of Engineering and Applied Sciences*, vol. 5, no. 11, pp. 17–23, 2018.

[2] R. M. Anderson and R. M. May, *Infectious diseases of humans: dynamics and control*. Oxford university press, 1991.
[3] P. Antoniou and A. Pitsillides, "Congestion control in autonomous decentralized networks based on the lotka-volterra competition model," in *International Conference on Artificial Neural Networks*. Springer, 2009, pp. 986–996.
[4] ——, "A bio-inspired approach for streaming applications in wireless sensor networks based on the lotka–volterra competition model," *Computer Communications*, vol. 33, no. 17, pp. 2039–2047, 2010.
[5] ——, "Congestion control in wireless sensor networks based on the lotka volterra competition model," in *Biologically Inspired Networking and Sensing: Algorithms and Architectures*. IGI Global, 2012, pp. 158–181.
[6] M. Beals, L. Gross, and S. Harrell, "Predator-prey dynamics: Lotka-volterra," 1999, accessed: 2025-03-09. [Online]. Available: http://www.tiem.utk.edu/~gross/bioed/bealsmodules/predator-prey.html
[7] W. E. Boyce and R. C. DiPrima, *Elementary differential equations and boundary value problems*, 7th ed. John Wiley & sons, 2001.
[8] J. BREARLEY and A. Soudack, "Approximate solutions to the lotka-volterra competition equations," *International Journal of Control*, vol. 27, no. 6, pp. 933–941, 1978.
[9] E. M. Cardona, C. A. Ramírez-Vanegas, and J. R. G. Granada, "Numerical Solution of the Lotka-Volterra Stochastic Differential Equation," *Statistics, Optimization & Information Computing*, 2025. [Online]. Available: http://www.iapress.org/index.php/soic/article/view/2307
[10] J. D. Davis, D. V. Olivença, S. P. Brown, and E. O. Voit, "Methods of quantifying interactions among populations using lotka-volterra models," *Frontiers in Systems Biology*, vol. 2, p. 1021897, 2022.
[11] O. Diekmann and J. A. P. Heesterbeek, *Mathematical epidemiology of infectious diseases: model building, analysis and interpretation*. John Wiley & Sons, 2000, vol. 5.
[12] F. N. Egerton, "History of ecological sciences, part 54: Succession, community, and continuum," *Bulletin of the Ecological Society of America*, vol. 96, no. 3, pp. 426–474, 2015.
[13] C. M. Evans and G. Findley, "Analytic solutions to the lotka-volterra model for sustained chemical oscillations," 1998.
[14] M. E. Gilpin, "Do hares eat lynx?" *The American Naturalist*, vol. 107, no. 957, pp. 727–730, 1973.
[15] D. Hundley, "Math 250: Introduction to mathematical logic," 2003, accessed: 2025-06-07. [Online]. Available: http://people.whitman.edu/~hundledr/courses/M250F03/M250.html
[16] C. Jost, G. Devulder, J. A. Vucetich, R. O. Peterson, and R. Arditi, "The wolves of isle royale display scale-invariant satiation and ratio-dependent predation on moose," *Journal of Animal Ecology*, pp. 809–816, 2005.
[17] M. Kawira, C. G. Ngari, and S. Karanja, "A theoretical model of corruption using modified lotka volterra model: A perspective of interactions between staff and students," 2020.
[18] A. J. Lotka, "Analytical note on certain rhythmic relations in organic systems," *Proceedings of the National Academy of Sciences*, vol. 6, no. 7, pp. 410–415, 1920.
[19] A. Marasco, A. Picucci, and A. Romano, "Market share dynamics using lotka–volterra models," *Technological forecasting and social change*, vol. 105, pp. 49–62, 2016.
[20] R. M. May and R. M. Anderson, "The transmission dynamics of human immunodeficiency virus (hiv)," *Philosophical Transactions of the Royal Society of London. B, Biological Sciences*, vol. 321, no. 1207, pp. 565–607, 1988.
[21] A. Meça, A. Uka, and M. Ali, "Parameter estimation of three cell interaction using lotka volterra differential equations," in *2021 International Conference on Computing, Networking, Telecommunications & Engineering Sciences Applications (CoNTESA)*. IEEE, 2021, pp. 12–18.
[22] V. Noonburg, "A neural network modeled by an adaptive lotka-volterra system," *SIAM Journal on Applied Mathematics*, vol. 49, no. 6, pp. 1779–1792, 1989.
[23] M. Passarella, "The paradox of tranquility revisited. a lotka-volterra model of the financial instability," *Rivista italiana degli economisti*, vol. 15, no. 1, pp. 69–104, 2010.
[24] D. Y. Regalado and E. C. Castillano, "Approximate analytic solution to the lotka-volterra predator â€"prey differential equations model," *Journal of Higher Education Research Disciplines*, vol. 4, no. 1, pp. 38–47, 2019.
[25] J. Toyoda and H. Saitoh, "Proposal of an open-electric-energy-network (oeen) to realize cooperative operations of iou and ipp," in *Proceedings of EMPD'98. 1998 International Conference on Energy Management and Power Delivery (Cat. No. 98EX137)*, vol. 1. IEEE, 1998, pp. 218–222.
[26] B. H. Tsai, "Forecasting ic design industrial clustering from taiwan to mainland of china using four-dimensional competitive lotka-volterra equations," *International Journal of Innovative Computing, Information and Control*, vol. 20, no. 1, pp. 249–261, 2024.

[27] V. Volterra, "Fluctuations in the abundance of a species considered mathematically," *Nature*, vol. 118, no. 2972, pp. 558–560, 1926.

[28] S.-Y. Wang, W.-M. Chen, and X.-L. Wu, "Competition analysis on industry populations based on a three-dimensional lotka–volterra model," *Discrete Dynamics in Nature and Society*, vol. 2021, no. 1, p. 9935127, 2021.

[29] P. J. Wangersky, "Lotka-volterra population models," *Annual Review of Ecology and Systematics*, vol. 9, pp. 189–218, 1978.

Everest Advances in Science and Technology (EAST), Vol. 1, No. 1, 2025
ISSN: 3102-0410(print), 3102-0429(online)

Analysis of Cost deviation in civil works of selected hydropower projects of Province No. 1 and Gandaki Province

AARSHIKA K.C.[1*]

Abstract. Cost of construction project is one of the major concerns of the parties involved in the project. The percentage of difference between the initial cost and final cost is known as cost deviation. In the context of developing countries like Nepal, inadequate planning often leads to significant cost deviation in construction projects. A case study has been done observing four hydropower projects: Rudi Khola A, Hewa Khola HEP, Midim Khola HEP and Mistri Khola HEP. The objective was to analyze the current scenarios of cost deviation, identifying underlying causes and suggesting remedial measures to mitigate such deviations. Data were collected through the bill of quantities, final Interim Payment Certificates (IPCs), and questionnaire survey. The qualitative response from the questionnaire survey has been quantified with five point ranking Likert scale for analysis.

The study revealed that the percentage deviation in cost lies between 18 % to 42 %. The main causes of cost deviation were identified separately .i.e. In Rudi Khola A HEP and Hewa Khola HEP, quantity overrun was the main cause. In Midim Khola HEP, change in design, quantity over run were identified as the major causes. In case of Mristi Khola HEP, seepage water management inside tunnel and price escalation were main causes of cost deviation.

Based on the feedback of the parties involved, the remedial measures suggested are to review and improve bid documents such as technical specifications, drawings, bill of quantities by the consultant; contractor should have enough cash before beginning of any project, frequent preventive maintenance of equipment by hiring full time skilled mechanics; client should ensure quality design of the project and other measures as effective strategic planning, geological investigation should be done

Keywords: Quantity over run, change in design, price escalation, preventive maintenance, technical specifications, geological investigation, cost deviation, Bill of quantities, quality design, bid document.

[1]Nepal Engineering College, Bhaktapur, Nepal
E-mail: kcrcka@gmail.com
* Corresponding author
Manuscript received: 27 July, 2025; revised: 13 August 2025; accepted: 5 September, 2025.
Everest Advances in Science and Technology (EAST), Vol. 1, No. 1, 2025

1. Introduction

1.1. **Background.** A successful project is one which has been completed as per the technical specification, the schedule, and within the budget. The cost of a construction project is one of the foremost imperative aspects in the construction industry. Due to numerous reasons, the total cost of a project notably deviates from the initially estimated cost [33]. The major concern of professionals in the construction industry is the wide gap between final account figures and the preliminary estimates arrived before the contract stage [23]. In the context of developing countries like Nepal, due to various reasons such as changes in scope of work, specifications, differing site conditions, increase in quantity of works, and unforeseen conditions, cost deviation exists [11].
Upper Trishuli 3A (60 MW), Middle Marsyangdi (70 MW), and Kulekhani-III (14 MW) are large hydropower projects having installation capacity greater than 10 MW, which were also completed with considerable deviation in project cost [29]. Similarly, in other small hydropower projects having installation capacity less than 10 MW, such as Lower Piluwa Hydropower Project and Hadi Khola Hydropower Project, there was deviation in the original cost by the time the project was completed [36]. Despite the size and nature of the project, deviation was seen in the cost of hydropower projects.
Also, the largest share of installed costs for hydropower projects is usually taken up by civil works for the construction of the hydropower plant, such as headworks, dam, tunnels, canal, and powerhouse [21].
Therefore, it is necessary to study the construction phase of hydropower projects in order to identify the causes of deviation so that the negative impact of deviation can be minimized in future hydropower projects.

1.2. **Statement of the Problem.** In the Nepalese construction industry, hydropower construction projects are being implemented without proper planning, estimation, and detailed study, which results in cost deviation of the projects by the time they are completed [31]. The final project cost of completed hydropower projects has considerable deviation from the original cost [28].
National pride projects like Middle Marsyangdi Hydropower Project (70 MW) and Kulekhani-III Hydroelectric Project (14 MW) faced cost deviation of more than 50% [29]. Delay and cost overrun occur in all phases of a project's life span. However, significant cost deviations usually occur during the construction phase [38].
Identifying the factors that lead to cost deviation is a way to control project costs. Very few studies have been done to identify cost deviation in the hydropower sector of Nepal. Therefore, studies in this field are very important to explore matters related to project cost deviation and make possible recommendations based on findings so that the parties involved in the projects can benefit.

1.3. **Research Objectives.** The general objective of this study is to analyse cost deviation in selected hydropower projects of Nepal.
The specific objectives of the study are as follows:

(1) To analyse the current scenarios of cost deviation of selected hydropower projects.
(2) To find out the major causes of cost deviation in selected hydropower projects.
(3) To find out the remedial measures of cost deviation of hydropower projects.

1.4. **Significance of the Study.** This study identifies the causes of cost deviation and recommends remedial measures for cost deviation in the construction of hydropower projects. Hence, all parties involved in the project—such as clients, consultants, and contractors—will benefit from the study.

The developers (clients) of hydropower projects will be able to minimize the wide gap between final and initial estimated costs. The consultants involved in the projects can gain better insight for proper estimation during the feasibility study stage. Contractors of hydropower construction projects will be able to clearly identify the possible causes of deviation during construction and will incorporate the rate of major works accordingly so that the negative impact of deviation can be avoided.

1.5. **Scope and Limitation.**

Scope. This study mainly focuses on major activities of civil works to analyse the current scenario of cost deviation in hydropower projects. In addition, it also focuses on analysing the causes and remedial measures of cost deviation in selected hydropower projects of Nepal.

Limitation. This research is limited to the civil construction works of hydropower projects, as civil works cover a major percentage of total project cost. Furthermore, the research only covers hydropower projects developed by Independent Power Producers (IPPs).

2. Literature Review

2.1. **General background.** Cost deviation may be expressed as a percent difference between the final cost of the project (actual cost) and the contract award amount (estimated cost). Generally, the success of project is defined by accomplishing it within specified cost, time and quality. However, the construction industry is full of projects that were completed with significant time and cost overruns [3]. The cost deviation can be either positive or negative (i.e., the final cost is above, or below the initial one). When it is positive, there is a cost overrun.

2.2. **Causes of cost deviation in construction projects.** From the preliminary survey conducted in water drilling projects in Ghana attributed the cost overruns to irregular monthly payment, the escalation of material prices, inadequate cash flow during construction, deficiencies in cost estimates prepared [38]. Some researchers like [25] and [5] have criticized bill of quantities lacking precision as one of the major reason for cost deviation. A fuzzy model was developed for forecasting the probability of cost overrun risk for Indian construction project. Among major factors shortage of construction material, fluctuation in price of material, inappropriate government policies and laws, unrealistic contract duration, differing site (ground) conditions, inflation, contractor' lack of experience and frequent design change are commonly occurred cost deviation factors [34]. Similarly, research done in delay and cost overrun in Vietnam construction project identified cost overrun factors such as financial difficulties of owner and contractor, , slow payment of completed works by owner, slow inspection of completed works by consultant and delay of works etc. [26].

2.3. **Causes of Cost Deviation in Hydropower Construction Projects.** In order to identify the various causes of variation orders in the construction of hydropower projects in Pakistan, a survey questionnaire was conducted. The most significant factors identified were:

(1) Change of scope,
(2) Omission and mistakes in design,
(3) Change in design,
(4) Owner's financial problems, and

(5) Unavailability of equipment [18].

The impact of such variation orders on time and cost of the project was reported as 20% time overrun and 31% cost overrun with respect to the planned schedule and budget [19]. A study of the construction of the underground powerhouse at the Dagachhu Hydropower Project in Bhutan revealed challenges such as seepage water management during construction. According to another study carried out on small hydropower projects, the main causes of cost deviation were time overrun and variation in quantity in civil and hydromechanical works [10].

A newspaper article published in the *Himalayan Times* regarding construction delays mentioned contractor-, client-, and employer-related factors, as well as external factors, as primary causes of delay and cost overrun in construction projects of Nepal [31]. Contractor-related factors included shortage of manpower. Consultant-related factors included delays in approving major changes in the scope of work, discrepancies in design documents, unclear and inadequate details in drawings, and insufficient data collection and survey before design.

Similarly, external factors included problems of land acquisition, tree cutting, price escalation, labour disputes, government regulations, slow permit approval by government agencies, and unforeseen ground conditions. According to [30, 31], construction delays lengthen project schedules, increase project costs, and hinder economic growth.

A paper published by [30] in *Hydro Nepal* analyzed the following major contractual problems faced by hydropower construction projects in Nepal:

- Payment disputes between contract parties in construction,
- Changed circumstances during construction,
- Unforeseeable conditions such as rugged terrain and varying geology, and
- Force majeure conditions.

A paper on predicted versus actual rock mass conditions for tunnel projects in the Nepal Himalaya revealed discrepancies between predicted and actual rock mass conditions, which affected the overall cost and construction time of projects [24]. Studies of tunnel projects in Nepal showed that the ground conditions encountered were quite different from what was anticipated during pre-construction phase planning and design. This mismatch caused additional cost, considerable delay, and led to claims and contractual disputes. The study of hydropower projects such as Khimti I and Modi Khola revealed that rock mass quality assessment, stability analysis, and rock support quantity predictions were mainly based on desk studies, aerial photo interpretation, and surface geological mapping.

2.4. **Remedial Measures of Cost Deviation in Hydropower Construction Projects.**

As cost deviation is inevitable in any project, it is necessary to adopt certain measures to minimize its impact in construction projects. A research article published by [1] recommended several measures to be adopted by contractors, clients, and consultants to minimize deviation in civil construction projects.

Contractors, being the main builders of the project, are recommended to have sufficient cash flow before beginning any project to minimize financial problems. Owners are advised to review and improve bid documents such as technical specifications, drawings, and bills of quantities, and to ensure the quality design of the project. Consultants are advised to hire qualified technical staff, provide timely instructions to contractors, and promptly

resolve any issues raised by the contractors, as delays in resolution can directly or indirectly affect project costs (either positively or negatively) [1].
[38] also suggested that appropriate funding levels should always be determined at the planning stage of a project so that regular payments can be made to contractors for the work completed.
In addition, mitigation measures to control cost overrun factors in construction projects in Malaysia have been identified as follows [6]:

(1) Proper project planning and scheduling,
(2) Effective site management and supervision,
(3) Frequent progress meetings,
(4) Use of experienced subcontractors and suppliers,
(5) Utilization of up-to-date technology,
(6) Clear information and communication channels,
(7) Frequent coordination between the parties,
(8) Comprehensive contract administration, and
(9) Systematic control mechanisms.

Furthermore, [24] suggested maintaining a minimum level of geological investigation to improve the predictability of geological conditions. This helps reduce the discrepancy between predicted and actual rock mass conditions to an acceptable level, thereby minimizing unexpected cost deviations.

3. Methodology

3.1. **Study Area.** The study area of the research was selected as hydropower construction projects developed by Independent Power Producers (IPP). There are altogether 42 hydropower projects developed by IPPs in Province No. 1 and Province No. 4 which have already started generation and are under operation. Among the 42 hydropower projects, only four hydropower projects were purposively selected for the study. The selected projects for the study are mentioned in Table 1 below:

Table 1. List of Selected Hydropower Projects with Key Details

S.N.	Name of Project	Installed Capacity / Type	Location	Project Commencement Date / Start Date	Status of the Project / Civil Works Completion Date
1	Rudi Khola A Small Hydropower Project	8.8 MW / RoR project with pipe	Lamjung District, Province 4 (Gandaki Pradesh)	March 24, 2016	May, 2019
2	Hewa Khola 'A' Hydroelectric Project	14.9 MW / RoR Project with Tunnel	Panchthar District, Province 1	September 30, 2012	February 4, 2017
3	Midim Khola Hydropower Project	3 MW / RoR Project with Tunnel	Lamjung District, Province 4 (Gandaki Pradesh)	April 15, 2016	August, 2017
4	Mistri Khola Hydroelectric Project	42 MW / RoR Project with Tunnel	Myagdi District, Province 4 (Gandaki Pradesh)	June 30, 2016	July, 2021

3.2. **Study population and Sample selection.** The parties related to the project such as client, consultant and contractor were interviewed on the subject.

3.3. **Data Collection.** To fulfil the purpose of study both primary as well as secondary data were collected.

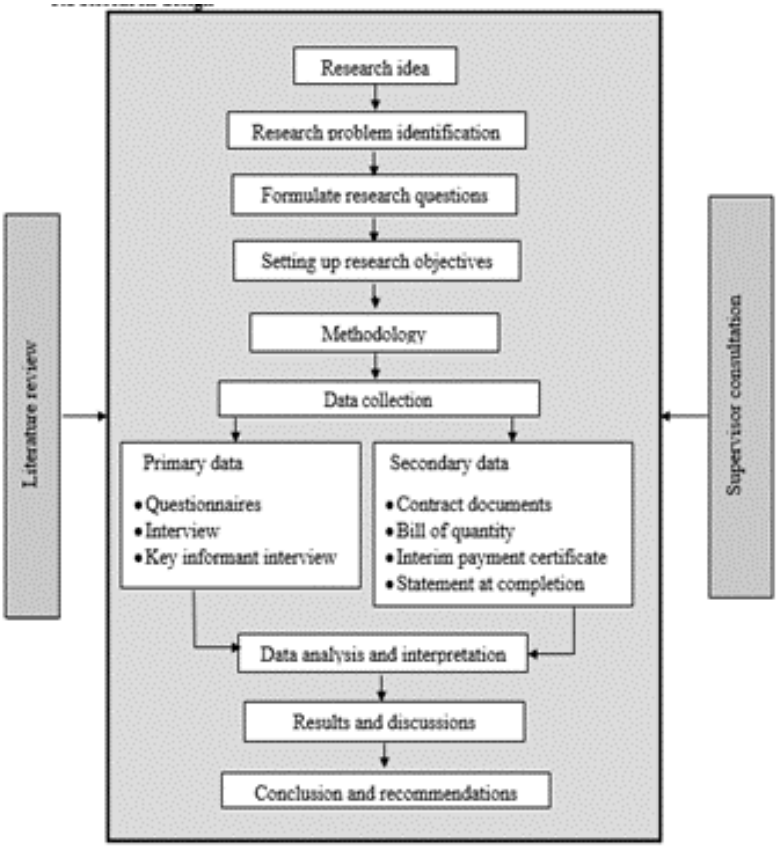

FIGURE 1. Research methodology flow chart

TABLE 2. Details of Respondents from Different Target Groups

S.N.	Target Group	Total No. of Respondents
1	Client's Representative	10
2	Consultant's Representative	10
3	Contractor's Representative	20
	Total	**40**

TABLE 3. Response Rate by Target Group

S.N.	Target Group	No. of Respondents	Responses Received	Non-response Rate
1	Client's Representative	10	8	20%
2	Consultant's Representative	10	8	20%
3	Contractor's Representative	20	16	20%
	Total	**40**	**32**	**20%**

3.3.1. *Primary Data Collection.* Primary data refers to the first-hand data gathered by the researcher himself. Various sources of primary data are surveys, observations, questionnaires, and interviews [2].

3.3.2. *Questionnaire Method.* Questionnaires is an observational technique which comprises series of items presented to a respondent in a written form, in which the individual is expected to respond in writing [2]. In this research, a set of questionnaires was developed which was provided to all the concerned parties (Client, Consultant and Contractor) who were directly involved in the projects.
The factors related to causes and remedial measures for the selected hydropower project were identified from the literature review.
The respondents were asked to rate the factors in a 5-point Likert scale. However, the numbers assigned to the agreement or degree of influence (1, 2, 3, 4, 5) do not indicate that the interval between scales is equal, nor do they indicate absolute quantities. The ranking detail is as shown below:

- E.S. = extremely significant (5 marks)
- M.S. = moderately significant (3 marks)
- V.S. = very significant (4 marks)
- S.S. = slightly significant (2 marks)
- N.S. = not significant (1 marks) [36]

3.3.3. *Key Informant Interview (KII).* Interviewing is a technique that is primarily used to gain an understanding of underlying reasons [2]. Key informant interview of managing director of hydropower construction company and design team leader of reputed consultant for hydropower projects who have experience in hydropower sector for more than 10 years was done to identify the challenges faced by hydropower sector which results in cost deviation. In total KII of three personnel were taken.

3.3.4. *Secondary Data Collection.* Secondary data are those which have already been collected by someone else earlier [2]. For the purpose of the study, secondary data were collected from the final interim payment certificate or statement at completion certified by the client after the work completion and Bill of Quantity agreed at the time of contract agreement and signed by the authorized representative of client and consultant were collected from the concerned authorities to get the information regarding actual cost and final cost of the project.

3.4. **Validity and Reliability.**

3.4.1. *Validity of Research Tools.* Validity refers to the degree to which an instrument measures what is supposed to be measured [26]. In order to establish content validity, literature reviews and then follow-ups with the evaluation by expert needs to be done [7]. The questionnaire developed for this study was based on Likert 5-point scale. Similar type of questionnaire was used in similar research by [20, 32, 33, 36, 22]. Similarly, in order to rank the factors, RII was used in similar research done by [20, 32, 33, 36, 22]. The results obtained in the research done by the previous researchers were also in agreement with the findings obtained after the analysis of questionnaire survey in this study.
In order to fulfil the objective of this research, questionnaire for the research were prepared with the help of literature review and concerned engineer having experience of more than 10 years in hydropower construction. Prior to the questionnaire survey, the questionnaire was thoroughly discussed and consulted with the supervisor for the validity of the research.

3.4.2. *Reliability of Research Tools.* Reliability concerns the extent to which a measurement of a phenomenon provides stable and consistent result [7]. The most commonly used internal consistency measure is the Cronbach Alpha coefficient [37]. Cronbach's alpha (α)

developed by Lee Cronbach in 1951, measures reliability of multiple questions to see if multiple surveys are reliable.
The formula for Cronbach's alpha is:

$$\alpha = \frac{k}{k-1}\left(1 - \frac{\sum s_y^2}{s_x^2}\right) \tag{1}$$

where,
k = number of test items
Σs_y^2 = sum of item variance
s_x^2 = variance of total score

TABLE 4. Cronbach's Alpha and Internal Consistency Levels

Cronbach's Alpha (α)	**Internal Consistency**
$0.9 \leq \alpha \leq 1.0$	Excellent
$0.8 \leq \alpha < 0.9$	Good
$0.7 \leq \alpha < 0.8$	Acceptable
$0.6 \leq \alpha < 0.7$	Questionable
$0.5 \leq \alpha < 0.6$	Poor
$0.0 \leq \alpha < 0.5$	Unacceptable

Cronbach's alpha test was carried out in MS-Excel, for the purpose of analysis, responses from questionnaire sets were tabulated in MS- Excel. There were 93 items in questionnaire of which the reliability of its measurements needs to be measured. Using the formula, the value of Cronbach's alpha was calculated for the causes and remedial measures which is presented in the table 5:

TABLE 5. Cronbach's Alpha Values for Different Sections of the Study

S.N.	**Description**	**Cronbach's Alpha Value (α)**	**Remarks**
1	Causes of cost deviation in selected hydropower projects of Nepal	0.982	Excellent
2	Remedial measures to mitigate the cost deviation	0.980	Excellent

As per prescribed values and range illustrated in table above, the consistency of questions within the questionnaire was found to be excellent.

3.5. **Data Analysis.** The data collected from both primary and secondary sources were summarized, classified, tabulated, and categorized in various categories. The method used in data analysis was primarily focused on calculating Relative Importance Index (RII), ranking the factors based on obtained RII, and checking the correlation between the views of respondents. To achieve the research goal, Microsoft Excel was used for analyzing the data.

Likert's scale is used for the ordinal scale measurement for the study. In this research, the scales are represented as not significant = 1 to extremely significant = 5.

3.6. **Relative Importance Index (RII).** Relative Importance Index has been widely used in construction research for measuring attitudes [13]. Many researchers like [1, 14, 35] used the relative importance index in their analysis.
Likert scaling was used to rank the causes of cost deviation and remedial measures to mitigate cost deviation [36]. After the ranking of the causes and remedial measures by the respondents, the combined ranking of client, consultant, and contractor was used to calculate the Relative Importance Index (RII) value using the following equation [15]:

$$\text{RII} = \frac{\sum_{i=1}^{5} W_i \times X_i}{A \times N} \tag{2}$$

where,
RII = Relative Importance Index
W_i = Weighting given to each factor by the respondents and ranges from 1 to 5
X_i = Frequency of i-th response given for each cause
A = Highest weight (i.e., 5 in this case)
N = Total number of respondents
The value of RII ranges from 0 to 1. Higher the value, more important is the factor that is responsible for the causes of cost deviation and remedial measures to mitigate cost deviation.

3.7. **Spearman's Rank Order Correlation.** According to Glen [35], Spearman's correlation coefficient is a statistical measure of the strength of a monotonic relationship among paired data. It means that if one variable increases (or decreases), then the other one also increases (or decreases). It is denoted by r_s or simply r and is constrained as $-1 \leq r \leq 1$. The formula for calculating Spearman's rank order correlation given by Charles Spearman in 1904 is:

$$\rho = 1 - \frac{6 \sum d_i^2}{n(n^2 - 1)} \tag{3}$$

where,
d_i = difference between two ranks of each observation
n = number of observations
It is interpreted based on the strength of correlation as follows:

- -1 = a perfect negative correlation between ranks
- 0 = no correlation between ranks
- 0 to 0.19 = very weak
- 0.2 to 0.39 = weak
- 0.4 to 0.59 = moderate
- 0.6 to 0.79 = strong
- 0.8 to 1.0 = very strong
- +1 = a perfect positive correlation between ranks

In a similar study done by Khanal [22] for the study of impact of variation order on project cost and time of building construction, Spearman rank correlation coefficient was calculated to determine the correlation among the control measures to minimize variation orders.

In this research study, correlation coefficient was calculated to find the correlation among the rank given by the respondents for the factors causing deviation and remedial measures to mitigate cost deviation.

3.8. **Research Matrix.** Following research matrix was used to meet the objective of the proposed research.

TABLE 6. Research Matrix

S.N.	Objectives	Data Required	Data Source	Analysis Tools	Outcome
1	To analyse the current scenario of cost deviations of selected hydropower projects	Percentage deviation in cost of major activities of civil works due to quantity overrun	Bill of quantities, interim payment certificates, contract documents, correspondences with client and consultant	Descriptive statistics	The cost deviation scenario that exists in selected hydropower projects
2	To find out the major causes of cost deviation in hydropower projects	Major causes resulting in cost deviation	Questionnaire survey, key informant interviews (KII)	Relative Importance Index (RII), Spearman's rank correlation	Various major causes of cost deviation in selected hydropower projects
3	To find out the remedial measures of cost deviation	Various remedial measures adopted to avoid cost deviation	Questionnaire survey, key informant interviews (KII)	Relative Importance Index (RII), Spearman's rank correlation	Mitigation measures to minimize the gap between final and initial cost

4. Results and Discussion

In order to study the current scenarios of cost deviation in construction of civil structures of selected hydropower projects, the contract document, interim payment certificated (IPC) and final certified bills and correspondence documents (i.e. , letters from client, consultant and contractor, minutes of meetings) were studied. The result of the selected project is tabulated below (Table 7):

TABLE 7. Current scenarios of cost deviation of selected hydropower projects

S.N.	Description	Rudi Khola A HPP (8.8 MW)	Hewa Khola 'A' HEP (14.9 MW)	Midim Khola (Karapu) HPP (3 MW)	Mistri Khola HEP (42 MW)
1	Contract Agreement Date / Project Commencement Date	March 24, 2016 / March 31, 2016	September 30, 2012	January 8, 2015	May 8, 2015 / June 30, 2016
2	Initial Project Completion Date	September 15, 2017	November 19, 2014	April 15, 2016	December 17, 2018
3	Actual Completion Date	May 30, 2019	February 4, 2017	November 16, 2017	July 8, 2021
4	Time Overrun	1.7 years	2.25 years	2.67 years	2.58 years
5	Original Contract Amount / Revised Contract Amount (Including VAT)	NRs. 320,920,000	NRs. 1,008,584,059.45 / 1,039,619,696.02	NRs. 244,975,338.29 / 323,943,814.38	NRs. 1,382,942,393.38
6	Final Certified Amount (Including VAT)	NRs. 458,984,846.00	NRs. 1,203,113,550.00	NRs. 433,991,644.47	NRs. 1,634,042,758.93
7	Cost Overrun	43.02%	15.73%	33.97%	18.16%

The percentage deviation in cost of major activities due to quantity variation is presented in the table 8 below separately for all projects:

Table 8. Percentage of Cost Deviation in Rudi Khola A HEP

S.N.	Item of Works	% Deviation in Cost due to Quantity Variation
1	Excavation of earth soil / common material / boulder mix	10.14%
2	Excavation in hard rock without blasting	63.48%
3	M10 Concrete	28.86%
4	M15 Concrete	15.72%
5	M20 Concrete	-69.47%
6	Plum M15/40	50.06%
7	M25 Concrete	747.15%
8	Formworks	37.99%
9	Reinforcement	4.62%

Table 9. Percentage of Cost Deviation in Hewa Khola HEP

S.N.	Item of Works	% Deviation in Cost due to Quantity Variation
1	Excavation of Common Material / Boulder	18.54%
2	Hard Rock Excavation	104.89%
3	Rock Excavation by Drilling and Blasting	-1.25%
4	75 mm thick C15 Blinding Concrete	8.76%
5	C25 Concrete	98.54%
6	Formwork	-8.76%
7	Reinforcement	101.83%
8	Fiber Reinforced Shotcrete	-3.63%
9	Rock Bolt and Spilling Rod	-3.63%
10	Steel Rib	193.37%

Table 10. Percentage of Cost Deviation in Midim Khola HEP

S.N.	Item of Works	% Deviation in Cost due to Quantity Variation
1	All types of Excavation	7%
2	Formwork	35.3%
3	Various Grades of Concrete	10.93%
4	Reinforcement Works	43%
5	Tunnel Support Works	-16%

Table 11. Percentage of Cost Deviation in Mistri Khola HEP

S.N.	Item of Works	% Deviation in Cost due to Quantity Variation
1	All types of Excavation	-8%
2	Formwork	2%
3	Various Grades of Concrete	54%
4	Reinforcement Works	18%
5	Tunnel Support Works	-27%

4.0.1. *Causes of cost deviation in the selected hydropower project.* Based on the combined views of all the parties involved and analysis of causes of cost deviation, the value of RII given to the following factors were most significant:

5. Relative Importance Index (RII) for Selected Hydropower Projects

Table 12. RII Values for Rudi Khola - A HEP

Factor	**RII**
Quantity overrun of the various activities of the project due to site condition	0.88
Additional work / New Item	0.825
Inadequate cash flow during construction / Cash flow problem / Financial difficulties faced by the contractor / Poor cost control	0.775
Bill of quantities lacking precision	0.775

Table 13. RII Values for Hewa Khola - A HEP

Factor	**RII**
Quantity overrun of the various activities of the project due to site condition	0.7
Strikes, bandhs	0.7
Inadequate cash flow during construction / Cash flow problem / Financial difficulties faced by the contractor / Poor cost control	0.675

Table 14. RII Values for Midim Khola HEP

Factor	**RII**
Change in design	0.93
Quantity overrun of the various activities of the project due to site condition	0.83
Insufficient data collection and survey before design / Inadequate detail study before execution of works	0.825
Strikes, bandhs	0.825

Table 15. RII Values for Mistri Khola HEP

Factor	**RII**
Seepage water management inside tunnel	0.95
Fluctuation in price of construction materials	0.9
Provision for price escalation	0.83

5.0.1. *Remedial measures of cost deviation in selected hydropower project.* Based on the combined views of all the parties involved and analysis of remedial measures of cost deviation, the value of RII given to the following factors were most significant:

Table 16. RII Values for Remedial Measures - Rudi Khola HEP

Remedial Measure	**RII**
Review and improve bid documents such as technical specifications, bill of quantities	0.825
Minimize change orders, design to reduce any time and cost overruns	0.775
Frequent preventive maintenance of equipment to avoid sudden breakdown	0.775

Table 17. RII Values for Remedial Measures - Hewa Khola HEP

Remedial Measure	**RII**
Review and improve bid documents such as technical specifications, bill of quantities	0.775
Hire full time skilled mechanics for proper maintenance of equipment	0.775
Frequent preventive maintenance of equipment to avoid sudden breakdown	0.75

Table 18. RII Values for Remedial Measures - Midim Khola HEP

Remedial Measure	**RII**
Review and improve bid documents such as technical specifications, bill of quantities	0.875
Ensure quality design of project	0.85
Minimize change orders, design to reduce any time and cost overruns	0.8

Table 19. RII Values for Remedial Measures - Mistri Khola HEP

Remedial Measure	**RII**
For the geophysical studies, seismic refraction, reflection seismic and electrical resistivity should be done to get more accurate information regarding weathering depth, ground water conditions	0.825
Minimum level of geological investigation to improve the predictability of geological conditions	0.8
Effective strategic planning by all parties involved	0.775
Realistic prediction and evaluation of rock mass quality	0.775

6. Conclusions and Recommendations

6.1. **Conclusions.** Based on the results and discussions, the following conclusions are made: From the study of all 4 hydropower projects, it was found that in all hydropower projects except Mistri Khola HEP, there was quantity overrun of major activities of the construction which resulted in cost deviation of civil construction works of the project. Besides that various client related factors such as irregular monthly payment; consultant related factors such as bill of quantities lacking precision, change in design, insufficient

data collection and survey before design; contractor related factors such as inadequate cash flow during construction/ cash flow problem/ financial difficulties faced by contractor; project related factors such as quantity overrun of the various activities of the project due to site condition, additional work, new item, seepage water management inside tunnel, provision for price escalation; external factors such as strikes, bandhs, natural disaster (landslide and flood triggered by heavy rainfall); equipment related factors such as frequent equipment breakdown/ frequent maintenance of equipment ; material related factors such as fluctuation in price of construction materials were some of the significant factors that led to cost deviation of the selected hydropower project.

6.2. **Recommendations.** From the analysis of the result of the questionnaire survey, it is observed that in order to minimize the cost deviation of hydropower project, the remedial measures to be adopted by client is to ensure quality design of the project, have appropriate funding levels so that contractor can be regularly paid; consultant related factor such as review and improve bid documents such as technical specifications, drawings, bill of quantities, minimize change orders, detail and comprehensive site investigation during the preparation of bill of quantities; contractor related measures are contractor should have enough cash before beginning of any project, frequent preventive maintenance of equipment to avoid sudden breakdown . Besides that the remedial measures to be adopted by all parties involved are effective strategic planning by all parties in order to find appropriate way to tackle various problems that arise during construction.

References

[1] A. Enhassi and J. A.-N., "Delays and cost overruns in the construction projects in the Gaza Strip," *Journal of Financial Management of Property and Construction*, vol. 14, no. 2, pp. 126–151, 2009.

[2] V. Ajayi, "Primary sources of data and secondary sources of data," 2017.

[3] A. M. Belay and O. T., "Do longer projects have larger cost deviation than shorter construction project," Elsevier Ltd, Primosten, Croatia, 2017.

[4] S. Assaf and H., "Causes of delay in large construction projects," *International Journal of Project Management*, pp. 349–357, 2006.

[5] A. Razali and A. T., "Applicability of Bill of Quantities in Construction Procurement," *International Journal of Engineering Science Invention*, vol. 3, no. 4, pp. 31–34, 2014.

[6] A. Azis et al., "Controlling Cost Overrun Factors in Construction Projects in Malaysia," *Research Journal of Applied Sciences, Engineering and Technology*, pp. 2621–2629, 2013.

[7] E. Carmines et al., *Reliability and validity assessment*, SAGE, Newbury Park, CA, 1979.

[8] M. M. Chabota Kaliba, "Cost escalation and schedule delays in road construction projects in Zambia," *International Journal of Project Management*, pp. 522–531, 2009.

[9] D. Chan et al., "Comparative Study of Causes of Time Overruns in Hong Kong Construction Projects," *International Journal of Project Management*, vol. 15, no. 1, pp. 55–63, 1996.

[10] K. Chiluwal, "Factors affecting construction performance and its impact on profitability of small hydropower projects," MSc thesis, Nepal Engineering College, CPS, Pokhara University, Bhaktapur, Nepal, 2017.

[11] S. L. Dahal, "Cost Variation in Construction Projects (A Case Study on Road Projects of RSDP in Department of Roads)," MSc thesis, Nepal Engineering College, CPS, Pokhara University, Bhaktapur, Nepal, 2015.

[12] E. Drost, "Validity and Reliability in Social Science Research," 2011.

[13] M. Egemen et al., "Different approaches of clients and consultants to contractors' qualification and selection," *Journal of Civil Engineering and Management*, 2005.

[14] M. El-Razek, "Causes of Delay in Building Construction Projects in Egypt," *Journal of Construction Engineering and Management*, 2008.

[15] O. Fagbenle, "Factor affecting the performance of labour in Nigeria Construction," 2004.

[16] S. Glen, "StatisticsHowTo," 2013. [Online]. Available: https://www.statisticshowto.com/probability-and-statistics/correlation-coefficient-formula/spearman-rank-correlation-definition-calculate/. [Accessed Feb. 2022].

[17] T. Hamed, "Validity and Reliability of the Research Instrument," *International Journal of Academic Research in Management*, pp. 28–36, 2016.
[18] M. B. Hashim Hanif, "Causes of Variation Orders in Construction of Hydropower Projects in Pakistan," in *International Conference on Management and Engineering*, Pakistan, 2014.
[19] M. B. Hashim Hanif, "Impact of Variation Orders on Time and Cost in Mega Hydropower Projects of Pakistan," *Journal of Construction in Developing Countries*, vol. 21, no. 2, pp. 37–53, 2016.
[20] S. R. Hillis, "Delay Management in Construction Projects in the Gaza Strip Clients perspectives," The Islamic University- Gaza, 2010.
[21] B. 36, "Clean Leap," 2015. [Online]. Available: https://cleanleap.com/4current-cost-hydropower/42-breakdown-hydropower-costs-source. [Accessed Jan. 30, 2015].
[22] S. Khanal, "Study of Impact of Variation Order on Project Cost and Time of Building Construction (A Study of Building Projects Inside Tribhuvan University Premises, Kathmandu)," 2020.
[23] L. C. Kofi Offei-Nyako, "Deviations between Contract Sums and Final Accounts: The Case of Capital Projects in Ghana," *Journal of Construction Engineering*, vol. 2016, p. 8, 2016.
[24] B. N. Krishna Kanta Panthi, "Predicted versus actual rock mass conditions: A review of tunnel projects in Nepal Himalaya," *Tunnelling and Underground Space Technology*, vol. 22, pp. 173–184, 2007.
[25] K. M. L.S. Pheng, "Formulating a strategic marketing mix for quantity surveyors," *Marketing Intelligence & Planning*, vol. 15, no. 6, pp. 273–280, 1997.
[26] Y. D. Long Le-Hoai, "Delay and Cost Overrun in Vietnam Large Construction Projects: A Comparison with Other Selected Countries," *KSCE Journal of Civil Engineering*, vol. 12, no. 6, pp. 367–377, 2008.
[27] Ministry of Energy, Water Resources and Irrigation, Department of Electricity Development, "Department of Electricity Development," 2020. [Online]. Available: https://www.doed.gov.np/license/54. [Accessed Aug. 23, 2020].
[28] Nepal Electricity Authority, *A Year in Review, Fiscal Year 2011/12*, Kathmandu, Nepal, 2012.
[29] Nepal Electricity Authority, *A Year in Review - Fiscal Year 2018/19*, Kathmandu, Nepal, 2019.
[30] A. Neupane, "Contractual Issues for Hydropower Construction in Nepal," *HYDRO NEPAL*, no. 23, pp. 56–57, 2018.
[31] U. Neupane, "Construction delay: poor planning to blame," *Himalayan Times*, Sep. 11, 2019. [Online]. Available: https://thehimalayantimes.com/opinion/construction-delay-poor-planning-to-blame.
[32] S. Sharma and P. G., "Cost overrun factors and project cost risk assessment in construction industry - a state of the art review," *Internal Journal of Civil Engineering*, pp. 139–154, 2014.
[33] S. Ahmed and I. B., "Deviation in the Cost of Projects," in *Construction Maeconomics Conference 2014*, p. 10, 2014.
[34] P. K. Savita Sharma, "Forecasting the Probability of Cost Overrun Risk of Indian Construction Projects using Fuzzy Model," *International Journal on Emerging Technologies*, vol. 14, 2019.
[35] G. Sweis, "Factors Affecting Time Overruns in Public Construction Projects: The Case of Jordan," *International Journal of Business and Management*, 2013.
[36] S. 29, "Time Overrun and Its Impact on Cost of Construction of Small Hydropower Projects," MSc thesis, Nepal Engineering College, CPS, Pokhara University, Bhaktapur, Nepal, 2014.
[37] B. Whitley, *Principals of Research and Behavioural Science*, Boston: McGraw-Hill, 2002.
[38] J. O. Yaw Frimpong, "Causes of delay and cost overruns in construction of groundwater projects in a developing countries; Ghana as a case study," *International Journal of Project Management*, pp. 321–326, 2003.

Journal Name: Everest Advances in Science and Technology (EAST)
Volume: 1
Issue: 1
Date: November, 2025
ISSN: 3102-0410 (print), 3102-0429 (online)
Publisher: Everest Engineering College, Sanepa-2, Lalitpur